The Observation of Extended Sources with the Hartebeesthoek Radio Telescope

THESIS

Submitted in Fulfilment of the

Requirements for the Degree of

DOCTOR OF PHILOSOPHY

of Rhodes University

by

PETER IAN MOUNTFORT

February 1989

Abstract

The Hartebeesthoek Radio Telescope is well suited to mapping large areas of sky at 2.3 GHz because of the stability and sensitivity of the noise-adding radiometer (Nicolson, 1970) and cryogenic amplifier used at this frequency, the relatively large 20′ beam of the 26 m dish antenna, and its high-speed drive capability. Telescope control programs were written for the Observatory's online computer for automated mapping.

Effort centred on removing the curved baseline or 'background' from each Declination (Dec) scan, due to atmospheric and ground radiation contributions varying as the antenna is scanned. Initially these backgrounds were measured over a wide range of Hour Angle (HA) for the Dec range of a map, and an interpolated curve subtracted from each on-source scan for its HA. A common baselevel was established by comparison with drift scans (observed with the antenna stationary).

These different observations (on- and off-source Dec scans and drift scans) were combined into one in the Skymap system by performing Dec scans at a fixed starting HA for a period long enough to permit 'cold sky' and the source to drift through. A background formed by fitting a smooth curve through the lowest sample at each Dec provides a consistent relative baselevel for all the scans in an observation. A high scanning speed is used so that observations may fruitfully be repeated three times and interleaved to build a reliable, fully sampled map. As each observation has its own background removed, it may be made at any HA.

For comparison, maps of Upper Scorpio produced by the earlier method (Baart *et al.*, 1980) and the Magellanic Cloud region produced by Skymap (Mountfort *et al.*, 1987) are shown.

Skymap provides a simple and flexible mapping method which relies on the stability of the noise-adding radiometer and high-speed repeated scans to produce good maps of large or small extent with little computation. Correction for drift is more difficult than with systems which use intersecting scans, such as the 'nodding' scans used by Haslam *et al.* (1981) or the Azimuth scans of Reich (1982).

Table of Contents

List of Tables

Page

List of Figures

List of Plates

Preface

This work was supported by grants from the Rhodes University Council and the CSIR.

I should like to thank my supervisor, Prof. de Jager, and Prof. Baart and Dr. Nicolson for supplying inspiration and guidance throughout the undertaking. Thanks are due to the RAO staff, especially Gunther Krantz and Don Cameron, for taking care of the hardware side of the telescope control system and for many invaluable discussions on the software, and Mike Gaylard for taking the telescope control software under his wing. Credit is due to a long line of people who worked in the Radio Astronomy group during the course of this project: Graham Oberem, Clive Way-Jones, Fiona Jackson, Pete Clayton, Mike Levey, Johan Fourie, Dave Maclennan, Margie Campbell, and especially Justin Jonas who has developed Skymap far beyond its simple beginnings.

Thanks to the Rhodes Computer Centre staff who were sympathetic to our needs, and to Prof. Terry of Computer Science for access to his library of subroutines..

Any project which stretches over 14 years becomes somewhat of an endurance test, and for their unflagging support through it all, I should like to thank Mr. and Mrs. Pearson, Prof. de Jager, Prof. Baart and my current employer in the person of my research head, Mr. van Zyl Brink, and, last but not least, Mrs. Daphne Hartley for her assistance in finalising this manuscript.

To Sheelagh
and Francesca

Chapter One: Introduction

Radio Astronomy Observatories in the Southern Hemisphere are fairly few and far between, as a quick glance at the Astronomical Ephemeris will testify, thus the Radio Astronomy Group of the Rhodes University Department of Physics and Electronics were fortunate to be offered the use of a facility 1000 km from the university. The Hartebeeshoek Radio Astronomy Observatory (RAO) was operated by the National Institute for Telecommunications Research (NITR) of the South African Council for Scientific and Industrial Research (CSIR). (It is now part of the Foundation for Research and Development). The facility had been operated on behalf of the United States National Aeronautics and Space Administration (NASA) as a deep space satellite tracking station, and converted to an observatory when these activites ceased. From September, 1975, the Rhodes Group were generously offered 20% of the available observing time. Because of the paucity of observatories, it follows that the Southern sky has not been exhaustively explored at radio frequencies, and much thought was given to the most useful way of employing the instrument which had thus become available. This, of course, depended largely on the characteristics of the instrument itself compared with others in the Southern Hemisphere. The telescope's 26 m dish antenna was equipped with a very sensitive receiver for 2300 MHz (13 cm). The 26 m antenna and 13 cm wavelength combine to produce a beamwidth of $^1/_3^\circ$, and the system temperature with the MASER receiver is 27 K (the telescope is described in detail in Chapter 2). The most prominent competitor was the 64 m dish at Parkes, which is used at a frequency of 2700 MHz, amongst others, for extensive surveys. However, there is a large area to be covered, and undaunted by the size of the competition, the problem was considered afresh.

Radio telescopes excel relative to their optical counterparts at measuring very distant sources of radiation, or those, relatively nearby within the Galaxy, which are obscured by gas and dust at optical wavelengths. The obvious problem with the very distant sources is that they cover very small angles in the sky, at most the order of arcseconds, not the sort of thing to explore with $^1/_3^\circ$ resolution. Likewise, a 26 m antenna does not have the large collecting area necessary to capture the minute amount of energy which reaches us over such distances.

Turning to the galaxy, we note other limitations. Our Earthbound view of the Galactic disc is necessarily edge on, the radio picture being one of source confusingly superimposed on source to a staggering degree. Thus most useful information about Galactic structure is obtained by a method which can at least estimate the distance of the emitting region, that is, spectral line observation. Unfortunately, at that early stage of development of the RAO, no spectrometer was available. Also, the Galactic Plane had been mapped several times before in the radio continuum, in particular from Parkes at 1410 MHz (Hill, 1968) and 2700 MHz (Day *et al.*, 1972) and later at 5000 MHz (Haynes *et al.*, 1978) with the good resolution yielded by their 64 m antenna. However, these surveys had been restricted to very low Galactic Latitude, less than 4° in most areas. Also, presumably because the sources within this region are so strong, low sensitivity had been used. Because of the Hartebeeshoek telescope's broader beamwidth and lower system temperature, it was feasible for a much broader area to be surveyed to higher sensitivity, albeit with lower resolution, in a reasonable amount of time.

Thus it was considered optimum to exploit the telescope's large beamwidth and low system temperature by mapping extended areas of low-level emission at low to middle Galactic Latitudes. To produce maps of large areas in search of large scale structures, rather in the tradition of the metre wavelength surveys, with the increase in frequency hopefully producing a different picture.

With the objectives thus set out, a brief overview of the current work is in order.

1.1. Overview

The overall purpose of this thesis is to present the techniques developed for the observation of extended sources and describe the implementation thereof by the author. This involved a study of the telescope operation in order to develop a suitably efficient observing method, an implementation under computer control, and the observation of a source area utilizing the completed system. The successive chapters have been delimited by subject, rather than chronology. Some background information is still lacking, and will be supplied in the remaining paragraphs of this chapter. Chapter 2 furnishes particulars of the observing environment, with a detailed description of the telescope instrumentation, including the radiometer, the antenna control system and the observatory computer system, though the latter evolved during the course of the work described. Chapter 3, in fact, recounts

the earliest version of the mapping system, which was operated without the help of computer controlled observing.

Chapter 4 then draws together all the information used in the design and development of the computer controlled fast mapping system, while Chapter 5 follows the operation of this system from observation through data reduction to map display.

Chapters 6 and 7 present and discuss two sets of results produced by the two different generations of the system described in Chapters 3 and 5 respectively, the first covering the Sco OB2 stellar association and the ρ Ophiuchus dark cloud, and the second the Magellanic Clouds and their surroundings. Finally Chapter 8 is an attempt to evaluate critically the performance of the system in the light of its objectives.

1.2. Mapping

It will be recalled that the key word in the objective stated above was "mapping". This is never a simple process for a radio astronomer, compared with the ease with which his optical counterpart may, in one observation, record the intensity of millions of points on a single photographic plate. The radio telescope can only measure the intensity of emission at one point at a time. Thus a map must be painstakingly built up in the manner of a television picture by scanning the beam across the sky, each scan sampled along its length and separated from its neighbours by less than half a beamwidth.

If a small look ahead might be permitted at this stage, it can be said that most of the problems with mapping arise because each point is observed at a different time and thus under different conditions to all other points. For this reason the conditions and their effect upon the observation have to be very well specified to allow a map to be put together.

1.3. Previous Observations

Deciding to search for extended sources on the basis that they are well matched to the telescope characteristics is all very well, but it would be reassuring to know that such sources are likely to exist. Such reassurance is forthcoming from two separate sources.

The metre wavelength surveys show extended features such as loops and spurs leading out from the Galactic Plane to fairly high latitudes (Berkhuizen, 1971; Landecker and Wielebinski, 1970; Price, 1974), though there is nothing in the Southern Hemisphere to compare with the North Polar spur at these frequencies. Radiation from these sources is mostly attributed to the synchrotron mechanism, which, given the Galactic electron energy spectrum, usually falls off very rapidly with decreasing wavelength, so we cannot be sure of detecting all such features at 13 cm.

At the other end of the spectrum are the optical H α surveys (Rodgers et al, 1960; Sivan, 1974; Gum, 1955). These show many features which would appear extended even to a $^1/_3^\circ$ beam, and several very large features: the Gum Nebula, the Orion complex and others in the region around the Galactic centre.

Two other sets of radio observations bear mention. Haslam *et al.* (1975) were known to have undertaken an extensive survey of the Southern sky at 408 MHz with the Parkes 64 m telescope, complementing those observations made in the Northern Hemisphere with the 100 m telescope at the Max-Planck-Institut für Radioastronomie (MPIfR) at Bonn. These data would complement a survey of similar scope undertaken with the Hartebeeshoek telescope, the 408 MHz data having approximately the same resolution and being nearly a factor of six lower in frequency.

An extensive ongoing project at Parkes was the 2700 MHz series of surveys (Wright et al, 1976). However this was a deliberate search for extra-galactic sources of smaller angular extent: Areas of high obscuration near the Galactic Plane were avoided, and a dual beam correlation receiver was used which effectively precluded the observation of sources greater in size than the beam separation, some $18.'5$ (Emerson and Klein, 1979).

Both the usefulness and feasibility of a mapping program having been established, attention is now turned to the equipment to be used.

Chapter Two: The Telescope

As one of the principal objectives of this project was to make best use of the telescope, it is described here at the beginning of this work with an emphasis on the features which make it unique, and which largely determined the resultant course of the project.

The most visible part of the instrument is the 26 m paraboloid dish antenna, which is supported by an Equatorial mount. The feed is used in the Cassegrain configuration, and is mounted in a cone above the surface of the dish. The cone also contains the MASER amplifier and mixer from which the signal is fed down to the control room, where the backend of the receiver is housed. Other signals, equally important when the overall operation of the telescope is considered, convey position information. They start at the synchros mounted on each axis, are encoded digitally and fed to the antenna control system. This generates the appropriate error signal, which is fed back to the hydraulics on the antenna mount to position the antenna. Information from both subsystems is fed into the computer for storage and analysis. The signal flow is shown schematically in Figure 2.1.

While the radiometer is, of course, of prime interest to the astronomer, this part of the system had matured by the time the Rhodes group arrived on the scene, having been in use for nearly ten years (Nicolson, 1970). Although physically reorganized after the cessation of tracking operations, the principle of operation was not modified. The design was originally chosen for optimum use of the single feed and MASER amplifier configuration used for tracking operations. However, its unique features were very well suited to the program of variable source measurement being carried out at the

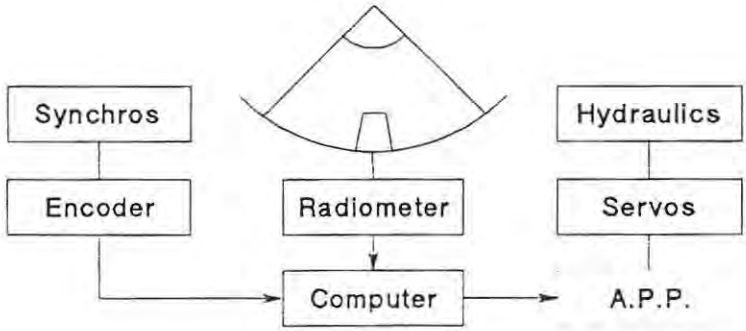

Figure 2.1. A block diagram of the telescope. Shown is the signal flow between the antenna and drive and the computer. The Antenna Position Programmer (APP), was retired in 1980.

RAO, as well as the planned Rhodes survey, and it was thus retained. For the extended source survey, little would have been gained from using sophisticated multiple beam techniques on the relatively small antenna (Emerson and Klein,1979), and in any case, these would require more than the single MASER front end amplifier available.

The antenna control system, by comparison with the radiometer, required a complete restructuring. This system had been driven by general purpose computers for NASA tracking operations. These computers were replaced by a purpose-built piece of hardware, the Antenna Position Programmer (APP) for RAO operation. Although obviously not as flexible as general purpose machines, the APP was used for the majority of observing until 1980, while new computers were acquired, interfaced to the servo electronics and programmed.

The computer system was built up over the years that the Rhodes mapping techniques were being developed. Indeed, the methods used were largely dependent on the state of computer development, and at each increase in the capability of the computer, a new observing system was implemented to make use of it. A large part of the effort of implementing the mapping system was thus expended on the computer, and for that reason it is dealt with in some detail here, together with its operating system and the extensions made to provide observing program support.

2.1. The Radiometer

The radiometer is shown in Figure 2.2 in block form. It operates in the noise-adding mode (Nicolson, 1970). In the terminology of Tiuri (1966), it is a gain-stabilized total power receiver. The gain of the entire radiometer is controlled so that a calibration noise source always produces the same increase in voltage at the output of the square-law detector. Nicolson's description of its operation is largely repeated here, with the updated hardware configuration.

Physically, the MASER and mixer are housed in the cone within the dish. The 2300 MHz signal produced by the MASER is mixed with one multiplied up from a digitally controlled synthesizer to produce an IF signal centred on 60 MHz. The MASER has the smallest bandwidth of any component in the system, namely 16 MHz.

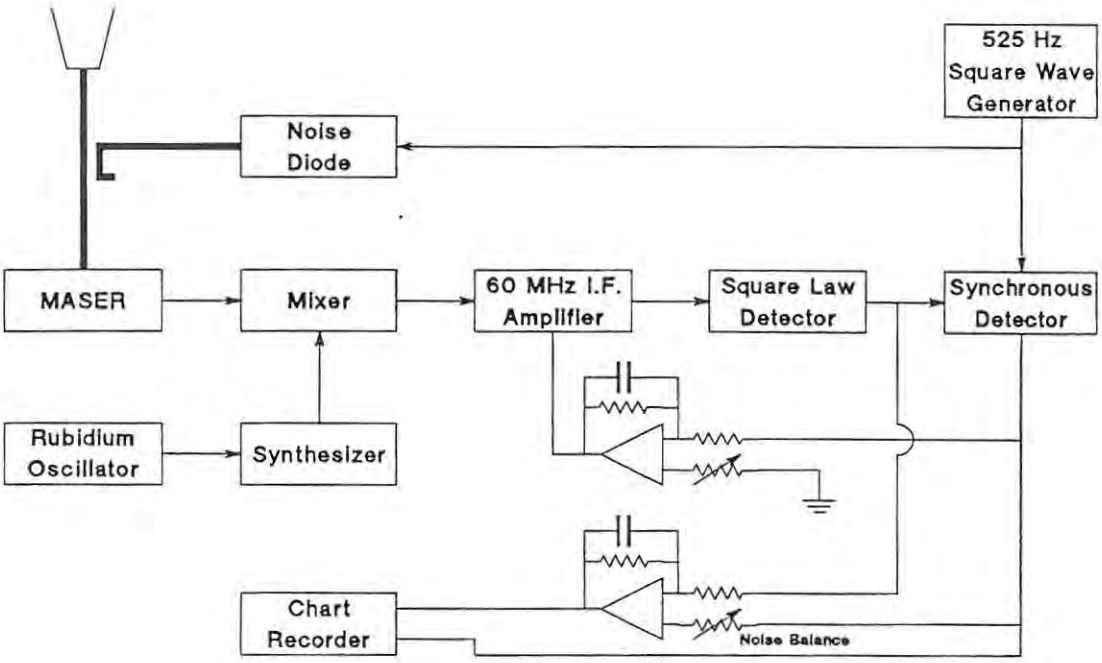

Figure 2.2. The noise adding radiometer. Note the output of the synchronous detector both controlling the gain of the IF amplifier and feeding the noise balance control for offsetting the receiver output. A DVM may be connected in parallel with the chart recorder.

2.1.1. Radiometer Operation

Stabilization is achieved by injecting noise from a noise diode into the signal path before the MASER via a directional coupler. The noise is modulated by a square wave of 525 Hz frequency. The signal resulting from the injected noise is extracted by a synchronous detector at the other end of the signal path, after the square-law detector, and used to control the gain of the IF amplifier which is thus able to reduce the effect of changes in the MASER gain.

However, the output of the receiver is proportional to the amount of IF power reaching the square-law detector, which power is in turn dependent on both the gain and noise temperature of the front end. Although the gain is stabilized, a control of better than 1% is not practically realizable. Even with a receiver noise temperature of less than 30 K, a 1% gain change means 300 mK change in output, far greater than the expected mimimum detectable source temperature. To alleviate this problem, the signal from the square-law detector is balanced against that produced by the synchronous detector. In other words, instead of a constant voltage being used to offset the large signal at the output due to receiver noise, a fraction of the synchronous detector voltage is used. Since

they are both equally dependent on the gain and bandwidth of the front end of the receiver, changes in these parameters have no effect on the receiver output while no source is present.

With an injected noise temperature T_n, the output of the synchronous detector is proportional to $gkBT_n$, where g and B are respectively the predetection gain and bandwidth of the system, and k is Boltzmann's constant. Similarly, the mean voltage output from the square-law detector is proportional to $gkB(T_e+T_n/2)$, where T_e is the receiver noise temperature. Thus if we use a fraction of the synchronous detector output to cancel this:

$$gkB(T_e + T_n/2) - cgkBT_n = 0$$

where c is the adjustable multiplying factor, the output should remain zero, independent of g and B. This provides a stable baseline for each source measurement, provided the balance is set at the start. A source, of course, appears as a slight increase in T_e, and provided the balance is not readjusted, appears at the output. T_n is usually set to about $2T_e$, to make c close to unity.

2.1.2. Stability and Noise Considerations

When mapping a large area, a single observing run may occupy a whole night, during which the noise balance cannot be adjusted. It is thus necessary that T_e should remain constant over the whole observing period, as a change in T_e cannot be distinguished at the output from a change due to a source. The stability of T_e over a time-scale of hours requires closer examination. T_n is supplied from a calibration noise source, and thus hopefully does not change. The observations of variable sources by Nicolson seem to bear this out.

T_e can be split into components from four sources: the atmosphere and dish surroundings, losses in the feed, the MASER and the second stage amplifier. The atmospheric contribution varies drastically as the antenna scans, and this must be dealt with during the reduction of the data. In clear dry weather which usually holds during the winter months, the atmospheric contribution appears to be stable, but any condensation in the antenna beam produces an increase in T_e. The surroundings cool after sunset, but their effect on the telescope output appears to stabilize after about two hours. These effects are seen on all-night drift scans, which provide the basis for confidence in the radiometer stability.

The feed can be considered a passive attenuator, so its contribution to the receiver noise temperature is a small fraction of its ambient temperature. The cone which houses the feed is airconditioned to minimize any variation in ambient temperature. There is a possibility that the attenuation factor might change due to a flexing of the feed structure while the antenna scans, but this is minimized by a rigid mounting, and would be removed together with the atmospheric contribution during processing, if repeatable from scan to scan.

The noise temperature of the MASER is inherently stable, as it operates immersed in boiling helium. Malfunction of some of the peripheral circuitry, for example the pump, can appear as an increase in MASER noise temperature, but under normal operating conditions the noise temperature is stable.

The noise temperature of the second stage amplifier is about 300 K, but this is divided by the MASER gain to find its contribution to the overall receiver noise temperature. The MASER is usually operated at about 34 dB gain (there is a trade-off between gain and bandwidth). A simple calculation shows that if the MASER gain should drop by 2 dB, a not uncommon occurrence, the second stage contribution should increase by 70 mK.

The expression for the minimum detectable signal is given by Nicolson

$$\Delta T = 2T_e(1 + T_e/T_n)/\sqrt{2B\tau}$$

where τ is the post-detection time constant. This is recognizable as the expression for the minimum detectable temperature of a total power receiver, with allowance made for the added noise. Remembering that T_n is usually set to $2T_e$ the bracketed expression evaluates to 1.5. It is interesting to compare this with a Dicke receiver, which has a penalty factor of 1.41 because only half the time is spent on-source. In addition, a Dicke receiver requires a switch in the feed before the amplifier, a component with higher attenuation than the coupler required by the noise-adding system. In the RAO radiometer, T_e is about 27 K, and T_n 45 K. The MASER bandwidth is 16 MHz, yielding a ΔT of 15 mK for τ = 1 s. The performance of the instrument expressed as a conversion factor from the flux of a point source to observed antenna temperature is 0.12 K Jy^{-1}.

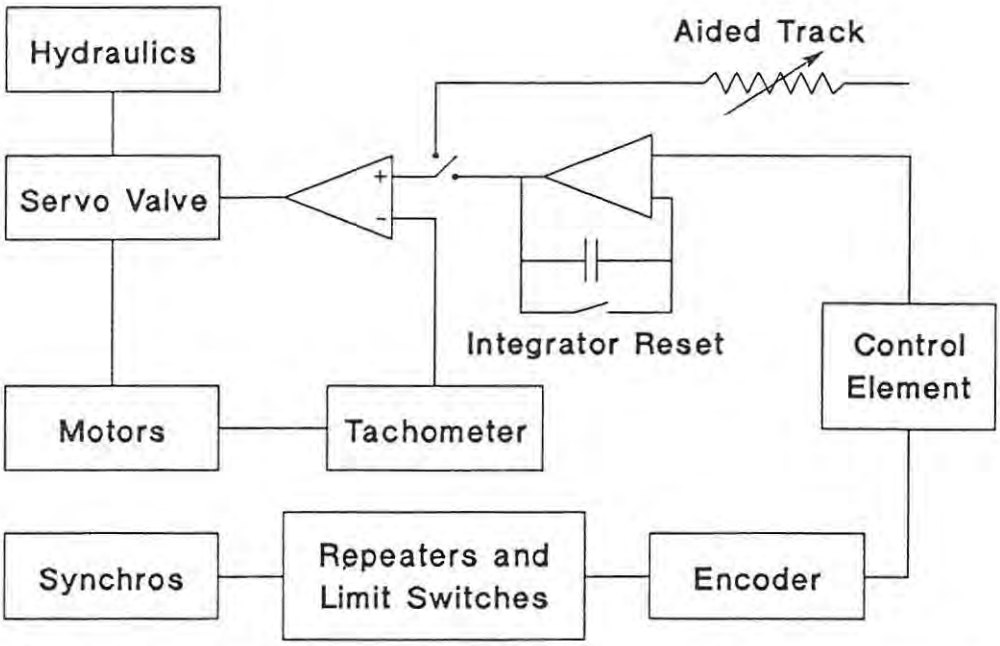

Figure 2.3. The Antenna Control System. There is one synchro/encoder system for each axis, and a total of four servosystem/motor combinations, one for each speed for each axis. The control element was initially the APP and later the computer. Integration of the error signal to control motor velocity provides a second order control system which tracks at constant velocity with zero error. Aided Track mode allows the velocity to be manually controlled from the console.

2.2. The Antenna Control System

A schematic layout of the control system is shown in Figure 2.3. The distinction must be made between the passive servo system and the programmable control element which allows the antenna to be driven in a meaningful way.

The encoder electronics measure the positions of both axes and return these to the control element. This generates an error signal which is fed back to the hydraulic system which actually drives the antenna.

The control element was, at the start of the Rhodes visits, the Antenna Position Programmer (APP), a dedicated piece of hardware which is thus described along with the servo system. This was later replaced by the computer, which will be described in the next section (2.3).

2.2.1. The Servo System and Encoders

The position of each axis is measured via a pair of synchros. The synchros mounted on the axes drive repeaters on the ground. Here a precision machined cam removes the errors introduced by the

synchros themselves, and encoders transform the position into a binary Gray code, to prevent ambiguous readings occurring while the antenna is in motion. The Gray code is in turn converted into binary coded decimal, and fed to the control element. The angles are represented as millidegrees (mdeg), and the resolution of the encoders is 2 units (7.2″). A system of limit switches is included on the antenna to prevent the dish from sustaining structural damage by being driven to any point where it might come into contact with the mount.

The electronics which condition the feedback signal consist mainly of an integrator. The error signal thus produces an acceleration by causing a change in the speed of the hydraulic motor, represented by the charge on the integrator. This second order feedback system allows the antenna to scan at constant velocity with zero error. Tachometers driven by the motors provide a negative feedback signal at the input to the summing amplifier, to leave the overall response of the system only slightly underdamped.

In fact there are two separate drive systems for each axis, one for high speed and one for low. The low speed motors drive the pinions through a reduction gearbox, and have their own tachometers and electronic integrators with longer time constants. The high speed drives are capable of reaching $1^{\circ}\ s^{-1}$ and the low speed drives 30 mdeg s^{-1}. There are two pinions on each ring gear, driving in opposite directions to prevent backlash, and thus two motors on each axis for each speed. Speed changes may be made only when the antenna is stationary, as the servo valves on the unused motors are closed, thus keeping the motors firmly stopped. There is no mechanism for matching motor speeds while the antenna is in motion. The high speed drive, if used at speeds below 30 mdeg s^{-1}, is unstable and does not track well.

There are thus several signals supplied by the control element. In addition to the error voltage, there is the high/low speed control, and for stopping there is an integrator reset which causes the servo valve to close gracefully, and a signal for the mechanical brakes which engage very abruptly.

A manual control console is provided to determine the source of the control signals. Apart from the APP and the computer, a manual mode called Aided Track is also used. In this mode, the integrators are bypassed, and voltages from two potentiometers are applied to the outputs, controlling the servo

valves and thus speed of each axis. Lighted push-button switches are provided to control the high/low speed, integrator resets and brakes for each axis. These serve as mode indicators when under computer control.

2.2.2. The Antenna Position Programmer

The APP may be regarded as a simple, fixed program computer. It reads command input co-ordinates, usually from paper tape, the real positions of the axes from the encoders, and real time from an external clock. From these it generates an error voltage which is fed back to the hydraulics.

Sets of co-ordinates, consisting of Hour Angle, Declination and time are input at one or ten second intervals. The difference in angle between the new command co-ordinates and the previous set is calculated for each axis. These differences are divided by 10 or 100 (depending on the difference in times being one or ten seconds) to obtain an increment value. Round off is a problem, especially when dividing by 100, as the quotient is truncated to 1 mdeg accuracy. Ten times a second, the increments are added to their respective angles, and the results compared with the values from the encoders to generate the feedback voltages. When real time from the clock reaches the latest command time read, this set of co-ordinates is moved to the old command register, and a new set read in.

In order to allow tracking at sidereal rate (4.17 mdeg s^{-1}) with 10 s updates, a 4 mdeg s^{-1} update was built into the Hour Angle register by the RAO staff. This was normally lost in the division by 100, causing a 42 millidegree jump every 10 seconds, with unsettling effects on the Hour Angle integrator.

During 1978 a system was tried whereby a computer supplied co-ordinates to the APP directly instead of via paper tape. This was later abandoned in favour of direct computer control mainly because of the age (about 15 years) and thus questionable reliability of the APP.

2.3. The computer system

The computers used at RAO since 1975 are Hewlett-Packard (HP) 21MX M-series. Duplicate systems were originally acquired for back-up purposes and this philosophy has been carried through whenever possible with later additions. Only the configuration used on-line to the telescope until 1980 will be described here. The configuration is summarized in Table 2.1.

Table 2.1. On-line computer configuration. The configuration of the RAO on-line computer (in 1980). The numbers are the octal I/O address in the case of peripherals, and channel numbers for the DIO.

Computer configuration:
Hewlett-Packard 21MX M-series
32 Kwords semiconductor memory with battery backup
Dual Channel Port Controller for Direct Memory Access
Memory Protect

Peripherals:

10 Time base generator	11 HP 7906 20 MB cartridge disc.
12 Digital I/O	13 Autocorrelation spectrometer
14,15 Magnetic Tape	16 TI Silent 700 printer terminal
17 HP 2620 visual display unit	20 HP A3-size Flatbed Plotter

Digital I/O Channels:

In	Out
1–3 Hour Angle Position	1 Servo System, DVM Reset
Declination Position	2 Digital to Analogue Converter
4–6 Digital Voltmeter 1	3 Noise Tubes
Digital Voltmeter 2	

There are two factors which determine the effectiveness of the computer in the observatory. The first is the way in which it is interfaced to the telescope, and the second is the degree of usefulness or usability of the supporting software available. The latter is directly linked to the type of mass storage used.

The telescope interface to the computer evolved from a 16-bit (4 decimal digit) digital voltmeter (DVM) interface and an 8-bit (one character) APP interface into a digital multiplexor with 14 x 16-bit input channels and 13 x 12-bit output channels. This device is known as the digital input/output module (DIO).

The software evolved slowly from a paper tape based system (actually using digital cassettes in the Texas Instruments Silent 700 terminals) through a magnetic tape based system until finally a magnetic disc drive was acquired in mid-1979. With this came RTE-II, a multi-user, multi-programming operating system, which, with its accompanying utility programs, considerably eased the development cycle for programs, as well as providing a more suitable execution environment. By this time most of the necessary signals could be exchanged with the telescope via the DIO.

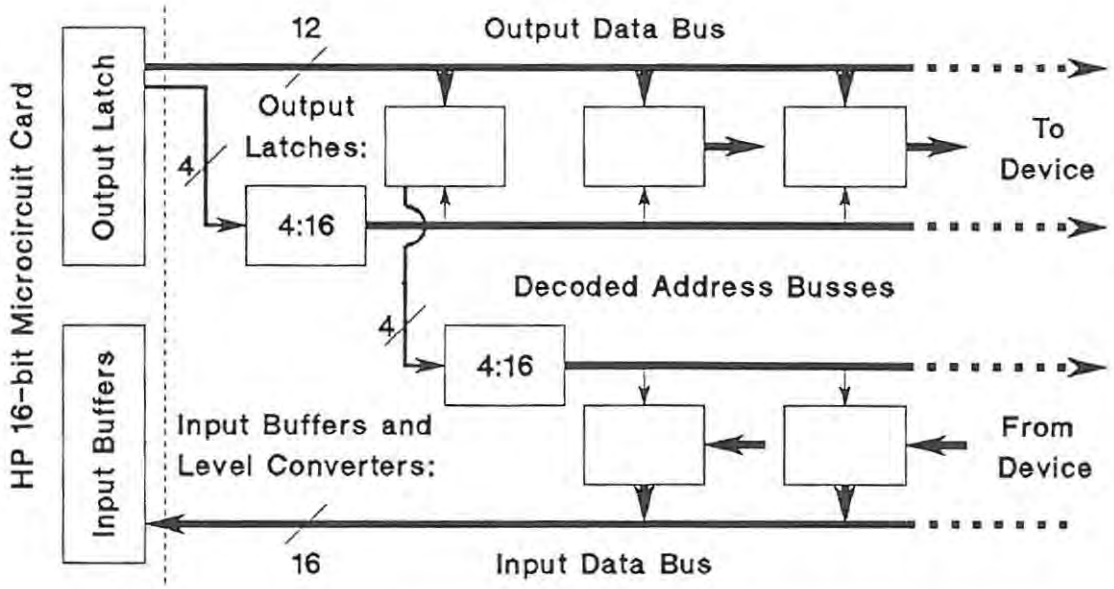

Figure 2.4. The Digital I/O Module schematic. Input and output address decoders and data buffers are shown. The address of the selected input channel is held in output latch 0.

Support software was written to enable programs running under RTE to access the telescope via the DIO. A function common to most observing programs is control of the antenna. The interprogram communication facilities of RTE allowed a separate program to be written to perform this function, both to simplify the special purpose observing programs, and to safeguard the antenna against incorrect programs.

2.3.1. The Digital I/O

The need for the DIO arose out of the large number of bits which had to be read by the computer (e.g. 24 for each antenna angle) and the restricted number of interfaces which could be physically accommodated by the computer chassis. Its purpose was thus to multiplex the required data signals so that they could be transferred via a single standard HP 16-bit bi-directional parallel interface card. It also provided a convenient place to convert from the diverse logic levels used by the telescope hardware (mostly 0 V and -12 V) to the TTL levels (0 V and 5 V) used by the computer interface.

A schematic diagram of the DIO logic is shown in Figure 2.4. The output word from the interface card was arranged so that the four most-significant bits (15 - 12) were used to specify an output channel address, and the remaining 12 bits were latched in the DIO as data for that channel.

When DIO output channel zero is specified, the data is interpreted as the address of an input channel. Of the 12 bits, the four most significant are used as the input address, i.e. bits 11 - 8. A full 16-bit word of data is then applied by that channel to the interface card input side, and this may be read by the computer.

The DIO was designed and constructed by RAO staff.

2.3.2. The Operating System

Real Time Executive (RTE) II is Hewlett-Packard's operating system for small memory 21MX computers. Briefly, it performs the following functions: Allows several programs to share the central processor time on a priority basis (Scheduling). Allows several programs to share time in two areas of main memory, the unsuccessful candidates for each area being stored on disc (foreground and background swapping). Allows programs to interact in a disciplined way. Presents programs with a clean (but unfortunately not device independent) interface to I/O devices. Executes operator commands for controlling programs.

Along with the operating system are supplied several programs which aid user program development. Most important is the File Manager/Batch Monitor called FMGR, which is more an extension to RTE than a separate program. On the one hand, it allows the disc to be divided up into named files for the storage of data sets, and on the other extends the RTE operator commands and allows sequences of commands to be stored in and executed directly from disc files, very useful for often used procedures. Other programs are an editor for creating and updating text files (e.g. program source) and compilers and a linking loader for translating source code into executable machine code.

The particular aspects of interest are I/O device drivers, as one had to be written to support the DIO, and the methods of interprogram communication, because these determined the overall structure of the suite of programs written to control the telescope.

2.3.2.1. The DIO driver

An I/O device driver is an Assembler program segment which is incorporated into the operating system. It interprets the standard I/O request parameters from I/O calls in user programs wishing to use the device under its control, and causes the device to perform the requested actions. At this level

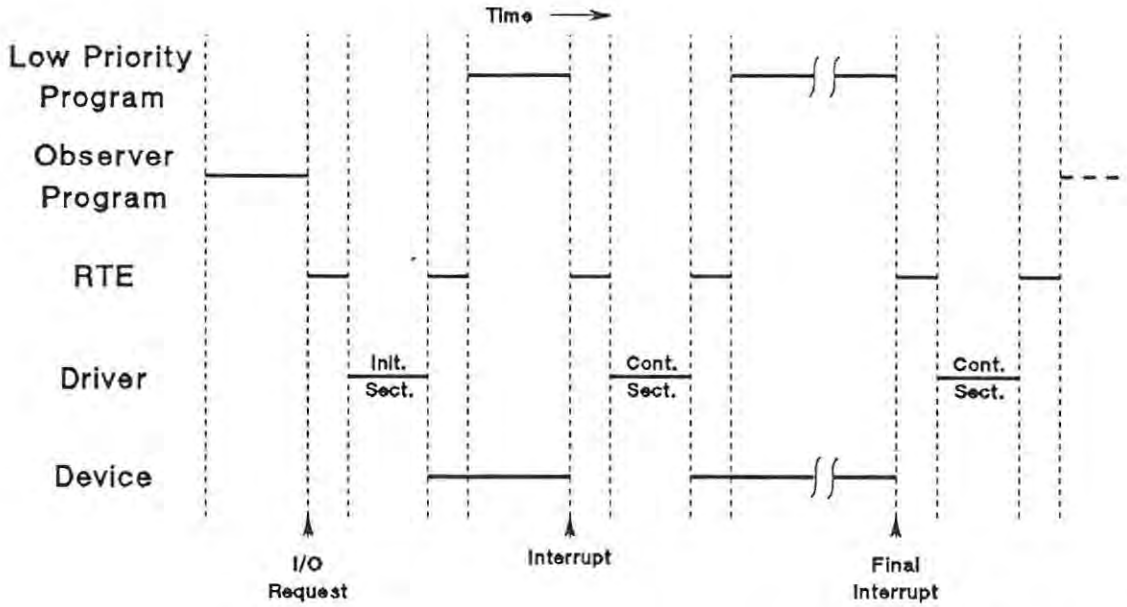

Figure 2.5. RTE device driver timing. The solid lines indicate program or device activity. Note that there is normally no concurrency of device activity with the program which made the I/O request (the observer program). The combination of program activity lines represents the CPU execution path. RTE always performs pre- and post-processing for the driver.

data transfer is performed by the record, e.g. a line of characters constitutes a record for a terminal. An important part of a driver's function is to hide the physical method of transfer from the user program. Transfer usually occurs word by word or character by character under interrupt, but this is handled by the driver, thus freeing the user program from any critical timing constraints or parallelism.

The driver consists of two parts called the initialization section and the continuation section. (A schematic diagram of the processor execution path during a hypothetical I/O operation is shown in Figure 2.5). The initialization section interprets the request parameters and starts the device operation. It then returns control to RTE which places the calling program in a suspended state and schedules any other program which might be ready to execute. When the device has completed the initial operation, it causes an interrupt which is recognized by RTE, and control is passed to the continuation section of the driver for the appropriate action to be taken. If more data is to be transferred, the driver will exit normally through RTE and await the next interrupt, which will be handled in the same way. When the driver recognises that the interrupt it is currently servicing will be

the last, it informs RTE on exit. RTE then places the calling program in the ready state once more, where it will be scheduled for execution according to its priority.

Two further points on driver operation are worth noting. The driver is only informed when entered from RTE of the physical address of the device. This means that all I/O instructions in the driver have to be overwritten immediately before they are executed (i.e. the code is self-modifying) as they each contain the physical address of the device on which they operate. This also determines the address in memory of the area where the parameters describing the device and its current operation are stored, known as the Equipment Table (EQT) entry. Because of the memory addressing scheme used by the 21MX, the operating system has to spend some time calculating the addresses of these parameters and storing them in a region of memory accessible to the driver prior to its entry, even into the continuation section, making the interrupt response time rather long. The advantages of this scheme are that only one driver is needed to service several devices of one type.

The second point is that one device can only transfer one record at a time. This is ensured by the operating system, which queues requests for a device that is busy on its EQT entry, even if accessed through a different logical unit number. This is done with devices such as a magnetic tape drive in mind. Four drives may be attached to one controller, and each drive treated as a different logical unit. However, the controller is occupied when any unit is busy, thus the queue of I/O requests must wait on the controller, which has only one EQT entry.

In writing the DIO driver, a general purpose approach was taken to the diverse categories of information to be passed through it. Data are written to or read from a contiguous set of channels with one I/O call. This was done primarily because the final configuration of the channels had not been decided upon when the driver was written, and updating a driver every time a change was made to the hardware was considered a greater complication than writing a user program to cater for the specific needs of each new configuration. Drivers are particularly difficult to update because installing a new version involves generating a new operating system (3 to 4 hours) and because it is very difficult to trap programming faults, as the driver operates in a privileged mode with none of the normal diagnostic facilities available.

Table 2.2. DIO driver function codes. The driver performs the following functions according to the request code and mode bits of the EXEC call. The channel numbers are passed to the driver as auxiliary parameters.

DIO driver functions:

Request Code	Mode Bit	Action
1	1	Read indicated channels as binary
1	0	Read indicated channels as BCD and convert to ASCII
2	1	Write data as binary to indicated channels
2	0	Convert data from ASCII to BCD and write to indicated channels

However, two specific problems were tackled in the driver. It was known that a lot of the information would be in a binary coded decimal format (BCD), so provision was made for converting BCD to ASCII on input and vice versa on output. The intention was that the normal FORTRAN I/O routines (contained in a program module known as the formatter) could then be used to convert ASCII to binary, as with other I/O devices. See Table 2.2 for the transfer modes supported.

The other problem for which specific provision had to be made was that of interrupts. RTE sees all the instruments connected through the DIO as a single physical device. For some of the instruments the data is always available (e.g. the angle readouts), but for others an interrupt signals that the data is valid (e.g. the DVM). However, it will be recalled from the preceding discussion of driver operation, that a device that is awaiting an interrupt is flagged as busy, and is prevented by the system from performing any operation in the interim. This would imply, for example, that during the DVM integration period (up to 1 s), any program trying to read the antenna position would be suspended awaiting the DVM interrupt. This sort of interaction is most undesirable.

The solution adopted was to create a fictitious DIO with a physical address higher than any real device, exactly 10_8 higher than the true address. The driver checks whether the device address passed to it is too high to be real, and if so, subtracts 10_8 from it and does the requested transfer immediately. If the device address does correspond to a real device, it is used unaltered, and the transfer is delayed until an interrupt is received. Because the system knows these as two different devices, it does not prevent an immediate transfer when an interrupt is pending.

Perhaps a better solution from a user programmer's point of view would have been to code the immediate response transfers as privileged subroutines. Like drivers, these operate in a privileged hardware mode with interrupts disabled, and are thus permitted to perform the necessary I/O. A separate subroutine could be written for each instrument to be serviced and the necessary code conversion (e.g. BCD to binary) performed in the subroutine. A driver could then be written to support only those instruments which actually require interrupts, and likewise give more complete support to these. As stated previously, this was not done because the final configuration of the multiplexor had not been settled, and the general purpose approach offered more flexibility and a shorter development time. By now, many programs have been written which use the driver in its present form, so change is unlikely in spite of the awkwardness of the arrangement.

One of the chief problems is that which Gray code was designed to overcome, namely values changing while being read. To illustrate, consider a BCD digit changing from 7 (0111_2) to 8 (1000_2). Depending on the underlying logic, the 8 bit might be set slightly before or slightly after the other three are cleared (e.g. in the case of a ripple carry counter, it would be slightly after). The first case would yield an embarrassing 15 and the second, an equally incorrect, but legal, zero, should the value be sampled at the crucial moment. The argument can be extended to a group of digits changing from 0999 to 1000.

The driver attempts to overcome this problem by reading each channel twice in quick succession, and only accepting a value obtained both times. A possible problem here is that the reads are too quick, as, especially where logic level conversion is involved (see 2.3.1), the signals from many instruments change slowly, so an error situation could extend over both readings. A more serious problem is that most instrument readings extend over more than 16 bits and thus two DIO channels. The driver does not have the knowledge of this relationship between channels, and thus cannot perform a consistency check.

It is the occurrence of this error within a single digit which causes the most trouble, however. As stated previously, the intention was for the driver to produce ASCII coded numbers, and the FORTRAN formatter be used to convert these to binary. However the illegal BCD digit 15 in the above example appropriately becomes an ASCII '?', and, occurring in the middle of a number

supplied to the formatter, causes the calling program to be aborted. Thus most programs laboriously and inefficiently perform the ASCII to binary conversion in FORTRAN, instead of using the Assembly coded formatter.

The ambiguous number problem only occurs on input. On output the main problem experienced so far occurs when control bits for diverse functions have been packed into the same output channel. Different functions are controlled by different programs and these must co-operate to ensure that they do not interfere. Again not an insuperable problem, but one which leads to clumsiness in user programs and lack of security in the system. A privileged subroutine would present a more elegant solution here, too.

There are also possible hardware solutions to each of these problems. In the case of the interfering outputs, the hardware could be constructed so that two bits are used to control each function, and that, if both bits are zero no change in the state of the function occurs. This is simply implemented with J-K flip flops. This solution has presumably been avoided by the DIO implementor because of a shortage of channels, or different functions would not have been packed into one word in the first place, and then perhaps this would be an unwarranted extravagance.

The hardware solution to the ambiguous input problem is not so simple, but relies on the fact that there is a quiescent time for each instrument during which the outputs are both stable and correct. In particular, the angle readouts may be latched at the Gray code stage, and the DVM data always change on the active edge of a master clock, so that the data are stable over the remainder of the cycle. The data could be latched into the DIO during these periods.

2.3.2.2. Program communication primitives

The most fundamental way in which data may be shared among programs running under RTE is via common blocks. These are contiguous sections of memory which may be referenced from any program. By itself, this is not a viable communications method, as there is no efficient means to prevent two programs from updating the same variable at the same time, thus destroying one or the other's result.

To facilitate program synchronization, RTE supports entities called resource numbers. They allow not only memory, but also peripherals, or indeed any other resource, to be shared by cooperating programs in a consistent fashion. Special system calls are available to perform uninterruptable 'lock' and 'unlock' operations on resource numbers. In operation, a resource number is obtained from the system and made available (perhaps through a common block) to all programs that need to access the associated resource. It should be noted that the association between resource number and resource is defined only by the programs which use them — the operating system is ignorant of the resource. In the case where a resource is a group of common variables, any program wishing to update the variables first locks the associated resource number. If the resource number is already locked, the program will be blocked by the system, until the resource number is unlocked. This provides a simple and efficient solution to the mutual exclusion problem. In this context, a resource number may be viewed as a binary semaphore.

The second communication method available under RTE is a buffered message passing system, which is implemented as a variation on input/output (I/O). If a program requests standard I/O through RTE, it is blocked until the operation has been performed. To allow concurrent I/O and computation to proceed within a single program, Class I/O is used. In this method, a program issues an I/O request associated with a Class number. The associated data and other parameters are copied into a buffer in system memory, and control is immediately returned to the calling program. When there is no more processing to be done by the calling program, a special Class Get call is issued to the system with the same Class number, which returns the result of the I/O operation.

The usefulness of this facility for interprogram communication relies on the fact that the I/O call and the Get call need not necessarily originate from the same program, as long as they use the same Class number. Another useful factor is that a nonexistent device may be nominated in the I/O call, causing the data to be immediately queued awaiting the Get call, thus removing the inevitable delay necessary if a real device was involved. It is the existence of the queue which gives this method its advantage in some cases over the resource number method. The program generating the messages may proceed unhindered by the speed at which the receiving program can process them. As with the resource

number, the Class number must be obtained from the system before it is used, and passed to other programs that need to use it.

A special case of interprogram communication exists when one program starts another (dormant) program running. These programs then have a 'father and son' relationship. The father may terminate the son's execution or wait for the son's voluntary termination, and data may be passed between them by a special string passage system call.

2.3.3. The COMND Antenna Control Program

As may be inferred from the sections describing the DIO (2.3.1) and its driver (2.3.2.1) the interface to the telescope, while functional, is far from friendly toward user programs. An attempt was therefore made to determine those functions that would be required by user observing programs, and to implement them as separate programs with friendly interfaces. One such program is the COMND antenna control program.

The first decision to be taken on the form of the program was the nature of its input and output. For input it was decided to use the Class I/O message system, as the buffering provided by this means would free observing programs from the constraint of having to generate commands in real time. This decision was admittedly biased in favour of the planned mapping system: no other programs with critical timing have yet been developed, and the buffering has proved an unnecessary complication with the more interactive programs, which do not know in advance where they are to drive. The output choice was between direct computer control of the servo system, or to route the control via the APP. Although the APP had performed faithfully for so many years, spares were running low (Germanium switching transistors are not easy to obtain these days), and direct control was decided upon. The RAO staff made the necessary additions to the DIO – a two channel digital to analogue converter (DAC) and the necessary signals for control of high/low speed, integrator reset and brakes for each axis. Later additions were sign and magnitude bits from the tachometers, as measuring antenna speed by differencing the readouts proved to be a problem. A major concern throughout the process of computerising the antenna control was the safety of the antenna itself. To safeguard against the computer program crashing and leaving a large error voltage on the DACs, a watchdog timer was

placed in the interface, which applies the integrator reset and later the brakes if the computer fails to address the readouts for more than one second.

2.3.3.1. The Command Message

The next step in the design phase was to decide on an input message format which would allow all the necessary commands to be coded. At first a very wide range of commands was considered, centred chiefly on flexible methods of co-ordinate specification. This was inspired by a description of the control program for the 100 m telescope of the MPIR at Bonn (Stumpf and Schraml, 1974). However, the limited time available for developing the system soon enforced a measure of practicality. The COMND control system and an observing program were developed in about 4 weeks at Hartebeesthoek.

The two user programs to be supported initially were the variable source program and the mapping program. Variable source observations consist of doing drift scans across the sources to be measured, i.e. the telescope is driven ahead (West) of the source and stopped, and the source allowed to drift through the beam. This procedure is then repeated for each source. The requirement for the control program is thus to be able to drive to a given Right Ascension (RA), and stop the telescope, in the shortest possible time. The requirements of the Rhodes mapping program were not then well defined, of course, but it was known to require scanning at constant speed and would probably need close control over the Hour Angle (HA), although scanning in RA and/or Dec. All of these requirements are fairly low level, and thus put an end to ambitious ideas of co-ordinate transforms. Such transforms are not necessary largely because of the Equatorial mount, which provides meaningful co-ordinates at the hardware level. The Altitude/Azimuth mount used at Bonn requires a fairly sophisticated control just for tracking.

The command capabilities and thus the message format were directly linked to the requirements discussed above. The message contents are as follows: (i) Longitude-like co-ordinate, Latitude-like co-ordinate and co-ordinate type. The types are restricted to the Equatorial system: uncorrected telescope HA and Dec; HA and Dec corrected for telescope pointing; RA and Dec of date; and RA and Dec of epoch 1950.0. (ii) An optional time at which the effectiveness of this command should cease, and the next command message be fetched. If this is omitted, the message is given a maximum

period of validity of one hour, and the next message is implemented as soon as it is received. (iii) A scan flag for each co-ordinate. If this flag is not set, the antenna is driven to the required co-ordinate as quickly as possible. If it is set, the antenna is programmed to scan at constant velocity from the previous command value for that co-ordinate to the new one, the speed being calculated so that the new co-ordinate is reached at the command end time specified in paragraph (ii). (iv) A stop flag for each axis. The particular axis is stopped when the corresponding requested co-ordinate is reached. This was included specifically with the idea of stopping the Hour Angle axis for a drift scan when the required Right Ascension is reached, instead of continuing to track. (v) A wake flag. This is in fact a Resource number, which is unlocked once the antenna has reached the command position. It is assumed that the observing program has locked the Resource number before transmitting the message, and attempted to lock it a second time after transmitting the message, and thus is being suspended until it is unlocked.

The last three parameters may be omitted from the message as transmitted, and are automatically set to zero (false) by COMND. Unfortunately 0.0 is a legal time (midnight), so if the end time is to be omitted, it must be specifically set to -1.0

2.3.3.2. Program Structure

A problem was encountered immediately on considering the implementation of COMND: lack of memory space. It was decided that the error voltages should be updated every 100 ms, as the APP had done. This response time could only be achieved by making the program permanently memory resident. However, of the 32 Kword of memory in the computer, the operating system occupied 17 Kword and 12 Kword had to be left open for the compilers to be run from the disc, leaving a scant 3 Kword for permanently resident programs. This immediately frustrated any plans for using the FORTRAN I/O routines to convert data from the DIO (see 2.3.2.1) as these alone occupy 3.5 Kword.

The program divided very neatly into two: an APP emulator program called STEER, which performs the feedback function for the antenna and interpolates between two successive command positions; and the command message processor program called COMND which receives the messages and processes the co-ordinates to the point where STEER can deal with them. This also solved the concurrency problem: how to wait for a command message and at the same time service the antenna.

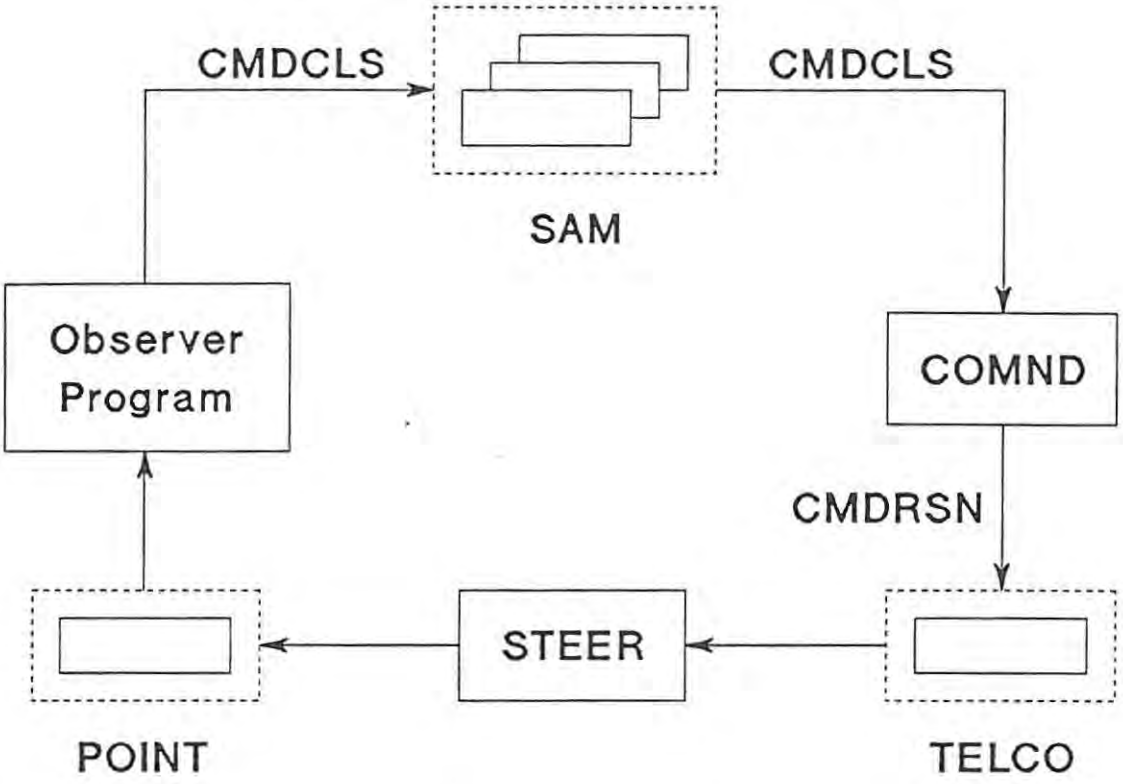

Figure 2.6. Data flow in the COMND system. Command messages from the Observer Program are associated with Class number CMDCLS and buffered by RTE in System Available Memory (SAM). These are fetched as needed by COMND, interpreted and passed to STEER through common block TELCO under control of Resource number CMDRSN. STEER keeps all telescope position information in common block POINT, which may be read, but not altered, by the Observer Program.

COMND spends most of its time blocked, either waiting for a new command message or waiting for STEER to complete the previous one, while STEER is run every 100 ms to update the antenna command position and error voltage. COMND thus shares the background swapping area of memory with other disc resident programs. COMND and STEER communicate through a named common block called TELCO, controlled by a resource number.

A summary of the programs and data movement are shown in Figure 2.6. The programs function as follows: COMND performs a GET call to receive a message. When a message arrives, it is checked for validity and converted into a parabolic trajectory in uncorrected telescope HA and Dec co-ordinates, which STEER can then follow. If the previous command did not specify an end time, the new co-ordinates are moved into TELCO, together with a break-in flag which causes STEER to abandon the old set of coefficients and switch immediately to the new. Otherwise COMND attempts

to lock the resource number which controls TELCO, and is thus suspended if there is still a valid set of co-ordinates in TELCO. As soon as the lock is permitted, COMND moves the new co-ordinates into TELCO and, leaving the lock on, goes to GET a new message.

STEER actually performs the initialization functions for both itself and COMND. When first turned on, it acquires a resource number to control TELCO and a Class number for command messages to be sent, and stores them in a named common block called POINT. It then starts COMND, and if no message is immediately forthcoming, stops the antenna at its current position.

STEER must be aware of the interval at which it is automatically scheduled to execute by RTE. This is usually 100 ms, but can be altered by the operator. When it receives a command in TELCO, it calculates how many times it must run before the end time contained in the command, and performs a count down, suspending itself after each check on the antenna, so that it arrives at the co-ordinates at the specified time. Only when the count expires, or when the break-in flag is set indicating that an unscheduled change is due, does STEER look for the next command in TELCO, and unlock the associated resource number, so that STEER performs all the timing functions for COMND. This includes waking the observing program by unlocking its resource number when the error in the antenna position first drops below 25 mdeg.

2.3.3.3. Antenna Control Algorithms

STEER has the responsibility of dealing with the antenna servo system. As the integrator has been retained, no further filtering is performed on the error signal. Likewise, a suitable time constant has been incorporated in the integrator reset function, so that it may be applied at any speed to stop the antenna gently. The functions which remain for STEER to perform are: choosing the appropriate speed setting, checking for servo system malfunctions, and checking the position limits.

The decision as to what speed to use is fairly straightforward: low speed is used unless the command speed exceeds 15 mdeg s^{-1} or the error exceeds 750 mdeg, when a change is made to high speed. Suitable hysteresis is included for the change down values, so that a switch is not made if the decision is marginal. The value of the error chosen for a change from high to low speed is important, as it determines the antenna performance when driving to a point, e.g. to stop for a drift scan. If the value

is too high, a change to low speed is made too soon and a long drive in low speed remains; if too low, the antenna overshoots and a long drive back must be made in low speed.

The change-over procedure itself involves stopping the axis whose drive is to be switched from one speed to the other. For this purpose the integrator is reset, and the program waits for the speed, as indicated by the tachometer magnitude bit, to drop to a reasonable level before switching over. The tachometer is digitized to two bits only – a direction bit and a 'too fast to change speed bit' – and read through the DIO. The sign bit was used to enable STEER to apply a reverse error voltage to stop the antenna, but this was dropped in favour of a gentle reset. The magnitude bit is necessitated by the difficulty of determining the antenna speed by differencing successive position readings. With STEER running 10 times per second, and a readout resolution of 2 mdeg, a speed of 20 mdeg s^{-1} is necessary before a difference can be detected every time. This is useless in low speed. The velocity could be averaged over a longer period, but the simplest and most accurate method was to provide access to the tachometer.

Servo system consistency is checked as far as possible as follows: (i) If the speed as measured from the changing readouts exceeds the preset limits, then the tachometer speed bit must be set. Conversely, (ii) in high speed, if the tachometer speed bit is set, the readouts must be changing. (iii) If maximum error voltage is applied, and the integrator reset and brakes are off, then the tach speed bit must be set, and the antenna must be moving in a direction which will decrease the error.

These errors are only trapped if they persist for more than five seconds, to allow for inertia in the antenna and delays in the servo system. If an error is trapped, an alarm is sounded, and STEER applies the integrator resets and stops checking the angles, which causes the watch-dog timer to trip out as well.

STEER applies a set of position limits to the command angles which are slightly inside those defined by the hardware switches in the synchro system. This check is applied to the interpolated command angles every time STEER runs. If a source sets during observation, or has not yet risen by the time the observation starts, STEER will cause the antenna to wait at the nearest permissible point. The way in which this limit is implemented, by altering the interpolated command angle, results in the command

error going to zero when the antenna reaches the limit. This causes the observing program to be woken immediately, instead of waiting for the source to rise. This is at least fail-safe, as the program will continue even if the source does not rise during the time allotted for observation.

2.3.3.4. Associated Utility Programs

Several auxiliary functions are carried out by separate programs. In general these were used while debugging COMND and STEER, and later made more friendly for general use, as they supplied useful functions.

The first need felt was for a display: of the command angles, the antenna position as seen by the computer, and the command errors. These were provided by a program called MONI (for monitor), which writes these angles on the VDU. MONI has been made permanently memory resident, and can be scheduled to run every second or so to provide a continuous display. This was not entirely satisfactory, especially for debugging purposes, and another program called FULMN (for full monitor) was written which also displays the values stored in TELCO and POINT. This is not usually necessary however, and FULMN has not been made memory resident.

The second was a manual antenna driving program called MANDR. This began as a simple way of feeding messages into the system for test purposes and then had mnemonic command facilities added, to allow the antenna to be easily positioned from the computer console, replacing a similar facility available from switches on the APP.

After regenerating the system several times to change constants in STEER, these were placed in a common block, and a program called PAMCH (for parameter change) written to update them from the console. The parameters include such features as the run frequency, the speed change distances and the program waking distance.

Chapter Three: An Early Mapping System

This mapping system is described because it was the fore-runner of the computerized fast scanning program which forms the basis of this thesis. Many of the concepts upon which the latter is based were formulated from experience with this system. It therefore provides a useful introduction to the design of the computerized system. A second reason is that an interesting region of sky, including the Sco OB2 stellar association and the ρ Ophiuchus dark cloud, was observed with this method, and is discussed later. Finally, the results obtained with this system provide a basis against which the success of the fast scanning system can be measured.

For observing with this system, the telescope was scanned manually in Declination (Dec), and tracked a constant Right Ascension (RA) with the help of the APP. The data were captured on paper tape, and recorded on an analogue X–Y recorder for backup. The reduction process required that scans be taken on-source and off-source over the same Dec range and approximately the same Hour Angle (HA). A smoothed off-source scan, or an interpolated version for the particular HA, was subtracted from each on-source scan to remove most of the systematic effects. A series of drift scans (scans in RA made with the antenna stationary) were also taken across the source area. The Dec scans and drift scans were finally combined into a self-consistent map.

3.1. The Observing Environment

When this series of observations was begun in July, 1976, the antenna was controlled by the APP. This was supplied with a paper tape which allowed it to track 0^h RA and 0° Dec. Offsets were supplied through switches in the control console to allow any RA and Dec of date to be tracked, so precession and pointing corrections had to be calculated separately.

In order to observe Dec scans, a hardware modification was made to the servo system. The APP error voltage was disconnected from the servo system, and a voltage from a potentiometer fed into the output stage, after the integrator, to provide a constant speed setting much like Aided Track mode (see Figure 2.3). A toggle switch was provided to determine the polarity of the voltage, and thus the direction of scan. These changes were made in such a way that they only applied to the Dec axis, and only when in low speed drive – in high speed the control was returned to the APP.

The data were captured on paper tape, via a separate data logger. This had originally been built to record the data from a filter-bank spectral line receiver. It was modified to digitize and punch two channels every two seconds. The analogue data supplied to it were the radiometer output and the APP Dec error voltage. The latter was proportional to the deviation of the antenna position from the Dec value entered in the switches. The proportionality constant was set to 1 V deg^{-1}, and the maximum amplitude was 10 V. The centre Dec value was usually entered in the switches to allow a 20° Dec range. Neither the time nor the Hour Angle could be directly captured, but were entered in a log book, together with the RA which was set in the switches.

The observing procedure for a Dec scan consisted of entering the RA and centre Dec in the switches, after correcting for precession and pointing. The antenna was then driven off in Dec manually, using the Aided Track mode (see section 2.2.1), to the start of the scan. The antenna was then placed under control of the APP, except the Dec axis, the speed of which was controlled by the potentiometer. When the Hour Angle axis was tracking satisfactorily, the potentiometer was turned up to give the Dec axis a speed of about 25 mdeg s^{-1}. After 1° had been covered, the HA and Sidereal Time (ST) were noted and recorded in the log book. A 20° scan would take about 13 minutes, then the whole procedure would be repeated for the next scan. Scans were driven South to North or North to South so as to minimize the change in Altitude during the scan, as the atmospheric and other unwanted radiation is a function principally of Altitude. This usually meant scanning North to South in the East and South to North in the West, so that the advance in HA due to tracking during a scan could partially compensate for the change in Altitude with Dec. Thus successive scans were usually driven in the same direction, and the antenna had to be driven the full length of the scan in high speed between each observation.

Two operators were required, as apart from the antenna manipulation described above, the paper tape punch and X–Y recorder also required attention at the start and end of each scan. The operation required a fair amount of concentration, and, particularly in the early morning, a scan could easily be spoilt by the omission of one of the steps from the operating procedure. Particularly demanding was the observation of background, or off-source, scans. Here it was not the RA but HA

that was specified, so the operator had to calculate the correct RA for setting in the switches, and start the scan so that one degree later the required HA would be crossed.

3.2. The Reduction Process

There were basically two operations to be carried out on the raw data: the subtraction of the atmospheric and other background effects, and determining the correct base level for each scan.

3.2.1. Background radiation

The use of the word background requires some elaboration. Originally, the word 'background' referred to the smooth curve, which, it was intuitively felt, represented the contribution of unwanted radiation to the change in radiometer output as the antenna scanned. This was extended to 'background areas' in the sky, referring to regions which were considered sufficiently devoid of emission to enable the background to be measured there, and to 'background radiation' which produced the effect. It has been pointed out (Nicolson, private communication) that the latter term is rather misleading, as in fact the radiation responsible for the background curve is emitted by foreground objects — the atmosphere and telescope surroundings. The background of a scan may be defined as the change in antenna temperature due only to scanning, as a function of the scan co-ordinate.

As a first attempt at fitting the background, it was assumed that each scan would pass over at least three cold or non-emitting regions. These sections of a scan were picked by eye, and a second order polynominal fitted to them by the least mean squares (l.m.s.) criterion to represent the background. The resulting scans, after this background had been subtracted, soon proved to be inconsistent, however. The difficulty, apart from that of guaranteeing that there actually were three cold sections on each scan, was recognizing these sections. A different background, resulting from the observation of the same RA at a different HA could completely change the appearance of a scan.

The second attempt, which was also unsuccessful, was to model the background as a function of Zenith Angle. This approach had been successfully used at Parkes (Day, Caswell and Cooke, 1972). The relationship assumed was $B = T_{60}(\sec z - 1)$ where B is the background, z is the Zenith Angle and T_{60} is the increase in antenna temperature when scanning from $z = 0°$ to $z = 60°$. In order to

measure T_{60}, the antenna was driven toward the Horizon at constant Azimuth. Scans were taken North, South, East and West and produced values of T_{60}, ranging from about 5 K to 7 K. Constant Zenith Angle scans were taken at $z = 60°$, 50° and 40° and showed a complex structure, even at the lower Zenith Angles. It was assumed that this was due to a combination of irregular Horizon (some features up to 7° Altitude) and the variation in the position angle of the feed causing different polarizations of spillover radiation to be seen as the antenna scanned. Since modifications to the feed configuration were carried out from time to time, it was considered better to measure the background than develop a model which would probably not be utilized for very long. A trial of the simple $\sec z$ model and the first implementation of the measuring system were carried out by Jackson (1976).

The background was systematically measured as a function of HA and Dec over the whole range for which scans were observed. This was usually $\pm 60°$ HA and the Dec range of the source. Scans were taken at 5° intervals in HA across the full 120° range. Low order polynominals were fitted to these scans as a function of Dec, as a smoothing measure, to remove noise and point sources. Polynominals were then fitted to the coefficients of these Dec polynominals as a function of HA. In this way a background scan could be generated for any Hour Angle at which an on-source scan was taken.

3.2.2. Reference Levels

In order to find the correct base level for each Dec scan, drift scans had to be taken, extending from some reference point which was judged to be free of emission and thus cold, right across the source area. These, of course, do not suffer from background effects, but again separately observed drift scans have no common reference level. Drift scans were taken every two degrees in Dec across the source, and each one was repeated at least three times to ensure the absence of receiver drift or interference.

For each source area one drift scan was selected as passing through the best reference area, or coldest Dec, and its level was then set by equating this reference area to 0 K, i.e. the effect of the 3 K cosmic background radiation was ignored. All other drift scans were then tied to the reference scan. This was done by taking the difference in temperature at the respective Decs on the Dec scans. Although the relative levels of the different Dec scans are not known, these differences can be measured once the background has been subtracted. The levels of the other drift scans were then

adjusted so that the mean difference in level from the reference scan matched that found from the Dec scans. This level difference was, of course, due to changes in the source level, and thus had to be retained.

Having generated a reliable framework of drift scans, the Dec scans were tied onto them, by adding a constant to each Dec scan to yield the least mean square error at those points which could be checked against the drift scans.

3.2.3. Implementation

The data was processed interactively on a Data General Nova 2 minicomputer. This was equipped with high speed paper tape reader and punch, an intelligent VDU and dual floppy disc drives. For the purposes of interactive data reduction, the machine was expanded by the construction of a 16 Kword memory board, and interfaces for an X–Y plotter and refresh vector CRT display. BASIC was chosen as the best language for support of interactive programs, and Assembler subroutines were written to make the new devices accessible to the BASIC interpreter. Later an asynchronous communications interface was constructed and a program written for the transfer of disc files containing data to the University ICL 1900 mainframe computer.

The interactive approach was ideal for the development of the data reduction system. In no other way can so good a 'feel' for the data be obtained, and while the principles of the reduction system were still being formulated, the interactive system provided the quickest method of experimenting with new techniques. However, once the reduction process had become routine, many man hours had to be spent in front of the terminal, steering the data through successive stages of reduction. This became a serious bottleneck in the reduction process, and it was realised that a more ambitious mapping program necessitated a more automatic reduction procedure.

Useful results were obtained with this system, as shown by the Sco OB2 map (discussed in Chapter 6), but the observations dragged out over two years. With the experience gained from this system, and the much expanded on-line computing capability in the offing, attention was turned to the design of a new observing system.

Chapter Four: Skymap Design

The observations of the Sco OB2 complex (results presented in Chapter 6) had proved that the mapping program was both workable and worthwhile. It was felt that with a suitable increase in the efficiency of the mapping method, the entire Southern Celestial Hemisphere could be mapped in this manner, within a reasonable space of time. Thus what became known as the Skymap project was launched, with the objectives of providing fully automated observing and data reduction facilities, and improving on the quality of data obtained with previous mapping systems. The sources of error in the old mapping methods were thus determined as far as possible, and selected for redress. The choice of scanning pattern turned out to be a difficult decision, and the options that were considered are described in some detail.

4.1. Efficiency and Errors

The efficiency of the observing process, in terms of man hours required, could be increased simply by using the newly acquired capabilities of the computer system to provide both automated telescope control and data capture, provided that the observing program could continue for extended periods of time without interaction. This would reduce the operator requirement from two active persons to one standing by in case of emergency. This was important as the RAO staff were occupied extending the facility and members of the Rhodes group could not spend extended periods at Hartebeesthoek. Operator time was thus a scarcer resource than telescope time.

A large part of the observing time was spent on surveying background, or off-source, areas. The time taken to observe a complete background map may be calculated as follows: scans were taken at 5° intervals from –60° to +60° in HA. This gave 25 scans, each of which had to be observed 3 times to check against gross errors or mistakes, giving a total of 75 observations. The rate of observation for 20° Dec scans averaged about 3 per hour, and because observations could only be made at night, this took three nights out of a visit of about two weeks. Since the whole Southern sky was ultimately to be surveyed, it was felt that observations should be arranged so that background measurement would not cause any increase in observing time. If background areas could be observed in the same manner as

source areas, and be reduced as such, some estimate could be obtained of how suitable they were for background measurement.

One reason why so much time was spent on background measurement was the fact that the observations themselves were slow and thus usually had to be spread out over several short Rhodes visits. Any change in the telescope configuration between visits — and the system was always evolving — meant that a complete new set of backgrounds would have to be taken. An embarrassing implication, of course, is that there was no way of checking whether the backgrounds remained consistent during a visit, either.

Another wastage of telescope time was caused by the slow scans. The scans are finally sampled at 1/3 beamwidth (100 mdeg) intervals. At the scan speed of 25 mdeg s^{-1}, this represented 4 s integration time per sample from just one observation, giving an expected r.m.s. noise level of 7 mK (see section 2.1.2). By the time three good observations of each scan had been made in order to check for consistency and gross errors, the noise level on the averaged scan was about 4 mK. This was further reduced by low-pass filtering once the final map was assembled. Greater errors than this occurred in determining the base level of a scan, as may be seen from the appearance of the Sco OB2 map (section 6.4), where the residual scanning errors are still noticeable.

Assuming that the new observing procedure would enable individual scans to be more accurately tied to a reference point, there is another limitation that prevents the low noise level from being achieved. An r.m.s. noise of 10 mK is produced by faint sources unresolved by the telescope beam (Nicolson, 1970). For total integration times as great as 4 s, the telescope may thus be described as confusion limited, rather than noise limited.

Another point can be made here, relating to the method of integration and faster scanning speeds. Considering the postdetection radiometer output as a function of time rather than antenna position, Jenkins (1976) discovered that the spectrum of noise power at the radiometer output is such that the noise increases with decreasing frequency. Thus scanning slowly and using a long time constant at the radiometer output is not the best method of reducing noise. The long time constant is a simple low-pass filter, which removes only the high frequencies from the signal, and passes the lower

frequencies which contribute the most noise. Assuming that little time is wasted between scans, then scanning fast and averaging the results of several repeated observations of the same scan has the following advantages: noise is reduced equally over the whole spectrum, and the variations in radiometer output caused by scanning across sources are increased in frequency, thus moving them to a less noisy part of the spectrum.

The source of errors in determining the base levels is not easy to isolate. Consider the Sco OB2 map (section 6.4). In determining the base level of each drift scan, 150 Dec scan measurements were averaged. Further, in determining the base level of each Dec scan, 10 samples were compared with their respective drift scan values. The errors on these values should thus be far lower than the errors on individual samples in the Dec scans, yet scanning effects are so prominently visible on the map. The scans obviously do not form a consistent set, and the reason appears to be inadequate background subtraction. This may be seen by following a scan which protrudes above its neighbours at one point on the map, and noticing that in other areas it is lower than its surroundings. The mean level is correct, but the shape is not.

Interaction in the reduction process was largely a continuation of manual operations in the observing procedure. Values that were written down by the operators during observations had to be typed into the computer during the reduction process. The data punched was not tagged with any information as to the purpose of the observation or even a run number, so each scan had to be steered through the appropriate operations. These problems could easily be rectified by a computerized data capture system. A related problem was the complete inability to log drift scans, as there was no way of capturing the time information. Drift scans were thus reduced by measuring values off the chart recorder output. Even with data capture by computer, separate observing and reduction programs are required for drift scans.

The most difficult problem to overcome is that of mistakes or errors during the observation. These have to be corrected on an individual basis, and always necessitate some extra interaction. Hopefully with automated observing there is less room for mistakes, but the data can never be expected to be error free.

Table 4.1. Inefficiencies in the early system. A summary of inefficiencies or errors in the early mapping system to be corrected in the new one.

Inefficiency or Error:	**Proposed Improvement:**
operator time	automate observing procedure
telecope time on backgrounds	include backgrounds with source, restrict HA range
telescope time on long integration	scan fast
inaccurate backgrounds	measure more often
interaction during reduction	log all necessary data, cope with errors

The problems are summarized in Table 4.1. Apart from the purely implementation problems of actually driving the antenna automatically and recording sufficient housekeeping information with the data, the improved solution was envisaged as follows: Observations would be long, usually a whole night at a time, and consist of many scans taken at high speed. All scans would be made either at the same HA or over a very narrow range of HA to reduce the magnitude of the background measurement problem. The long observations would always be arranged to include an area cold enough to be used to measure the background for the observation.

The restriction that scans should be made over a small range of Hour Angle does not entirely determine the scanning pattern. Several patterns were considered.

4.2. Scanning Patterns

Because the background radiation is produced by objects surrounding the telescope the background is fixed relative to the Earth, i.e. it is a function of local co-ordinates. The most obvious method of simplifying the measurement of the background was to restrict the range of local co-ordinates over which an observation was made. By confining the antenna to a simple zero or one dimensional path for the duration of an observation, a great reduction in background measurement over the full two dimensional case may be realized. As no symmetry in Azimuth had been observed, and the antenna mount was Equatorial, Hour Angle and Declination were chosen as the most convenient set of co-ordinates. Three restricted scanning patterns were considered: with the antenna stationary, moving in one axis only, and finally moving in both axes, but repeatedly following a fixed path. They are illustrated in Figure 4.1.

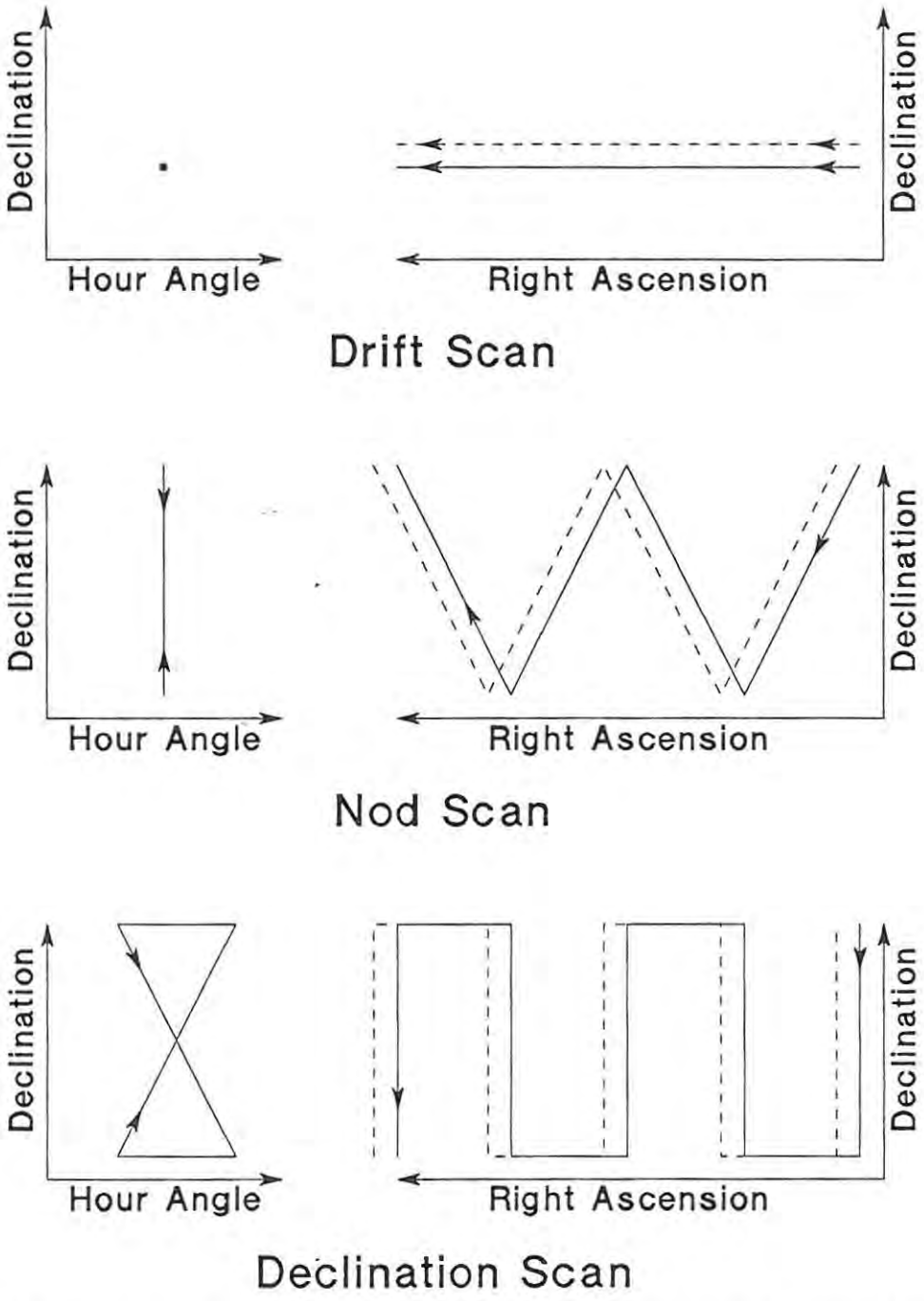

Figure 4.1. Scanning patterns. The patterns for observing using drift scans, nod scans and Dec scans are shown both as antenna movement in HA, Dec, and as the resulting pattern traced on the sky in RA, Dec. The dashed lines show the next observation in a fully sampled series.

4.2.1. Drift Scans

Although this method could be ruled out on the grounds of inefficient use of telescope time, it was given due consideration as the simplest method of scanning.

As the antenna is not moved at all, the contribution of background radiation is constant. The data reduction problem thus becomes one of relating adjacent, parallel scans in Right Ascension to a common reference point. This can only be achieved by measuring the change in source temperature with Declination at some particular RA, which necessitates scanning and thus introduces background problems, or extending each scan to an area of high Galactic Latitude where it might be assumed that there are no large scale sources. This method is particularly susceptible to receiver drift as there can be almost no check on receiver level over periods of hours while the source is drifting through.

The inefficiency may be calculated thus: as shown in section 4.1. above, the longest useful integration time for a single sample is 4 s. For longer integrations the fluctuations on the record are predominantly due to unresolved sources rather than receiver noise. The FWHP beam is at least 72 s (of time) in Right Ascension (at the Celestial Equator). Assuming that we oversample by taking three samples per beamwidth, this gives 24 s integration per sample, a factor of six too long. From the equation for ΔT given in section 2.1.2, this yields an r.m.s. contribution of 3 mK to the output noise from the receiver, compared to 10 mK from confused sources. It must be stressed that the only method of verifying an observation is to repeat it, and if there is disagreement, to repeat it yet again. Using drift scans, this would imply at least a factor of twelve wastage of telescope time.

4.2.2. Nod scans

The method used by Haslam et al (1970) for 408 Mhz surveys is the next most simple pattern. The antenna remains stationary in HA at the Meridian, scanning only in Declination. This limits the background to a single constant HA line in the HA, Dec plane. The restriction that the observation be made on the Meridian falls away when using an antenna with an Equatorial mount. The background must be measured by observing an area as part of each observation which can be considered free of extended sources. The originators of this method did not have to resort to this – at 408 Mhz, the source temperatures are so high that atmospheric effects are negligible by comparison.

The problem now arises in combining repeated observations of the same source area. Each raster scan is a zig-zag on the RA, Dec plane and in order to obtain a rectangular grid of samples, interpolation between different observations is required, a fairly complex and time consuming task to perform on a computer. Advantages cited for this method were mainly to do with removal of receiver

drift, which was not considered a serious problem in this case, though in practice more drift was encountered than had been foreseen. Moreover, these advantages depend on many scan crossings occurring, which would not be the case with high speed scans over relatively narrow Dec ranges.

At the other extreme, it was felt that this method would be extremely inefficient when mapping small areas. The diagonal scans result in large ragged edges around the area being observed, which cannot be reduced properly as they have been scanned in one direction only. It was envisaged that small areas including extra-galactic sources would be frequently surveyed for calibration purposes.

4.2.3. Declination scans

This differs from the nod scan in that the antenna tracks a constant Right Ascension while scanning in Declination, returning to a fixed Hour Angle to begin each scan. The antenna thus traces two fixed paths in HA, Dec for background measurement, one for upscans (observed South to North) and one for downscans (observed North to South). In its favour, however, we have to some extent achieved the goal of allowing the observer to scan in celestial co-ordinates. In fact, with a slight extension, we can scan in 1950.0 RA and Dec, the effect of precession being to blur and slightly lengthen the background trace in the HA, Dec plane. Provided that the starting HA is close to the meridian where the rate of change of background with HA is small, the slight change with RA of HA and thus background is small enough to be ignored.

Combining successive observations can be carried out on a scan for scan basis at each RA sampled, if computer store is at a premium. In practice, it turned out that the antenna drive was not always capable of tracking accurately enough under scan conditions to permit this simple merge.

We still have the problem of extending each observation into a region considered to be free of extended sources for background measurement, or relying on the background being constant over periods of days so that it may be measured in a subsequent observation.

4.3. Choice of scanning method

Chiefly because of past experience with Declination scans, they were chosen as the optimal scanning method. The advantages of parallel scans along lines of constant Right Ascension were thought to be: simplified combining of observations by merely interleaving scans, and no interpolation necessary to

place the data on a meaningful grid. As an extreme example of the latter, sources viewed on plots of the unprocessed scans could have their 1950.0 co-ordinates measured directly from the plot. This is very useful to confirm correct operation of the system.

The final scheme was then as follows: observations would consist of a night long series of Dec scans at a fixed starting HA. The shape of a background scan would be determined by finding the lowest temperature occurring at each Declination. This would be done separately for upscans and downscans. Once the appropriate background had been subtracted from each scan in the observation, the data would automatically be referred to the coldest point in the source area. Repeat observations could then be averaged. Because of the fixed starting HA requirement, scans from a single observation could not, except for the shortest scans, be separated by only 100 mdeg in RA as this would imply a scan time of only 24 s. The scans from observations covering different RAs would thus be interleaved to form a map.

Chapter Five: Skymap Implementation

A series of programs was written to implement the observing procedure of performing a series of Dec scans at constant HA, as derived in the previous chapter. These programs can be split neatly into three suites: the observing system for capturing the data, the reduction system for combining separate observations into maps, and finally a collection of programs to process and display entire maps.

The observing program was designed for fully automatic operation: it accepts details of the observation from the operator then proceeds without attention for the remainder of the observation. Off-line programs were also written to verify and display the data after the completion of an observation.

The suite of reduction programs are similarly designed to be as free from operator interaction as possible. The purpose of these programs is to remove all systematic errors from the data. It was originally hoped that this would be merely a matter of removing scanning effects, but inevitably receiver drift and interference contaminated a large number of observations to varying degrees and had to be dealt with. For this purpose some interaction had to be introduced, and median filtering was used as hedge against those errors which could not be easily detected by eye.

The process most often carried out on complete maps is smoothing. For this purpose a program was written to perform two dimensional (2-D) Fourier transforms, so that the filters could easily be specified in the spatial frequency domain. The chief complication here was the limited amount of computer immediate access memory available compared with the amount of data. Several types of display program were written: apart from the usual contouring, hidden line displays can also be generated, half tone reproductions made on the plotter or the line printer, and grey scale pictures on film.

5.1. The Observing System

The observing program called SKYMP was written for the RAO computer. SKYMP uses the antenna control program COMND as described in section 2.3.3. The observer's view of the system is presented, followed by some details of the program structure and implementation. Because there is

Table 5.1. Example SKYMP startup dialogue. The operator describes the source area and scan pattern, from which SKYMP calculates the antenna timing. Break times refer to the end and start of the up and down scans (in seconds). Operator responses are underlined. Note that the scan interval in RA and the scan rate have been defaulted to 0.1° and 0.250° s^{-1} respectively

```
INPUT OBS NO, LO DEC, HI DEC, RA INTVL, DEC RATE
19 297 336
PATTERN FOR OBS NO   19
LO DEC 297.000 HI DEC 336.000 DEC RATE  .250
RA INTERVAL  .100 NO OF RASTERS  8
BREAK TIMES  156.0  191.5  347.5  383.0
O.K.(1) ? 1
RASTER NO AND RA (H M S) ? 0 10 20
ADJUSTED RA  10:20:48.0 CURRENT HA  359.081 OK (1) ? 1
ARRIVED AT START
RUN        RA            UT            HA        DIRN
  1    10:20:48.0    15:11:29.8    359.176       1
  2    10:24:  0.0   15:14:41.3    359.756      -1
```

no display of data during an observation, support programs were written to provide verification and review of the captured data after an observation has been completed.

5.1.1. The Observer's view

Table 5.1 shows an example of the start-up dialogue. The source area is defined by its upper and lower Declination limits. Given these two values, the Right Ascension interval between scans and the scanning speed in Declination, a scanning pattern is defined. The RA interval between scans must be less than $^1/_2$ beamwidth for a fully sampled map. In practice $^1/_3$ beamwidth (100 mdeg) was usually used to allow subsequent smoothing of the data without loss of information. As noted in section 4.3, the constraint of a fixed starting HA for all scans means that neighbouring scans cannot be observed in succession. Scans which can be observed in the same observation are said to belong to the same raster. In this terminology, a scan is a fixed path on the sky, a run is one pass of the antenna beam over a scan and an observation is a continuous series of runs in alternate directions, covering a raster of scans.

Once the four above parameters have been defined, the system decides how many scans must be skipped between runs, i.e. which scan will next reach the starting Hour Angle after a run has been completed. Each of the intermediate scans will now be linked to a different raster. Rasters are

numbered according to the number of scans they would pass in front of 0^h RA, were they to extend across that point, i.e. raster 0 passes through 0^h, raster 1 includes the next scan, and so on. This gives an unambiguous interleaving of rasters, irrespective of the starting RA of the area of interest.

When the scan pattern has been established, the approximate start RA and a raster number complete the definition of an observation, which proceeds until manually terminated. Because of the necessity of maintaining a constant starting Hour Angle, there is no possibility of re-observing spoilt runs immediately, so no mechanism for changing position during an observation was included, and no on-line display of data. The radiometer output and AGC voltages are monitored on a chart recorder, providing sufficient information to establish the correct operation of the system.

5.1.2. Program Structure

As experienced with the COMND program, there are problems of obtaining a quick response and operating several devices in parallel. In this case the high speed response is required by the digital volt meter (DVM) measuring the radiometer output, which has to be sampled every 100 ms during high speed scans. The parallelism results from controlling the DVM and magnetic tape unit at the same time. The solution adopted was similar to that used with COMND: a small program called LOGER was written and made permanently memory resident. This program has sufficient speed of reaction to service the DVM.

SKYMP program structure is shown in Table 5.2. SKYMP begins by accepting the source parameters from the operator as defined in the section above. Once this phase is completed, there are two functions to perform: supply antenna commands to COMND, and record the radiometer data on magnetic tape.

Before each upscan run, a set of four messages is generated for COMND: (i) Scan South to North while tracking, (ii) track the start RA of the downscan, (iii) Scan North to South while tracking, and finally (iv) track the start RA of the next scan. The co-ordinates are supplied as RA and Dec, and the Universal Time (UT) is calculated so that a constant starting HA is maintained. This calculation assumes the simple relationship

$$HA = ST - RA$$

Table 5.2. The structure of program SKYMP. The parallelism is achieved by running concurrently with COMND and LOGER. Synchronisation with COMND is achieved by means of times passed in the antenna motion commands, whereas LOGER is turned on and off as needed.

```
begin
    read source description
    while observation number > 0 do
        drive to source
        repeat for each up/down scan
            generate command messages
            start LOGER
            repeat
                accept and log data messages
            until end time of upscan
            stop LOGER
            wait for start time of downscan
            start LOGER
            repeat
                accept and log data messages
            until end time of downscan
            stop LOGER
        until break flag
        read source description
    endwhile
end
```

and is thus rendered invalid if the co-ordinates are precessed in COMND before use. Although the change in precession in RA with RA for the starting Dec could easily be accommodated, thus keeping the starting HA constant, the effect of this change over the whole Dec range is not so easy to eliminate. This causes the shape of the scan on the HA, Dec plane to be a function of RA, thus if the background is very sensitive to changes in HA, RA of date must be used.

After these messages have been sent, SKYMP is free to concentrate on logging the data. When the scan is due to start, SKYMP turns LOGER on. LOGER immediately starts the DVM and each time it interrupts, the DVM reading together with those of the antenna position readouts and the computer time (expected to be UT) are decoded and transmitted by means of a Class message. These messages are received by SKYMP, and when sufficient samples have been collected (usually 40) or the end of the run is reached, SKYMP converts the data to ASCII and writes them to tape. When the end of run is reached, as determined from the time contained in a message, LOGER is turned off, and SKYMP prepares for the start of the next run. At the end of each downscan run, a check is made on the state of the break flag, which can be set by an operator command from the RTE console. When

the flag is set, the observation is terminated, a file mark is written to the magnetic tape, and SKYMP requests a new source description. If none is forthcoming, another file mark is written to tape, and SKYMP becomes dormant.

The method of passing messages from LOGER to SKYMP via Class messages is the only way that SKYMP can be freed from the critical timing constraints of servicing the DVM, but the sheer volume of data generated can cause problems. Messages are buffered in System Available Memory (SAM), which is allocated at RTE system generation time, and which is used to various purposes by RTE, apart from message buffering. Any other buffering scheme between SKYMP and LOGER would require dedicated memory. Only about 1.5 Kwords are available for SAM, and in practice, SKYMP can be inactive for 5 s to 7 s before SAM becomes clogged with messages from LOGER. If this happens, the whole system can become deadlocked, and SKYMP and LOGER have to be aborted. Even then, there is no way of destroying the now unwanted messages, and a special program, EATER, was written for this purpose. On occasion, I/O operations are blocked by the memory jam, and the operator commands necessary to abort SKYMP and LOGER, and run EATER, cannot be entered. The entire RTE system then has to be rebootstrapped from the disc, and usually SKYMP has to be recompiled. Because of these drastic results if SKYMP is pre-empted from execution for relatively short periods of time, other programs which compete for the same memory area are not usually run during observing sessions. Fortunately COMND operates between SKYMP runs, when LOGER is dormant.

5.1.3. Support Programs

There is no need for display of data during an observation, but there definitely is a need for verification of the data as logged on magnetic tape while the observer is still at the Observatory. To this end a suite of programs was written for the RAO computer for processing and displaying the data from magnetic tape.

The first program, called BINTD (for bin to disc), reads an observation from magnetic tape and writes the data to a random access disc file. To reduce the amount of data involved, the RAs of the individual samples are ignored, all assumed to have been taken at the nominal RA of the scan. Also, adjacent readings are averaged over equally spaced intervals of Dec (binned). This program serves a

purpose by merely proving that the data are readable, and presents the data in a useful format for further processing. The advantage of placing the data in a random access disc file is that any run may be selected at will for closer examination.

The next program, called BACOF, performs rough background subtraction. Up to 20 runs may be nominated as covering a background area. These are averaged and then smoothed by fitting a low order least mean squares polynominal. This smooth curve is then subtracted from all the scans in the input file and the results are written to a new file, together with a synthesized run in the shape of the fitted curve. Two further programs were written by J.L. Jonas of the Rhodes group. They provide for one dimensional smoothing of a file of scans, and display of a set of adjacent runs as a hidden line map on the plotter. Thus the observer may be assured of the validity and quality of his data before returning it to Rhodes for a more rigorous reduction process.

5.2. The Reduction System

If all the observations were perfect, then the reduction process would be as simple as that described in section 5.1.3 above for displaying scans on the RAO computer. Once the data had been converted to a format readable by the ICL computer, it would be simply a matter of constructing background scans and subtracting them from all the data in their respective observations, and then averaging observations of the same raster or interleaving those of separate rasters to form a map. But, of course, error free data can never be obtained.

A general defensive policy against errors was used in all the reduction programs. The rationale was that there would be far too much data for all observations to be individually examined by eye for errors, let alone have the errors edited out. Thus the programs have to treat each datum with suspicion. This is done at a gross level by checking each value against its own maximum and minimum possible values before use. On a finer level, use was made of the fact that it was intended to cover each raster with at least three separate observations, thus a reliable value for any sample could most likely be obtained by taking the median of the three readings, as any single reading in error would be rejected by this process. The obvious advantage of the median over the mean for combining readings in this case, is that it is not affected by the magnitude of the readings in error, but only by their number. For this reason medians were used wherever possible as part of the defensive policy. The

first specific problem to be dealt with was receiver drift. Problems were experienced with the cone airconditioning unit during the first few observations taken with the SKYMP system. Although these were soon cured, other problems arose to achieve the same effect, and the net result was a series of observations of which many were contaminated by drift. This neatly countered the proposed strategy for finding the background as the lowest sample taken at each Dec, as the low points on the affected observations were now determined more by drift than source temperatures. Even if complete runs could be nominated as being on cold background areas as with the reviewing system, subtracting them from the remaining runs in the observation would yield incorrect reference levels.

Drift is here considered as a very slow change in receiver output level. It is slow enough to leave data from individual runs intact, but destroys the information defining their levels relative to a reference point. The drift and scanning or background effects are thus orthogonal, and may largely be treated separately. In order to restore the correct levels, the uncorrupted observations or parts of observations must be specified by the observer, and used to set the levels of those observations which have been adversely affected. This process is complicated by the fact that it must be performed before the background is removed, and thus when runs from different observations are not directly comparable, owing to being superimposed on differing backgrounds. This means that separate estimates of the levels have to be obtained for each Declination at which samples were taken, as the background is an undefined function of Dec. This is in effect synthesizing a drift scan, by nature free from background effects, at each Dec covered by the observations. A helpful point is that, because the drift varies so slowly, the data may be heavily smoothed before the level comparisons are made, and the undersampling in RA of a single observation, caused by the wide spacing of successive runs, is not relevant. The number of samples necessary to represent the smoothed data is, by Nyquist's Theorem, much less than the original number of samples taken.

A lesser problem was the inability of the HA axis to track a constant RA consistently under scan conditions. More precisely, the time constant in the servo system was so long that a run was usually well under way before the drive settled down to a constant velocity. This could have been overcome simply by spending longer intervals between runs, tracking the RA of the run about to commence, but the reduced efficiency was considered too high a price to pay. The result of this problem was to

complicate the process of combining observations into maps, as many observations could now wander across a single column of constant RA in the final matrix. It is still assumed however, for the purposes of background determination, that all runs of a given observation follow the same path in the HA, Dec plane, albeit not the simple straight line originally planned.

The stages of processing are thus as follows: reformatting the data to ICL standards; removing the effects of receiver drift; determining and removing the background; and combining separate observations.

An implementation problem experienced throughout the processing, particularly with drift removal, was the small amount of memory available to user programs on the Rhodes ICL computer, usually only 20 Kwords if the program was to be run under routine conditions and have access to magnetic tapes and large disc files. To partly offset this problem two ICL packages, known as Find and Sort, are available for manipulating data stored in standard ICL record format on disc files. They perform the function of selection and sorting respectively, so that only that data required by a program may be presented to it, and then in the optimum order to match the structure of the program. These utility packages require key values to be stored in each data record, and on the basis of these values they perform their selection and sorting functions.

5.2.1. Medians and Binning

Two processes which are carried out at various stages of processing are binning the data in equally spaced slots by averaging, and median filtering. They are thus examined here in greater detail.

Binning is used where a function has been heavily oversampled, but at irregular intervals. This is particularly the case with the radiometer output, which is sampled approximately every 25 mdeg compared with the antenna beamwidth of 300 mdeg, but the DVM taking the samples is not in any way synchronised with the antenna position. Binning, a process of averaging all samples taken within each slot, provides a simple method of placing the data on a regular grid.

The process is illustrated schematically in Figure 5.1. It may be regarded as convolution of the irregularly spaced time series with a top hat function of the bin width, followed by a multiplication by a III (the shah function, Bracewell, 1965) which represents the sampling operation. The sample

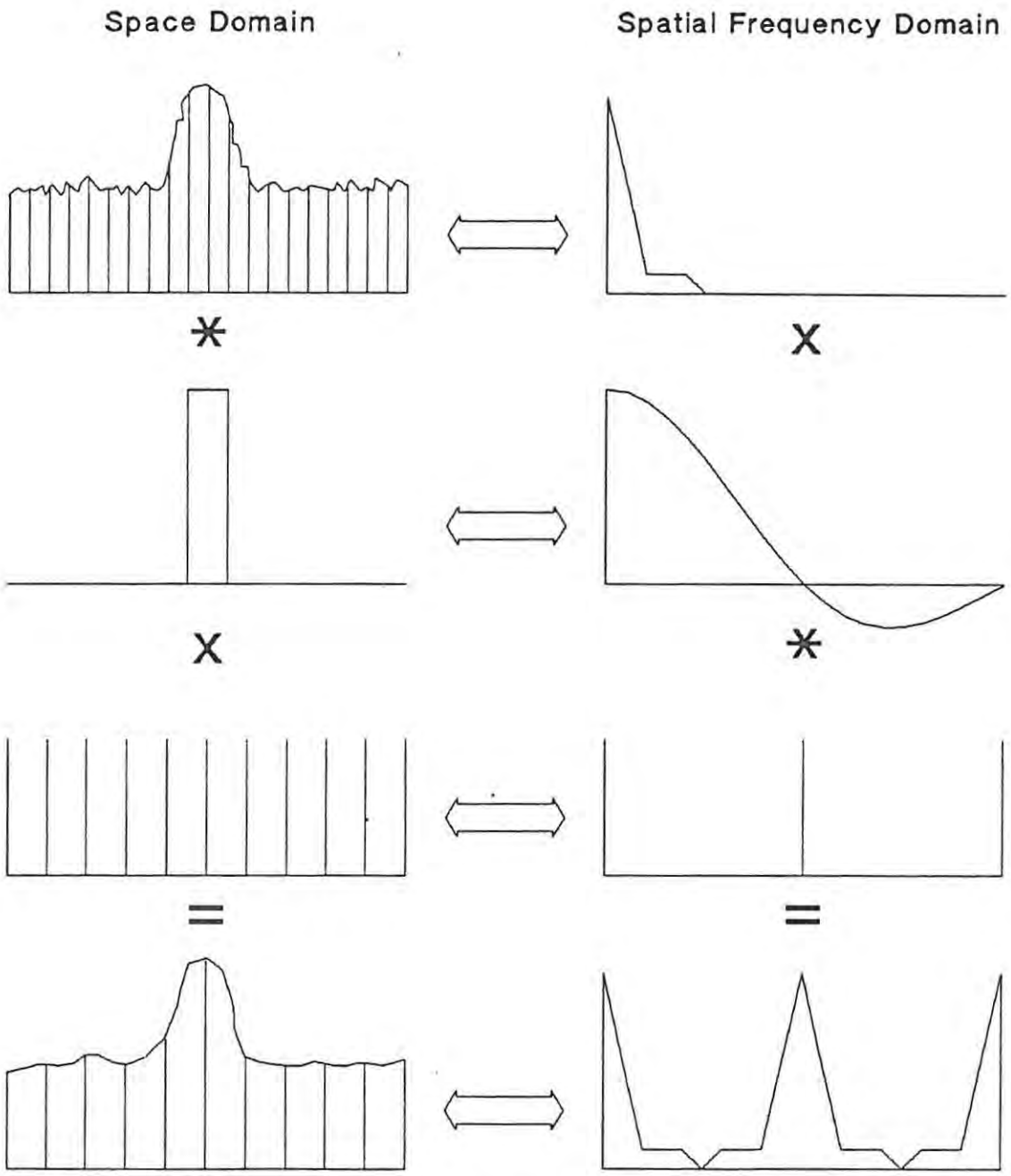

Figure 5.1. The binning operation. The binning operation, in which adjacent samples are averaged, is shown schematically in the space and spatial frequency domain. The original oversampled data with samples not necessarily equally spaced is represented by the top figures. In the frequency domain the triangle peaking at DC represents information gathered by the beam, and the plateau to the right is white noise generated by the receiver. This is then convolved (*) with a top-hat function equal in width to the desired final sampling rate. In the frequency domain this corresponds to a multiplication (x) by the sinc function. Resampling is represented as multiplication by III (Bracewell's shah function) with spacing equal to the width of the top-hat. In the frequency domain this corresponds to convolution by III with reciprocal spacing, producing the familiar replication of the original spectrum. Note that in this case the averaging operation does not prevent aliasing, and the data must be filtered before binning.

intervals are also equal to the bin width. In the frequency domain, this corresponds to multiplying the spectrum of the radiometer output by a sinc function corresponding to the top hat, and followed by a convolution by a III with the reciprocal interval of its counterpart in the time domain, which produces the expected replication of the original spectrum due to sampling.

The problem may clearly be seen here that the sinc function is not a good low-pass filter, as it suffers from side-bands of large amplitude which transmit high frequency noise. The more disturbing aspect is that the replication due to sampling occurs at the same frequency as the first null of the sinc, thus aliasing occurs even without considering that noise passed by the side-bands. The data must thus be smoothed before binning. In the case of the radiometer output, the information is smoothed by the telescope beam to less than 3 deg^{-1}, and the post-detection time constant is chosen so as to attenuate receiver noise of higher frequency than that of half the reciprocal bin width, depending on the scan speed. Thus for a scan speed of 250 mdeg s^{-1} and a bin width of 100 mdeg, the bin width corresponds to 0.4 s or 2.5 Hz, so a post-detection bandwidth of 1.25 Hz must be used.

Medians were first considered as an efficient method of determining the majority vote where three separate observations were to be compared. As long as at least two of the three are in reasonably good agreement, one of them will be nominated as the median. The alternative considered was taking the mean of the three readings, then discarding any reading which differs from the mean by more than four or five times the expected standard deviation and repeating the process. The difficulties of this approach are making a reasonable estimate of the standard deviation, and the fact that the procedure is iterative, although with only three original readings, there is not much room to maneuver.

The idea of using medians and median filtering as a way of discriminating against uncertain data was first obtained from Tukey (1977). However, no claims were made for the significance of the results obtained, the technique being presented more as an aid to reviewing data. However, Wall (1979) suggests that the median supplies a safer value than the mean in cases where the distribution of errors is unknown, or contains long tails, i.e., a very few large errors. This latter is certainly the case where digital errors in the data are concerned, or where one of a set of observations are contaminated by bad weather or other interference. These produce errors orders of magnitude greater than the noise

on a single record, and, as long as the minority of scans are so contaminated, have minimal effect on the value of the median.

Another case where the median was considered to have the desired properties, is that of discriminating against point sources in areas which are otherwise cold enough for background measurement. The median is taken over an interval in Dec at least two full beamwidths wide. Thus if one point source occurs in the interval, it will be largely removed by the process, regardless of its strength.

5.2.2. Reformatting

Because of the requirements of the Sort and Find packages, and because of the penalties in terms of poor job turnaround time when large data sets are involved, the reformatting procedure was not as trivial as one might expect.

The first need was to compress the data: a single observation as stored on tape occupied more space than could be obtained in one disc data file. The data as captured are very heavily oversampled, and samples are not equally spaced, there being some jitter in the speed with which the DVM is serviced. Thus the data can be immediately compressed by averaging adjacent samples into equally spaced 1/3 beamwidth bins in Declination. The co-ordinate data as stored on the tape is directly from the angle readouts, and thus has to be corrected for telescope pointing, and precession if necessary, before the binning operation is performed. After binning, each run is stored as a one-dimensional array of bins, with a starting Dec and a nominal RA. Because of the tracking problems, another array is kept with the mean RA of the samples in each bin, and in order for correctly weighted means to be taken when combining observations, the number of samples that went into each bin is also saved.

It is essential that the data used for background determination be unprecessed, even if the final map is binned in 1950.0 co-ordinates. It is therefore necessary to separate the data for finding backgrounds at this stage as well. The background is expected to be smooth, thus can be completely specified by widely spaced samples. To generate data for background determination, samples are collected in wide bins, usually about twice the beamwidth to first nulls (BWFN), and the median taken, rather

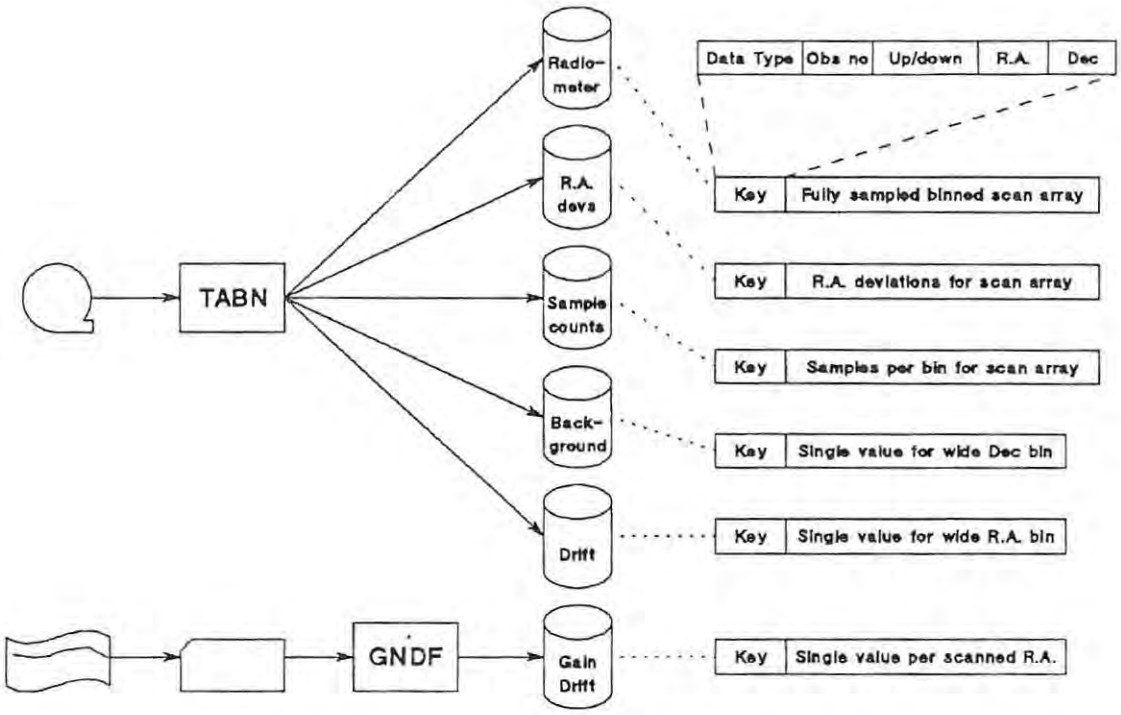

Figure 5.2. Translation of the raw data. Data from the magnetic tape is reformatted to ICL standards and key values are included with each record for manipulation by the FIND and SORT programs. The receiver AGC voltage is manually measured from the chart and converted to a similar format.

than the mean, to discriminate more effectively against digital errors and point sources in the background areas.

As noted above, the drift can also be determined from heavily smoothed data, so the same procedure of taking medians in large Dec bins is followed to obtain a set of data for drift determination. The difference is that these bins are formed in the observer's co-ordinates, i.e., in precessed Dec if so specified. For both background and drift data, the precise RA information is ignored. For the background, it is assumed that the scan path is the same for each run in a single observation, even if not at constant RA, and for the drift data, this is so heavily smoothed in use that a slight deviation in RA is negligible.

A program called TABN (for translate and bin) was written for the ICL computer to perform the reformatting procedure. Its operation is illustrated in Figure 5.2. Data are read directly from the ASCII tape written by the RAO computer and converted to ICL 6-bit character code for later

translation to binary by standard FORTRAN read statements. In this manner, various digital errors may be detected and corrected. A three point median filter is passed over the data before any binning is performed, as an added protection against digital errors. At this point the data is oversampled by a factor of at least 5, so no information is lost. The three streams of data, i.e., fully sampled runs, smoothed background data, and smoothed drift data are written to the same output file, but with appropriate key values, so that they may be separated later by the Find package. The fully sampled runs are written as one record each, but the background and drift data have to be read sometimes as Dec scans and sometimes as RA scans, and so each value is written in its own record with appropriate keys so that the reordering may be performed by Sort.

The key values written in each record are: data type, observation number, scan direction, nominal RA, and Dec. These have so far proved to be sufficient. Together with the ICL standard record header, this adds an overhead of five words to each record. Each sample occupies one word. RA causes some problems with sorting, because it is circular, and thus order is not easy to define. The approach taken was to store an extra sign bit with the RA value which ranges in mdeg between 0 and 360 000. If the sign bit is included in the sort key, the RAs effectively lie between -180 000 and 180 000 mdeg, and if it is ignored, they retain their basic values. Thus as long as a single observation does not cross both 0^h and 12^h RA, it can always be sorted into RA order. As no observation can be longer than 14 hours, the longest night at the RAO, this is not a crippling restriction.

With the data suitably formatted and reduced in volume, the next stage of processing is the removal or minimization of receiver drift effects.

5.2.3. Drift removal

The principle of the drift removal procedure is to build up a very heavily smoothed map of the source area from the observations not noticeably affected by drift. This map is called the median sky, from the manner in which it is obtained. Similarly smoothed versions of all the observations are then compared with the median sky, and the differences used to correct the unsmoothed data. Because the background due to scanning effects is not removed from the data before this operation is carried out, a separate estimate of the drift is obtained for each run for each Dec for which a smoothed sample

exists. Since the drift is considered to vary too slowly to have any effect on a single run, the median value of all the estimates for each run is used.

Drift from one source may be measured directly. Because the radiometer AGC voltage is recorded on a chart recorder, any change in system gain may be measured from the chart. If this is attributed to the MASER, then the appropriate increase in the second stage contribution to the system temperature may be calculated, and subtracted from the radiometer output. This change is called the gain drift, and is stored in a disc file with the help of program GNDF.

The data used throughout the drift determination process is that produced by TABN for this purpose as described in section 5.2.2. above. This has already been smoothed in the Dec direction by taking medians over large bins. Each observation is undersampled in RA because the skip distance between runs is usually larger than the beamwidth, thus no smoothing can immediately be performed in the RA direction.

The binned radiometer output, in this case the drift bins, may be thought of as a three dimensional array R_{ijk} with samples at RAs α_i and Decs δ_j and forming part of observation n_k. For the purposes of data reduction, upscans are considered to be part of a different observation from their associated downscans. The array is sparse, as a single observation will contain data for every $2N$th RA only, where N is the number of rasters in the scan pattern. The radiometer output is considered a superposition of five components:

$$R_{ijk} = S_{ij} + G_{ik} + D_{ik} + B_{jk} + O_k \qquad (5.1)$$

where S_{ij} is the output due to the source within the beam at (α_i,δ_j), G_{ik} is the gain drift when scanning at α_i during observation n_k, D_{ik} is receiver drift from any other cause at the same time (which we now wish to measure), B_{jk} is the background contribution at δ_j for observation n_k and O_k is the constant offset due to the arbitrary setting of the balance control during this observation.

The first problem is that O_k gives each observation a completely different level, thus not even drift scans synthesized for the same Dec from different observations are directly comparable. The first stage of the processing is thus to equalize levels, by subtracting the median value of each drift scan from its component samples.

In terms of our array, the measured gain drift is first subtracted:

$$R'_{ijk} = R_{ijk} - G_{ik}$$

and then the median value of the drift-free data in each RA scan is subtracted from that scan:

$$L_{ijk} = R'_{ijk} - \text{median}_I(R'_{Ijk})$$
$$I \in \{i:i = (r_k + 2mN), m = 0,1,2,\ldots,M_k\} \cap \{i:D_{ik} = 0\}$$

where the median is taken over I for each j and k, r_k is the raster number of the observation and M_k is the number of scans in the observation. From equation 5.1 and the fact that the background and offsets are independent of RA:

$$L_{ijk} = [S_{ij} - \text{median}_I(S_{Ij})]_k + D_{ik}$$

where again the median is taken over I for each j. In order for the bracketed expression above to be independent of k, so that synthesized RA scans from drift-free observations may be subtracted from those of affected observations to determine their drift, the $\text{median}_I(S_{Ij})$ must return the same value for each observation. While these values cannot be identical because of the interleaving of observations, they should be similar enough provided that (i) the I (indicating the set of drift-free runs) for different observations fall within the same range of i and thus RA, and (ii) taking medians in large *Dec* bins when generating these data has been successful in removing any sources with small extent in *RA*, which is not unreasonable when one considers the alternative, that sources should be aligned with the long axis in the Dec direction. Of course, single scans are not simply subtracted as suggested above, but the median of all the good data surrounding each scan is used as the reference (the 'median sky', as described below).

The operation is performed as follows (refer to Figure 5.3): The good, i.e. apparently drift free, observations or parts of observations are flagged using Find. All the data are then sorted into RA scans, separately for each Dec and each observation, i.e. synthesized drift scans. The data are corrected for gain drift, the median value of the good samples in each RA scan is found and this value is subtracted from the entire scan. This procedure is carried out by program RDDC (for remove gain drift and DC level).

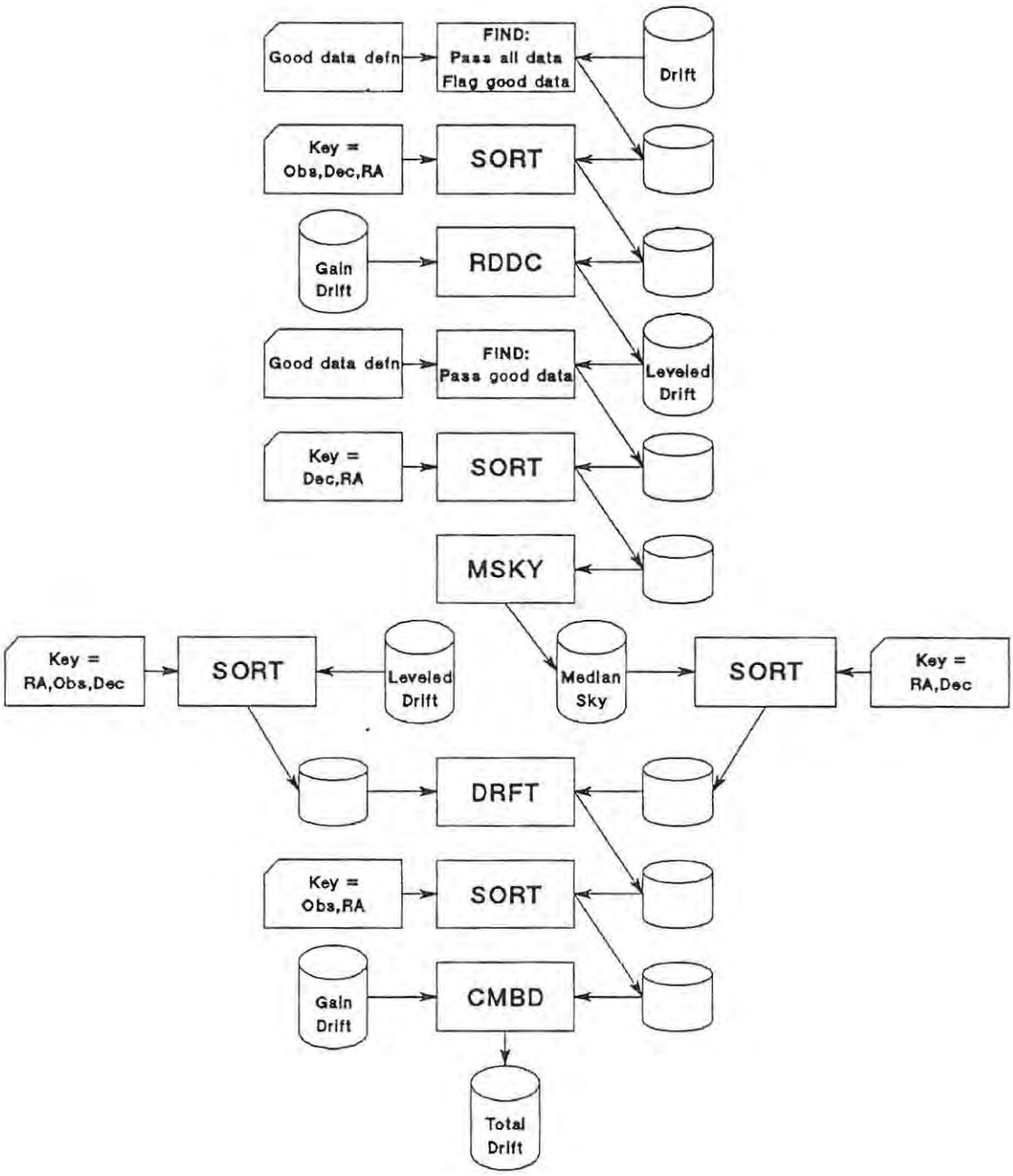

Figure 5.3. The removal of receiver drift. Provided that there are some observations free of receiver drift, they may be used to correct others by synthesizing a set of heavily smoothed drift scans to which the affected observations may be tied. The top input disc file labelled "Drift" is that produced by TABN (Figure 5.2). The drift-free data is flagged and all the data is sorted into RA scans, keeping observations separate. The sort keys are listed in decreasing order of significance. From the whole of each RA scan program RDDC subtracts the median value of good data in that scan, thus removing background and offset effects and placing all RA scans on a comparable level. MSKY takes good data from all observations and at each Dec produces a single smoothed median RA scan. DRFT finds the difference between these reference scans and all the drift data, and CMBD adds this to the gain drift which is measured separately.

The median sky can now be found from the RA scans. Only those samples which have been flagged as good are used. The data are again sorted into RA scans, but this time the values from different observations are interleaved, to give fully sampled scans, with probably several samples from different observations at each sample point. A wide median filter is then passed over each scan to remove any errors which might have escaped the attention of the observer, and to smooth it, and the resulting scans are written out as representing the median sky. Since the median filter preserves sharp edges, there is some argument for including a linear low-pass filter at this stage, but this has not been attempted. The median sky, although smoothed, is still fully sampled in RA, i.e. a sample exists at each Dec for each RA at which a run has been taken. The determination of the median sky is performed by program MSKY.

Now that a reliable, if heavily smoothed, set of synthesized drift scans across the source area has been obtained, the drift data with the background and offsets removed (array L_{ijk}) may be compared to them, and the differences then represent the drift on each observation. Although a separate value of the drift is obtained at each Dec, the value of the drift is considered to be constant over one run, so the median value is taken over the Dec range.

In operation then, all the data is sorted into Dec scans in strict RA order, i.e., Dec scans from different observations are interleaved in RA. The median sky is also sorted into Dec scans in RA order. The comparison is thus made by Dec scan at corresponding RA's, and the median difference value written out for each run of each observation. These values now represent the drift for each observation. This procedure is performed by program DRFT.

The final process consists of combining the drift found by the above procedure, and the gain drift as measured from the chart recorder trace of radiometer AGC voltage. This is simply done by sorting the drift values into RA order for each observation, and adding it to the gain drift. This is done by program CMBD (for combine drift). This combined drift data is now available to correct the other two streams of data produced by TABN, the background data and the fully sampled runs.

One problem has been glossed over here, and that is the method of determining which observations are good. In practice then, a first pass is made with RDDC with all the data flagged as good. This is a

crude method of removing the background from each observation, as a different level is subtracted from samples at each Dec. Another program, MDSC (written by M. Campbell) is then used to take a median value across the Dec range for each run. A plot of these median values is made as a single RA scan. Because the data are so heavily smoothed the signal to noise ratio is good, and bad observations or even individual runs can easily be seen.

It must be stressed that this procedure depends on the availability of several drift-free observations covering the entire source, and that for best effects, a portion of the source area should be free from drift on all observations.

5.2.4. Background removal

Once the magnitude of drift effects have been calculated for an observation, the backgrounds may be tackled. The procedure is simply to find the coldest sample at each Dec, with the assumption that this represents a source temperature of 0 K. Although this assumes that every observation will cover an area of cold sky at each Declination, it is not necessary that the RA of the cold area for each Dec be known beforehand, or that whole runs be on cold sky. It is assumed that all runs follow a fixed pattern in the HA, Dec plane, i.e., corresponding to a particular Dec position of the antenna are only two possible HA positions, one for upscans and one for downscans.

The data used is that supplied by TABN for background calculation. This consists of runs smoothed by taking medians in wide bins in unprecessed Dec. In terms of the five component model of Equation 5.1, all the drift has now been measured and may be subtracted:

$$R''_{ijk} = R_{ijk} - (G_{ik} + D_{ik})$$

and the background and offset are removed by subtracting the lowest value measured at each Dec:

$$R''_{ijk} - \min_i(R''_{ijk}) = (S_{ij})_k$$

where the minimum is taken over i for each j and k, thus cancelling the background and offset contributions without affecting the source, provided that the minimum source level at each Dec is zero.

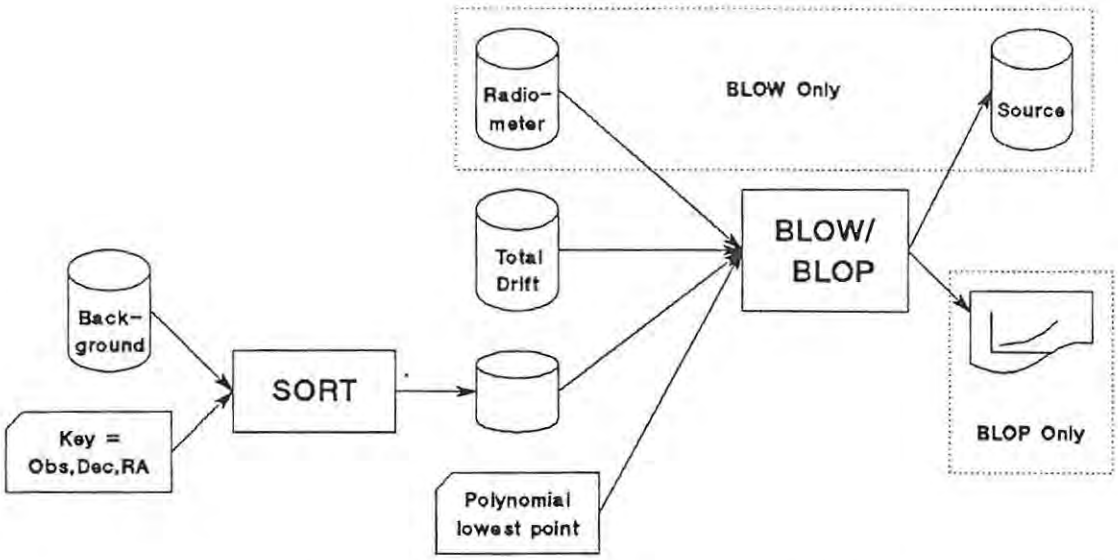

Figure 5.4. The background subtraction procedure. These programs take the data produced by TABN for background calculation (see Figure 5.2), correct it for receiver drift, find the *n*th lowest point at each Dec for each observation and finally fit a l.m.s. polynomial as a function of Dec to these points. Program BLOP fits several different polynomials and simply plots the results so that the goodness of fit can be judged. BLOW fits a single polynomial, then subtracts this and the drift from the fully sampled radiometer output.

The procedure followed (see Figure 5.4) is to sort the data into RA scans, one for each Dec at which a median was taken, and for each observation, treating upscans and downscans as belonging to separate observations. As each RA scan is read into the program the data are first corrected for drift and then sorted into ascending order, only the lowest 20 values being kept. When the end of a scan is reached, the *n*th lowest sample is saved, where *n* is a parameter supplied by the observer. All RA scans of a particular observation are treated in this way. When the end of the data for that observation is reached, an l.m.s. polynomial is fitted to the stored values as a function of Declination, where again the degree of polynomial may be specified by the observer. Each observation is processed in turn.

Two programs were written which perform the above procedure. The first, called BLOP (for low background plot), simply plots the stored points and fitted polynomials for each observation, and prints such useful information as the r.m.s. error of the fit. Several different levels and degrees of polynomial may be specified for each observation on a single pass. The second program is called BLOW (for low background) and only accepts one level and degree of polynomial for each observation. The fitted curve is subtracted from the fully sampled runs for the observation, together with the combined drift values. The observations are then ready to be combined into one map.

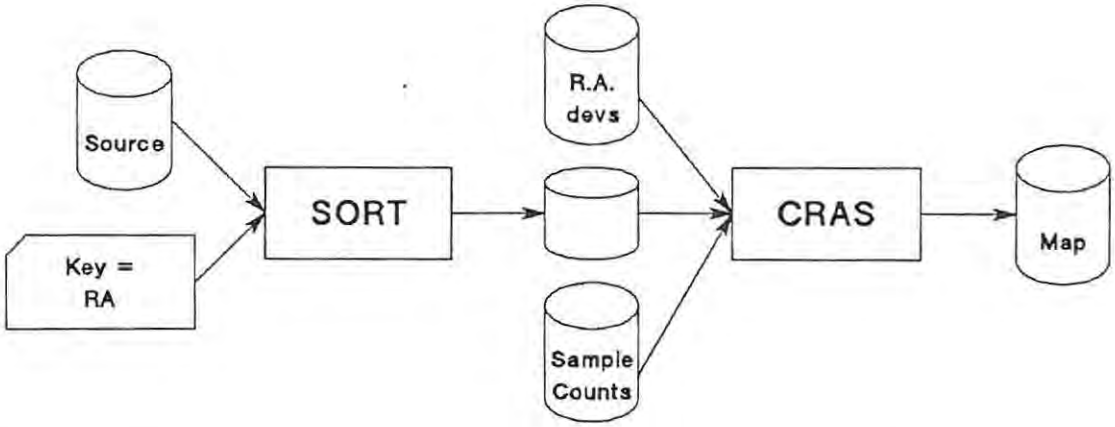

Figure 5.5. Combining observations into a map. The fully sampled scans produced by BLOW (Figure 5.4) are sorted into strict RA order and combined into one map. Because the antenna tracking is not perfect, several runs on either side of the RA of the output scan are searched for samples.

5.2.5. Combining observations

The combining operation consists essentially of taking medians of all samples which fall at a given point in the source area. Ideally there would be three runs covering each scan, and medians could simply be taken at each Dec. However, because the runs do not cover the nominal RA exactly, many runs must be searched for samples covering a particular scan.

The procedure, as performed by program CRAS, is illustrated in Figure 5.5. The input data are the fully sampled runs with background removed by program BLOW, sorted into strict RA order, together with the original RA deviations for each bin, produced by program TABN. Runs whose nominal RA's lie within about 1° of the RA of the scan whose image is being constructed are read into memory. At each Dec on the scan, all the runs are searched for samples of the correct Dec which have wandered over the scan in question. These samples are accumulated, and when the search is complete, the median value is found. When all the Decs have been covered, the resulting scan is written out, the runs which are now too distant to qualify for consideration are dropped, and new runs read in to take their places for the next scan. When all the scans have been covered, the final map has been built up as a matrix on a disc file, and is ready for display and picture processing.

5.3. Map processing

The first function required when a map has been assembled is display. The output devices available on the Rhodes computer are a Calcomp drum plotter and a Tektronix T4010 graphics VDU. Various methods of display were used, including contouring, half tone shading and hidden line maps. More recently, access has been obtained to an Optronics film writer, and this has provided very detailed grey scale displays.

The next function implemented was filtering. So that the filter could be specified exactly in the spatial frequency domain, filters were implemented by means of two dimensional Fourier transforms. These linear filters are still susceptible to digital errors in the data, so running median filters are also used to remove any such errors. A third and related function is that of co-ordinate transforms. The Fourier transform programs assume equidistant samples, but at high Decs, the spacing of an RA, Dec grid is far from equidistant. The data are thus rotated to a better grid before filtering.

5.3.1. Display

A contouring routine had been obtained by the Applied Maths Department and was pressed into service. Some modifications were made, mostly to improve the efficiency of memory usage, and others to allow for the fact that RA, Dec form a left-handed co-ordinate system. Subroutines were also written to superimpose co-ordinate grids on the maps. Although not very satisfactory on the point of visual impression, a labelled contour map provides a quantitative display which is necessary for the serious evaluation of data. This remained the primary display method, used for all purposes from detection of bad data to source flux measurement.

The second method of display used the hidden line technique. Again a routine was made available through the Applied Maths Dept, but this proved totally intractible owing to the amount of memory required, and a less generalized routine was written from scratch. This technique gives a good visual impression of the strong sources within a map, and was used for various displays.

Half tone representation seemed to offer the best display method from the point of visual impact and several attempts were made to produce them by various methods on the line printer as well as the graphic output devices.

Overprinting on the line printer produces output very quickly, but a linear scale could not be constructed from the available characters, even with as few as 20 levels, particularly near the ends of the scale. Even the smallest character (".") produced a marked darkening over blank paper, and when a character position was completely blacked in a gap was left before the next position, so that the overall effect was never very dark either. A factor which detracted from the speed with which the output could be obtained, was that a white border had to be manually removed from each page, making the assembly of a large map more time consuming than producing the printout.

On the plotter and graphics VDU, half tones were formed by dividing the drawing area into pixels which could selectively be coloured to varying degrees by drawing short vectors across them. Because of the comparatively low resolution of the VDU (1024 x 768 points), the pixel chosen was small (5 x 5), and within this area only 7 grey levels could be distinguished because of the width and nonuniformity of the writing beam. On the plotter (7000 steps in width) a much larger pixel, usually 12 x 12, could be used, and this could be resolved into the full expected number of levels, i.e., 145 levels for a 12 x 12 pixel. The chief problem with both these output devices was the speed of operation – the VDU limited by its 1200 baud link with the computer, and the plotter by its 30 mm s^{-1} pen speed. Various pattern generation algorithms were used to optimise the two cases. The VDU screen could be filled in about 15 to 20 minutes, displaying 200 x 150 data points. The same data took about 4 to 5 hours to reproduce on the plotter with its increased resolution. Eventually access was obtained to the Optronics film writer of NITR at the Hartebeesthoek Satellite Remote Sensing Centre. This has very high resolution and good dynamic range, but the three week travel time for data tape and photographs does not encourage use of this facility.

It is interesting to compare the visual efficiency of the different techniques. Both the contour and hidden line displays emphasize edges, the contour by drawing many lines on a steep edge and the hide by leaving a blank area as a high object interrupts scans passing "behind" it. For this reason both techniques can obscure extended sources, as the visibility depends not on relative height, but the steepness of the edges. The advantage in the case of contouring is that there is no problem with dynamic range – contours may be drawn at ever higher levels without restriction. Contour maps do suffer from a resolution related problem – when a map is very detailed it looks cluttered, so major

features are difficult to pick out, and there is not always sufficient room to label small contours, which then become ambiguous. The labelling problem may be alleviated by marking every second contour in some way – using a different colour or tracing twice. Because the contour positions can be accurately interpolated between sample points, the true strength of contouring lies in the display of minute detail in data up to about 100 beam areas. When the data cover a larger area, some detail must be sacrificed for visibility.

The grey scale reproductions, on the other hand, are limited more by the performance of the eye, especially when a machine with the accuracy of the Optronics is available. Between white and black, the eye can only distinguish a certain number of grey levels. Using more levels than this, as with the 256 levels available on the Optronics, serves only to allow smooth transitions between visibly distinct levels, but does not increase the visibility of features. This problem is compounded by the fact that the eye's response is logarithmic, so that the photographic density must increase exponentially in order to produce a linear response. The result is that the grey scale displays are much more sensitive to the choice of zero level than the other methods.

5.3.2. Filtering

An inherent part of the Skymap philosophy was a high scanning speed, with only a short integration time on each sample point. One of the reasons that this was accepted, was the assurance that once a map had been assembled, the signal to noise ratio (S/N) could be improved at the cost of resolution by low-pass filtering. As the chief interest lay in extended sources, the loss of resolution was not considered serious. In the two dimensional case, the S/N improves in direct proportion to the loss of resolution, not the square root thereof, as might be expected from the one dimensional case. As the maps are always sampled at 1/3 beamwidth, an increase in S/N of 1.5 may be obtained without loss of resolution.

A further use envisaged for filtering was the simulation of other observing techniques. Thus by using a suitable low-pass filter, the Skymap data might be made directly comparable in resolution to the metre-wavelength surveys, or with the use of a suitable high-pass filter, to the beam-switched surveys.

To provide maximum flexibility in the specification of the spatial frequency response of the filters, a program was written to perform a two dimensional Fourier transform, multiply the result by a specified function, and then perform the reverse transform. As usual, the main difficulty encountered was lack of memory space. For this reason a generalized mixed radix Fast Fourier Transform subroutine was used (Brenner, 1976) so that the arrays would not have to be extended to the nearest power of two, and use made of the fact that the data were purely Real rather than Complex, to achieve a further reduction in storage. Disc files were used for intermediate storage. This program was implemented by P. Clayton. Although time consuming to run, this program allowed the computation of the exact discrete Fourier transform (DFT) of a large array of data.

A problem with the DFT arises from the replication of the interval of data due to sampling. This effectively juxtaposes the ends of the data, causing a step if, as is usually the case, the samples at the ends are not equal. If the data is then smoothed to any degree, the step is also spread out, into the ends of the data.

The first order solution to this is to reflect the data about the Y-axis before transforming a double sized array. This ensures that there is no discontinuity in the data. A routine was found (Brenner, 1976) which performs this operation almost as efficiently as the straight transform, and this was used in the filter program.

This solution still leaves a discontinuity in the slope. This discontinuity may be removed by subtracting a straight line which passes through the two end points, from the data, and then reflecting the data through the origin. The straight line may optionally be restored after filtering. Unfortunately this technique relies heavily on the reliability of the individual samples at the ends of the data.

If an isolated sample in error makes its way into the assembled map, as may be the case if more than one observation is corrupted in the same place, the result of using the usual low-pass filter is to spread the error out into neighbouring samples until it resembles a point source. This is very confusing. As a final effort to remove such gross errors from a map, a running three point median filter is used (called a 3S filter after Tukey) in the RA direction only, as such errors are likely to occur in individual scans. This should not strictly be used unless the data is oversampled by at least a factor of two, as the value

of a correct sample might be used to replace that of its neighbour. This level of oversampling often occurs in a map, since the scans are brought closer together than the nominal $^1/_3$ beamwidth by the cos δ compression factor.

It is now time to look at some of the results produced by the systems which have been described.

Chapter Six: The Upper Scorpio Region

By July, 1976, sufficient experience had been gained with the telescope for an observing program to be undertaken with some chance of producing useful data. The source associated with the H II region Gum 65 was settled on as an ideal test object for the system, and was duly mapped. While the map was being processed, attention was turned to the interpretation of the data. In order to produce useful results, the boundaries of the extended sources must be defined and the radio flux from within these boundaries measured. If it is assumed that the source is an H II region, the ultraviolet flux necessary to cause the ionization may be deduced, and this in turn related to the characteristics of nearby early type stars, in this case the Sco OB2 association. The results of this work and a more detailed discussion have been presented elsewhere (Baart, de Jager and Mountfort, 1980).

6.1. Observations and processing

At the time these observations were begun, the reduction method involving the measurement of background radiation (as described in Chapter 3) had been developed in theory but not implemented. The paper tape data logger system had been adapted for use on the noise-adding radiometer to provide a means of capturing reasonable quantities of data in machine readable form, thus making an implementation of the reduction process feasible.

An extended source of radio emission associated with the H II region Gum 65 was pointed out by Nicolson. This source produced a peak antenna temperature of about 0.5 K, and on exploratory drift scans was seen to be surrounded by extended structures. Situated at $+17°$ Galactic Latitude (b), this source was well outside the range covered by the high frequency Galactic plane surveys, and its association with an H II region implied that it would not be as easily observable at the lower frequencies. It was thus an ideal source to be mapped with the Hartebeesthoek telescope, and an observing program was duly begun. An advantage which only later became apparent was the location of the source at an RA which was well placed for observing during the long clear winter nights.

The area observed initially was from 16^h00^m to 16^h40^m in RA and $-15°$ to $-35°$ in Dec. It became apparent during the early phases of the reduction process that the source area extended to earlier RA, thus the region from 15^h40^m to 16^h00^m was mapped as well. Unfortunately, in an attempt to

speed up the observing process, this second region was scanned at intervals of 150 mdeg in RA, a full half beamwidth, instead of the customary 100 mdeg, thus low-pass filtering on the final map was particularly ineffective in removing scanning effects in this region.

Backgrounds were measured around 22^h RA. The observations extended over two years (the last were taken in July, 1978) and five different background maps were measured during this period. Tie-in drift scans were made from before 10^h through the source region at Decs of –15°, –17°, –19°, –22°, –24°, –28°, –30°, –31° and –33°. This was done so that a 'cold' reference area could be found to which the level of the map might be referred. This area was eventually selected as 10^h15^m on the –22° scan, and all temperatures on the map were measured relative to this point. It is conservatively estimated that the levels across the whole map are accurate to within 30 mK.

The map as first produced has a noticeable tilt from the Southeast corner down toward the Northwest, i.e., away from the Galactic Plane, which tended to obscure faint sources of large extent. It was decided that this radiation was due to the Galactic disc (see for example Price, 1974). A Gaussian function of Galactic latitude was fitted to the lowest point at each latitude, and subtracted from the map. This had the form

$$T = 515 \exp(-4.669 \times 10^{-3} b^2) \qquad [\text{mK}]$$

This corrected map was used for the flux measurements, and is shown as a contour map in Figure 6.1, with boundaries of individual sources emphasized.

6.2. Measurable parameters

The first problem when analysing data from extended sources is the definition of the boundaries of the individual sources. For the analysis of this region a map was drawn with contour intervals of 10 mK and the source-defining criteria used were as follows: (i) there must be at least two closed contours (ii) these must be virtually parallel and within one beamwidth of each other (iii) they must not mimic the shape of lower contours, and (iv) to ensure that it is extended, the source thus defined must have an area of greater than one square degree. The sources are outlined in Figure 6.1, and the observed parameters shown in Table 6.1. The galactic co-ordinates refer to the geometrical centre of the source unless there is a distinct peak, in which case those of the peak are given. The linear

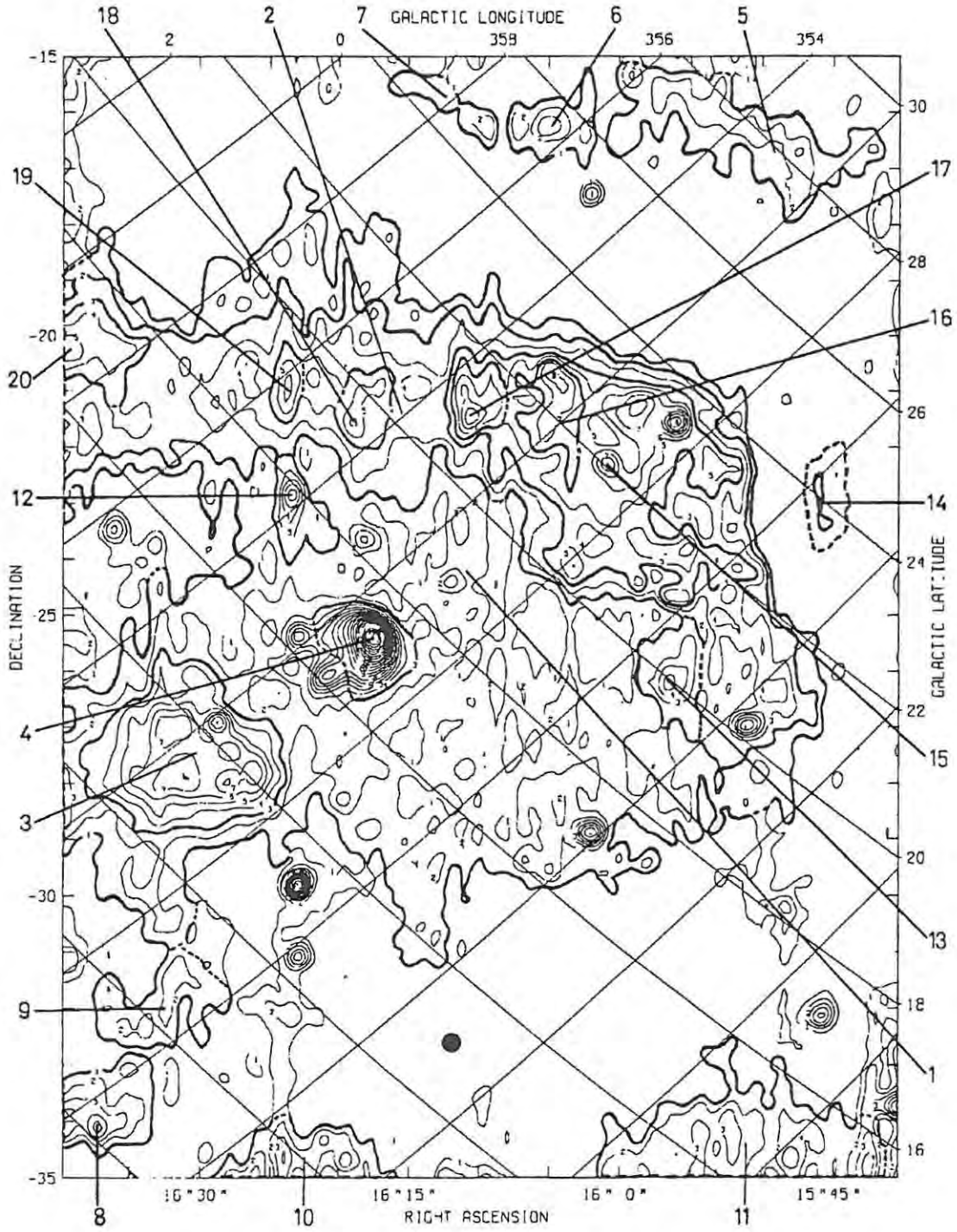

Figure 6.1. Extended sources of the Upper Sco Region. The boundaries of extended sources are marked by heavy contours in this map of the Upper Scorpio Region. The contour interval is 20 mK and the lowest contour is 80 mK. A Gaussian function of Galactic Latitude, representing Galactic disc radiation, has been subtracted from the data. Note that the method of defining source boundaries permits one source to enclose another. The filled circle in the lower centre represents the 20′ FWHP beam.

Table 6.1. Measured source parameters. The parameters of extended sources defined within the mapped region in Upper Scorpio, as measured from the 10 mK contour map. The size is calculated from the apparent extent by assuming a distance of 170 pc.

Source number	Galactic coordinates		η_B	T_b(max)	S	Area	Approx. Extent	Size	Optical Features
	l	b		[mK]	[Jy]	[deg^2]	[deg × deg]	[pc × pc]	
1	351	19	1.0	80	496	114	>12×10	>36×30	Sco OB2
2	354	20	1.0	30	60	40.4	>12×5	>36×15	
3	351.5	13.5	0.95	137	27.5	8.64	4×3	12×9	RCW 129
4	351.3	17.2	0.78	564	15	1.86	1.5×1.5	4.5×4.5	S9,Gum 65
5	353	28	0.95	126	37	8.30	4.5×2	14×6	
6	356.5	25.5	0.8	125	81	2.16	1.5×1.5	4.5×4.5	
7	358	24.5	0.77	104	5.5	1.6	2×1	6×3	
8	347.6	8.2	0.78	167	8.9	1.83	1.5×>1.5	4.5×>4.5	
9	348.5	10.3	0.79	101	6.7	2.08	2.5×1.5	7.5×4.5	
10	345	10	0.78	141	8.2	1.81	3×>1	9×>3	
11	340.5	14.5	0.95	137	32.5	8.21	5×>2	15×>6	
12	354.3	17.9	0.75	120	2.4	1.18	2×1	6×3	
13	347.2	20	0.76	99	29	1.5	2×1.3	6×4	S1
14	347.5	24	0.75	113	4.7	1.07	2×0.7	6×2	
15	351	22	1	110	26.2	14.3	7×4	21×12	S7
16	352	22	0.79	89	3.5	1.85	2.5×1.3	7.5×4	
17	353.2	21	0.74	74	2.4	1	1.5×1	4.5×3	
18	354.5	19.5	0.73	82	2.4	1.06	1.5×1	4.5×3	
19	355.7	19	0.76	79	2.6	1.39	1.7×1.3	5×4	
20	358.8	16.5	0.77	78	3.1	1.61	2×>1.5	6×>4.5	

co-ordinates have been calculated using a distance of 170 pc, the mean distance of the Sco OB2 association as measured by Hardie and Crawford (1961). The beam efficiency, brightness temperature and flux are discussed in the following paragraphs.

The fundamental parameter of an extended source measured with a radio telescope is the surface brightness. This is defined as the power received per unit area of the antenna, per unit receiver bandwidth, per unit source solid angle. The integral of brightness over the entire source area yields the flux of the source at the frequency received.

When a source is observed by scanning the antenna beam across it, the source brightness distribution is convolved with the beam shape. As the beam may be regarded as suitably normalized (volume = 1), the convolution does not affect the flux measurement, provided that the integral of brightness is taken over the "smeared" source area. The parameter measured is then the antenna

temperature, rather than the source brightness temperature. For a source much smaller than the beam (a point source), the smeared area becomes the beam area, which in practice is limited to the main lobe. The reduction from brightness temperature to antenna temperature for a point source convolved with a large beam is called beam dilution. For a given telescope, the integral of antenna temperature over the beam for a point source is not usually performed to determine the flux, because it is proportional to the peak antenna temperature obtained, a more easily measurable quantity, which may be calibrated in terms of flux by observing standard sources.

When the flux of an extended source is measured, however, two further steps must be performed. Firstly the integral of antenna temperature must be taken over the full source area as it appears after broadening by convolution, and the contribution by the beam side lobes must be taken into consideration, as the radiation received through the side lobes is indistinguishable from that received through the main lobe if the source is large enough to fill both the main and side lobes at the same time. This contribution is usually included in the form of a beam efficiency factor (η_B), which is 1 for a source large enough to fill all the side lobes, and reduces to the main/side lobe ratio for a small source.

Introducing the Rayleigh-Jeans approximation to Planck's Law for converting a temperature to the equivalent radiated power, the flux at the frequency observed may be expressed as (Kraus, 1966):

$$S = 2k/(\lambda^2 \eta_B) \iint T_a \, d\Omega$$

where T_a is antenna temperature which for an extended source is integrated over the source solid angle Ω, λ is the wavelength of the received radiation, and k is Boltzman's constant.

If the source area is known or is large enough to be measured, the mean source brightness temperature may be calculated from

$$T_b = (1/\eta_B) \int T_a \, d\Omega \, / \int d\Omega$$

where the upper integral is over the broadened source area and the lower one is the actual source area.

Table 6.2. Derived source parameters. The source parameters derived for some of the sources listed in Table 6.1, assuming that they are H II regions excited by stars of the Sco OB2 association. The Lyman continuum fluxes for the suggested exciting stars are taken from Churchwell and Walmsley (1973), Panagia (1973), Higgs and Ramana (1968a,b) and Kazès, Le Squeren and Gadea (1975).

Source Number	S [Jy]	$<E>$ [pc cm^{-6}]	$<N_e>$ [cm^{-3}]	M_{HII} [$M_\odot$]	U_{rad} [pc cm^{-2}]	Possible Exciting stars	L_c flux [10^{45} photons s^{-1}] Obsvd	CW	P	HR	KSG
1	496	155	2.2	1502	33		1175				
2	60	53	1.5	351	16		141				
3	28	114	3.3	73	13	τ Sco B0 V	65	955	427	952	212
4	15	296	8.2	14.2	10	σ Sco B1 III	35	6.0	7.4	330	0.6
5	37	161	4.3	60	14		87				
6	8.1	134	5.5	9.5	84		19				
7	5.5	122	5.4	7.6	7.4		13				
9	6.7	116	5.1	19	7.9		16				
12	2.4	72	4.2	5.9	5.6		5.6				
13	2.9	68	3.9	6.8	6.0	π Sco B1 V + B2 V	6.8	2.6	3.3	155	0.4
14	4.7	158	6.7	5.9	7.0		11				
15	26	66	2.0	153	12	δ Sco B0.5 IV	62				
16	3.5	67	3.6	9.1	6.4	ω' Sco B1 V	8.3				
17	2.4	84	4.8	4.3	5.6		5.6				
18	2.4	81	4.8	4.3	5.6		5.6				
19	2.6	68	4.0	5.6	5.8		6.2				

6.3. Derived parameters

Once the flux of a source has been calculated, no more information can be extracted from the continuum observation without some assumption being made as to the nature of the generating mechanism. Here it was assumed that the sources were H II regions excited by ionizing radiation from stars of the Sco OB2 association. The derived parameters are shown in Table 6.2.

The model of the H II region used follows model II of Mezger and Henderson (1967). It is assumed that the optical depth of the H II region is much less than 1, and that the electron temperature is a constant 10^4 K. The emission measure has then been calculated from the brightness temperature for these conditions. The source was modelled as a cylinder of depth equal to its diameter. The average electron density has then been found using

$$N_e = \sqrt{<E>/2R}$$

where $<E>$ is the average emission measure and R is the radius of the source. Also calculated are the mass of ionized Hydrogen and the excitation parameter U_{rad} following Churchwell and Walmsley (1973). The Lyman continuum fluxes corresponding to the observed fluxes have been calculated from

the formula given by Rubin (1968). The fluxes for the suggested exciting stars are taken from Churchwell and Walmsley (1973), Panagia (1973), Higgs and Ramana (1968a,b) and Kazès, Le Squeren and Gadea (1975).

6.4. Discussion of Results

The final contour map is compared with optical observations of the Sco OB2 region, and the excitation of individual sources by nearby early type stars are discussed. Finally consideration is given to possible evolutionary sequences for the association.

6.4.1. Comparison with optical features

It is significant that source 1 coincides very nearly with the Sco OB2 association. This is illustrated in Figure 6.2 where all stars of type B9 and earlier in the association are plotted. Members of the association have been taken from papers of Garrison (1967) and Gutierrez-Moreno and Moreno (1968).

Source 3 coincides with the emission nebula RCW 129 and is about the same size. The suggested exciting star of this H II region is τ Sco (B0 V). Source 4 is the most intense in the whole map. It coincides with the Hα feature Gum 65 or Sharpless 9. This is an H II region with exciting star σ Sco (B1 III). Source 12 lies just North of the Ophiuchus dark cloud. ρ Oph lies on the Southern edge of this source. Source 13 is an H II region associated with π Sco (B1 V). Sharpless 1 occurs in the same region, but the size quoted is larger than that of source 13.

6.4.2. Excitation of H II regions

There is considerable disagreement concerning the theoretical Lyman continuum fluxes of B stars as can be seen from Table 6.2. The radio sources associated with τ Sco, σ Sco, and π Sco are clearly defined and their associations with Hα nebulosity makes them identifiable as H II regions. Cappa de Nicolau and Pöppel (1986) note a good agreement between the mass of 'missing' H I and that of the H II given in Table 6.2. for sources 13 and 15

In the case of τ Sco the observations yield a Lyman continuum flux much less than any of the theoretical values, which suggests that the H II region RCW 129 is density bounded. This in turn

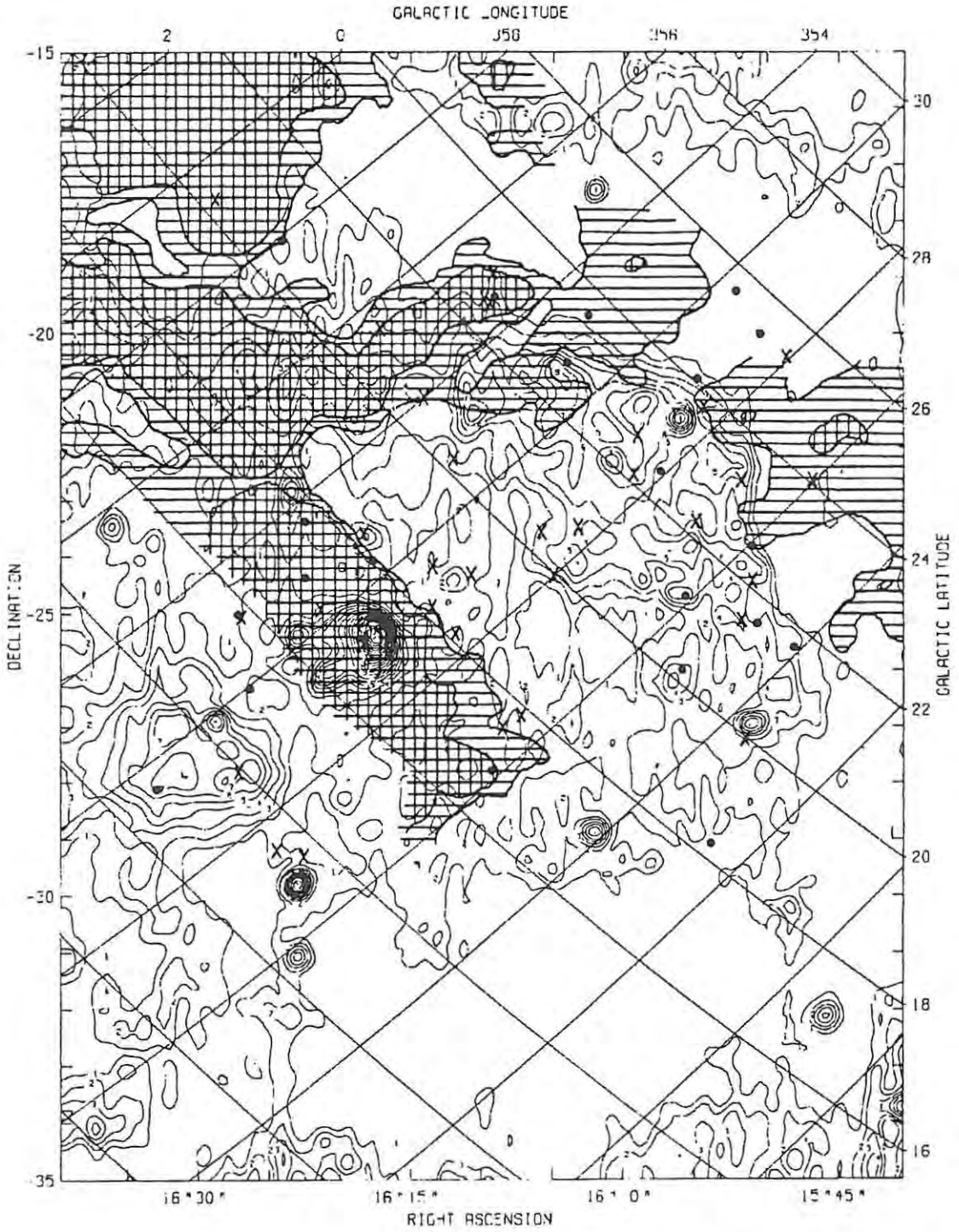

Figure 6.2. Stars and obscuration in Upper Scorpio. The coutour map of Figure 6.1 with B0–B5 stars (•) and B6–B9 stars (×) belonging to the Sco OB2 association plotted on the radio contours. Areas of constant obscuration from Rossano (1978) are superimposed.

suggests that τ Sco could be responsible for most of the ionization contained within the boundary of source 1, if this source is assumed to be of thermal origin.

In the Sco OB2 association there are one B0, two B0.5, three B1, one B2 III and two B2 IV stars. Local enhancements in the radio emission are detectable on the 10 mK contour map for all the stars earlier than B2.

6.4.3. Structure of the Sco OB2 Association

Near the centre of source 1 the radio emission is weak and there are no early B type stars, as noted by Garrison (1967). On the other hand the B type stars, the strong radio emission, the obscuration and an H I shell (Sancisi, 1974) tend to occur near the edge of the association. If the initial star formation took place near the centre of source 1, the expanding H II region would drive the neutral gas and dust outwards. Early B stars could form in this compressed material and they would then have the outward velocities observed by Blaauw (1978). These early type stars would then ionize the neutral gas near them, giving rise to the strong emission regions observed. The same effect could be produced if a supernova explosion had occurred at the centre of source 1. In this connection it should be noted that ζ Oph, a runaway star, appears to come from this area of sky. In the absence of any known SNRs or sufficiently luminous early type stars, however, Cappa de Nicolau and Pöppel (1986) suggest that star formation in the entire Sco-Cen association could be caused by an expanding shell of H I associated with the Gould belt.

Chapter Seven: The Magellanic Cloud Region

The Sco OB2 association had proved to be a fruitful testing ground for the old mapping system. For testing the Skymap system a much larger area was required, and preferably a region which had been well observed at other frequencies so that the results could be verified to some extent.

The choice of source region and the objectives of the tests to be applied are next described, followed by a description of the observations and the processing carried out on the data. The results are presented in the form of source lists and contour maps. Sources for which a flux of greater than 600 mJy at 2300 MHz was predicted from the Parkes catalogue were measured to estimate pointing and flux errors, and the maps were compared with the 408 MHz continuum survey (Haslam *et al.*, 1981) and H I observations (Mathewson *et al*, 1979). The Parkes catalogue used is a machine readable version of about 1979 vintage obtained via Dr. G.D. Nicolson of RAO.

7.1. Choice of tests

A tempting option was the idea of observing an area polewards of –60° Declination. The closeness of adjacent scans on the sky in this region due to the cos δ compression factor meant that only half as many interleaving rasters would be required to fully sample the sky as would be required at lower Declination.

The Skymap observing programs became operational towards the end of 1979. At that time of year the possible start RAs, which can be observed within 30° of the meridian at sunset, range from 16^h to 20^h, and the observations may continue for 11 hours until sunrise. It was decided to allow a two hour period after sunset for the telescope surroundings to cool before the source region drifted into the telescope beam as the background is partly due to spillover from the secondary reflector seeing the ground around the dish. Drift scans allowed to run over night (as used for the Sco map) usually showed a slight downward trend during this period, which could not always be attributed to the source.

A Declination range of 19° was chosen to match the timing of antenna movements, and allowed the source to be completely sampled with only two interleaved rasters of Dec scans.

7.1.1. Other Extended Source Surveys of the Region

The region from 22^h to 7^h RA includes both Magellanic Clouds and part of the Magellanic Stream between Declination –80° and –61°. The former objects provided two well observed extended sources and the latter an ideal faint extended source which had been detected only in H I. Numerous sources documented in the Parkes catalogue also permit the verification of pointing errors and comparison of flux measurements of compact sources.

From the 150 MHz map of Landecker and Wielebinski (1970), it appeared that sufficient 'cold' sky occurred between the Magellanic Clouds to provide good backgrounds for each observation.

When considering other radio continuum surveys of the region, the 408 MHz all-sky survey of Haslam *et al.* (1981) is the comparison of choice with the present work, because it covers the whole area, maintains accurate baselevels and has comparable resolution. Others, such as the 1.4 GHz survey of Haynes *et al.* (1986), cover only the Magellanic Clouds, or, like the 5009 MHz survey of McGee, Brooks and Batchelor (1972), the 2700 MHz survey of Broten (1972) and the 8400 MHz survey of McGee, Newton and Butler (1978), concentrate only on individual sources within the Clouds. Earlier, Mathewson and Healey (1964) produced similar maps including one of the whole region at 408 MHz, maps of the clouds at 1410 MHz and selective observations at 136 MHz and 2650 MHz. All the above surveys were made with the 64 m antenna at Parkes. Maps produced with synthesis telescopes, including those of Mills, Turtle and Watkinson (1978) at 1415 MHz with the Fleurs Synthesis Telescope and Mills *et al.* (1984) at 843 MHz with the Molonglo Observatory Synthesis Telescope, offer high resolution, but as a result only cover small areas and suffer from the difficulty of establishing good base levels. Longer wavelength surveys such as Shain (1959) at 19.7 MHz, Alvarez, Aparici and May (1987) at 45 MHz and Mills (1955) at 85.5 MHz provide a base for calculating the spectral index of the integrated flux of the Clouds.

Large quantities of H I have been observed in the intercloud region. These observations, including those of the LMC by McGee and Milton (1966), the SMC by Hindman (1967) (which have been confirmed by McGee and Newton (1981) using higher resolution and better sensitivity) and the intercloud region by Mathewson *et al.* (1979) have been combined by Mathewson and Ford (1984). While the neutral Hydrogen is not expected to be visible on the continuum observations, optical Hα

observations by Johnson, Meaburn and Osman (1982) and Marcelin, Boulesteix and Georgelin (1985) have shown that some ionization is taking place.

Large scale optical features of the Clouds expressed as star count isopleths and smoothed red and blue isophotes are given by de Vaucouleurs and Freeman (1973).

King, Taylor and Tritton (1979) measured optical nebulosity near the South Celestial Pole from the SRC survey Schmidt plates, including some in the area $4^h > \alpha > 5^h$ and $-80° > \delta > -75°$ with a surface brightness < 26 mag arcsec^{-2}. They determined that these were reflection nebulae in the Galaxy.

The photographic representation of the IRAS sky brightness images do not show any extended features in this region outside the Clouds, apart from the so-called infrared 'cirrus' at 100 μm wavelength (Neugebauer and Beichman, 1985), but this could be due to the limited dynamic range of this form of representation.

7.2. Observations and Processing

The area was observed twice, as the first set of observations were found to contain systematic errors which rendered them useless. Both sets of observations and their respective processing steps are now described. The final data have been published elsewhere (Mountfort *et al.*, 1987)

7.2.1. Precessed Observations

The first observations were made in six nights during October and November 1979, each raster being observed three times. Scanning was performed in 1950.0 co-ordinates. It was argued that this would greatly simplify the data reduction process, as the data would fall naturally upon a grid in 1950.0 RA and Dec which would facilitate comparison with other published data.

These data were used to develop the reduction programs as described in section 5.2. When the map was produced it was noticed that there was a general trend which caused a high at around 0^h RA and fell toward 6^h, only to increase again toward the end of the map at 7^h, with an amplitude of about 200 mK. At first this was thought to be caused by streamers from the Galaxy, but comparison with some early 408 MHz data (Haslam *et al.*, 1981) showed that this was not so.

Examination of printouts produced during observations showed that the SKYMP observing program was calculating the starting time for each scan using the 1950.0 RA of the scan and attempting to keep the starting Hour Angle constant. As the COMND program adjusted the RA for Precession, the net result was a wander in starting Hour Angle which varied as sin α with an amplitude $\sim 1°$. This was more than sufficient to produce the 200 mK variation in level observed on the map. It was thus decided to remove the Precession option from SKYMP and to re-observe the Magellanic Cloud region.

7.2.2. The Final Observations

The area was finally observed between September 23 and December 4, 1982, by which time some experience in the reduction of Skymap data had been gained through the observation of regions which could be observed at more favourable times of the year (Jonas, de Jager and Baart, 1985). Unfortunately insufficient drift-free observations were obtained to provide baselevels across the whole range of RA observed, but, since problems with the MASER receiver precluded the possibility of obtaining yet a third set of observations, these data were reduced.

By the time these observations were made, changes to time constants in the antenna control system necessitated the observation of three separate rasters. Scans were separated in RA by 0°.2 to compensate for the cos δ compression factor, and each raster was observed three times. Because these observations were made slightly later in the year than the first set, the useable data covered 23^h to 7^h in RA.

7.2.3. Data Reduction

Because of the lack of drift free observations, the standard procedure for reducing the data as described in section 5.2. could not be followed. As there was insufficient data for construction of a median sky a similar approach was used to determine the drift as is described for finding the background in section 5.2.4. The lower 10th percentile point on each Dec scan was found and its value subtracted from the entire scan.

This value is obviously dependent on the background, which is in turn dependent on the drift, so that an iterative procedure was followed. First a rough background was subtracted from each observation,

the resulting data used to calculate the drift and then a second estimate of the background found and subtracted. The second approximation to the drift appeared as random noise, so the procedure was terminated at this point. This reduction procedure effectively removes any source area which extends across the whole map at one particular RA or Dec. Those features which have sufficient cold sky on the same Dec and RA scan will survive unaffected.

The observations were then combined into one map by program CRAS (described in section 5.2.5.) which takes a median value at each output sample point. At this stage the raw map was transferred into the STARLINK system for further processing. The STARLINK package on the Physics Dept VAX 11/730 computer provides a uniform, user friendly environment for processing maps. Some of the functions of display, filtering and co-ordinate transforms as discussed under map processing in section 5.3. were supplied with STARLINK and the remainder were implemented by Jonas (1982).

A very valuable addition to the display peripherals attached to the VAX was the Tektronix 4115B graphics terminal. This display was of inestimable value, providing confirmation at each stage of map processing that the desired result had, in fact, been effected.

An efficient two dimensional Fourier Transform program was implemented by Jonas, and filter profiles could be constructed for various purposes. In particular filters were constructed for removing all frequencies above those present in the beam (3.5 degree^{-1}), and for smoothing the data to the 0°.85 beamwidth of the 408 MHz survey (Haslam *et al.*, 1982).

Programs were also available for performing co-ordinate conversion, as it was necessary to precess the maps before measuring source co-ordinates, and to rotate them onto a field centred co-ordinate system with a more equally spaced grid before Fourier filtering, returning them to 1950.0 Equatorial co-ordinates for display.

7.3. Results

The filtered data are presented in Figure 7.1 as overlapping contour plots of antenna temperature. The scale for degrees of Right Ascension was chosen to be half that for degrees of Declination so that geometric distortions are reduced. The zero level for the data is chosen so that the amplitude

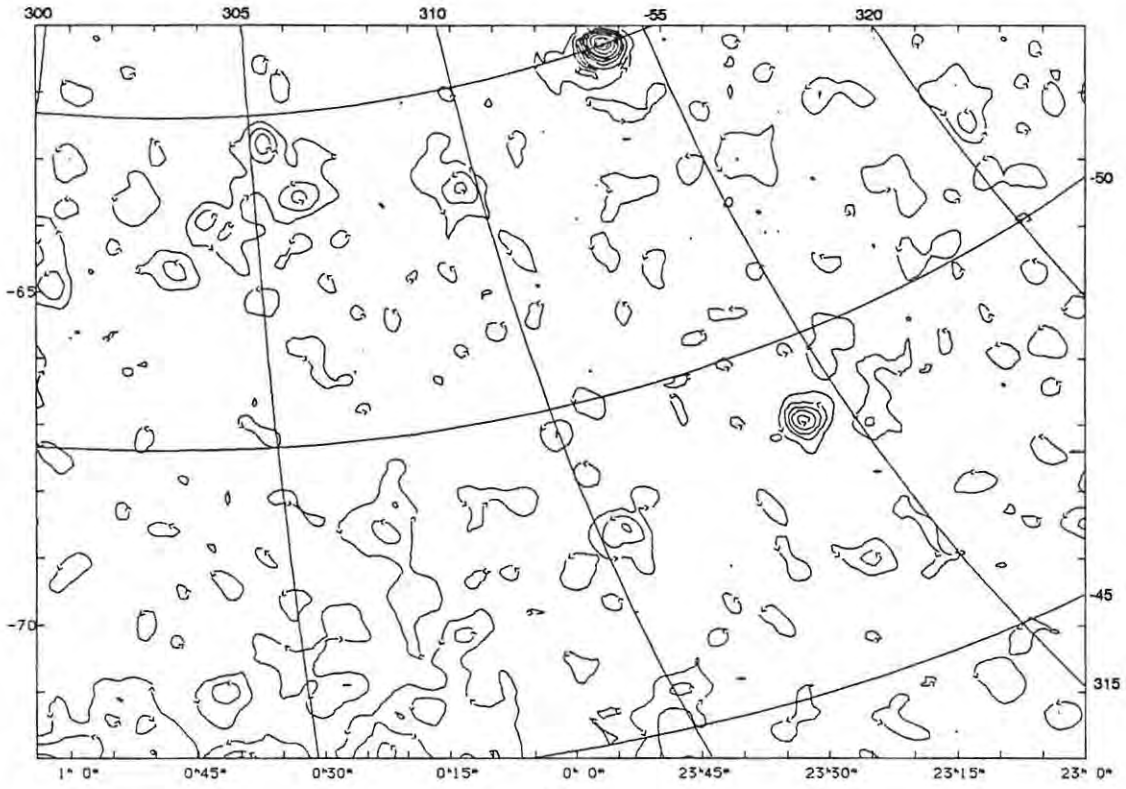

(a)

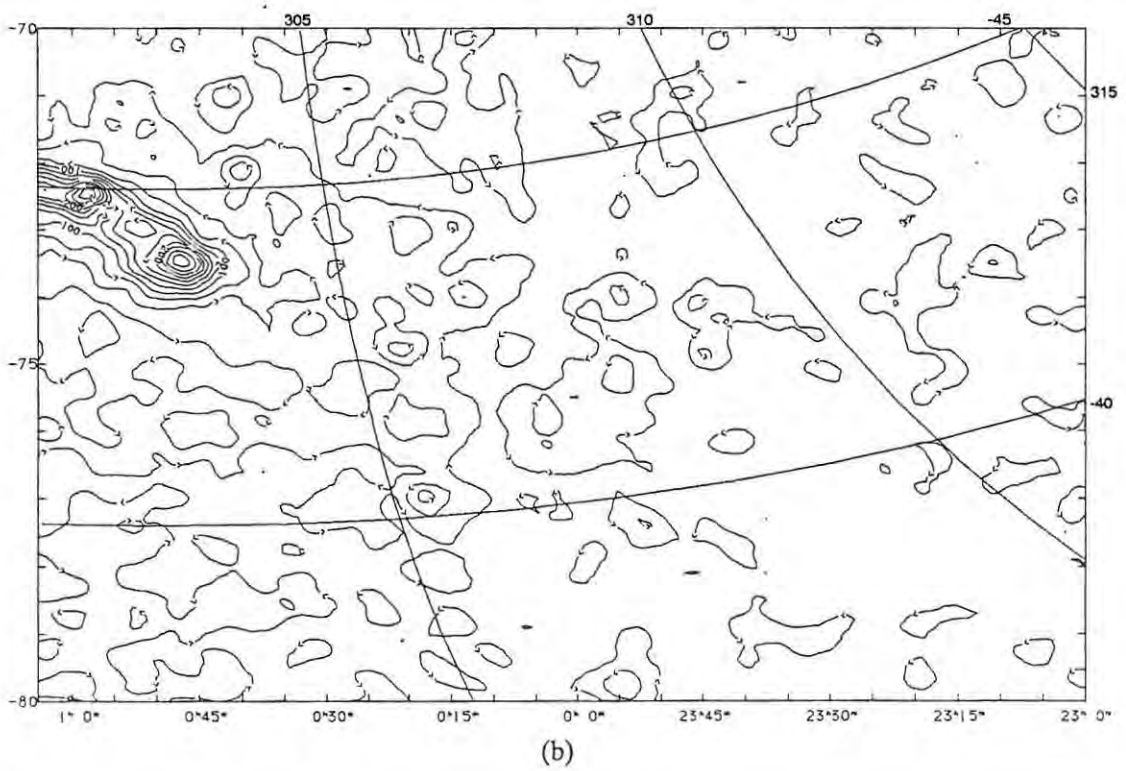

(b)

Figure 7.1.(a)-(h). Contour maps of the Cloud Region. Contour maps of antenna temperature in 1950.0 Equatorial coordinates with a grid of Galactic coordinates superimposed. The contour levels and labelling are described in section 7.3. The maps are presented in order of increasing Right Ascension.

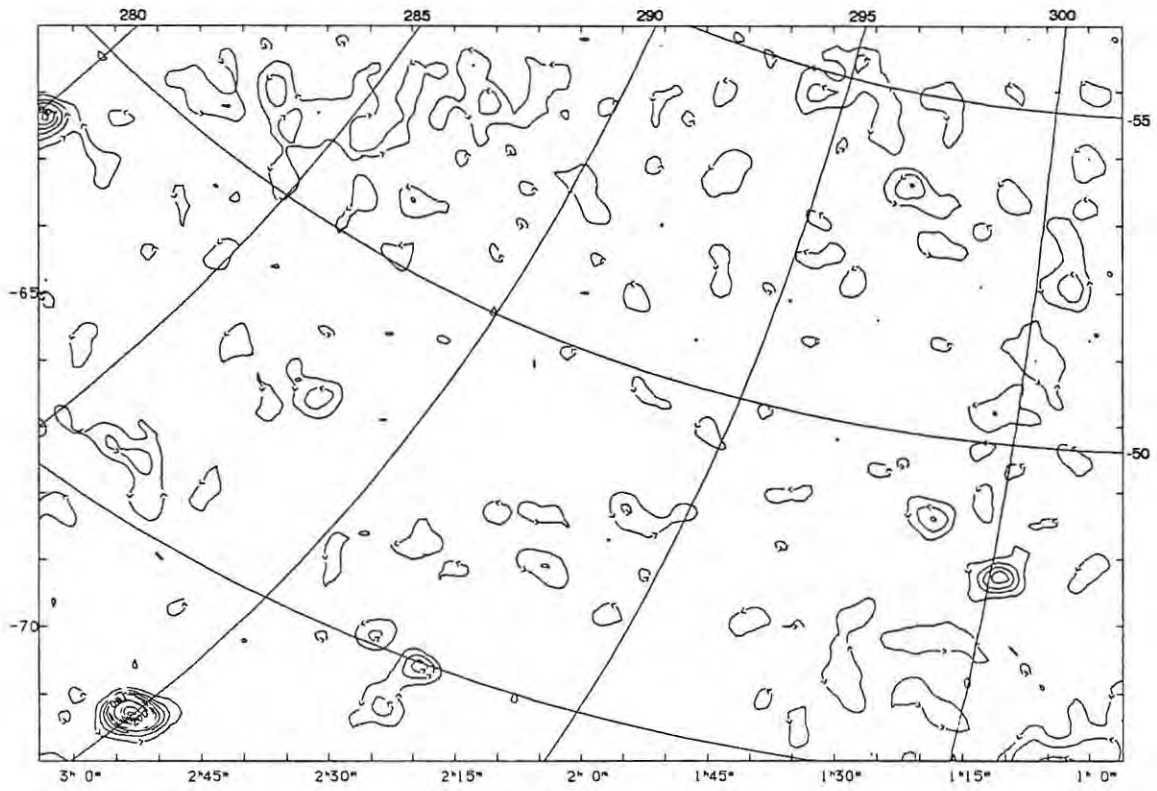
280
285
290
295
300
-55
-65
-50
-70
3h 0m
2h45m
2h30m
2h15m
2h 0m
1h45m
1h30m
1h15m
1h 0m

(c)

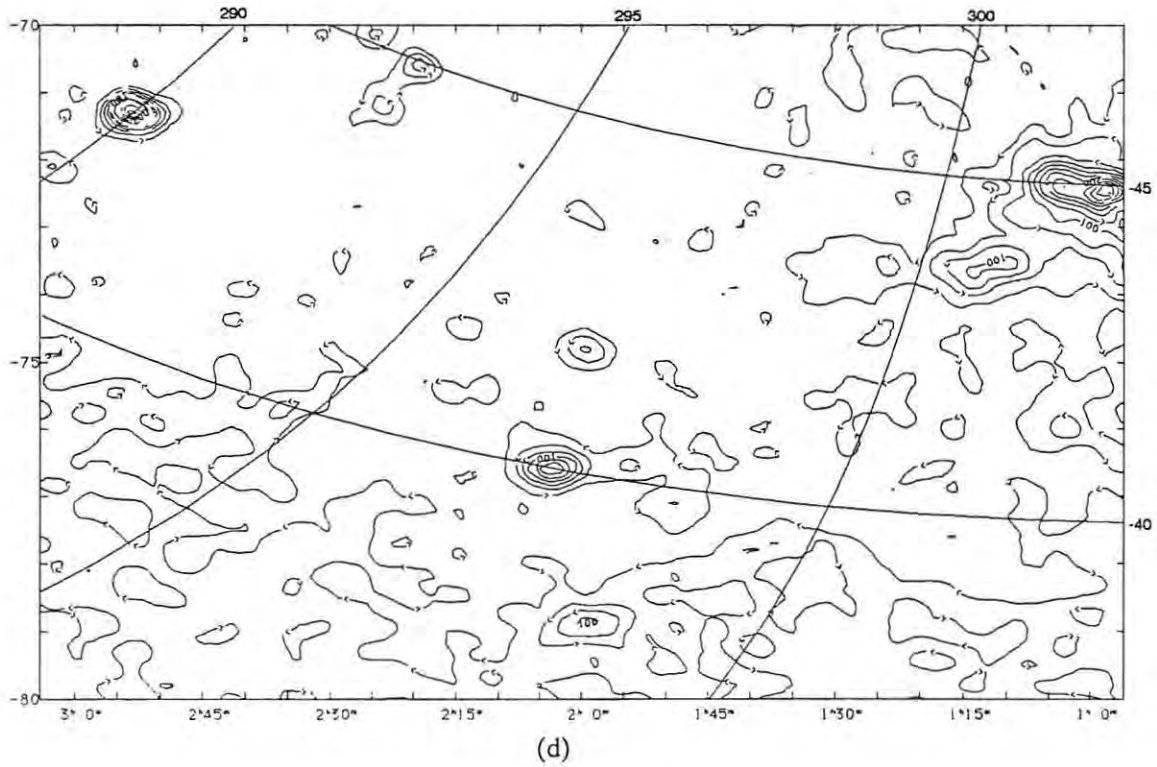
290
295
300
-70
-45
-75
-40
-80
3h 0m
2h45m
2h30m
2h15m
2h 0m
1h45m
1h30m
1h15m
1h 0m

(d)

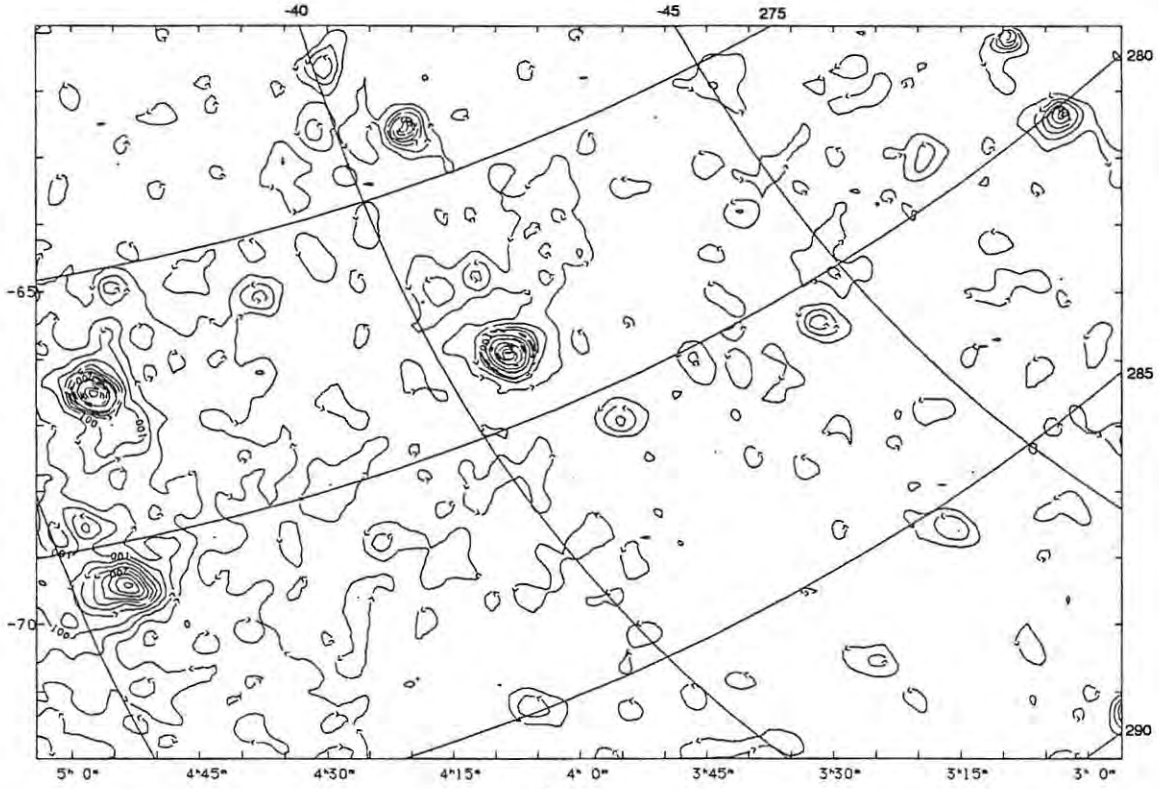
-40
-45
275
280
-65
285
-70
290
5h 0m
4h45m
4h30m
4h15m
4h 0m
3h45m
3h30m
3h15m
3h 0m

(e)

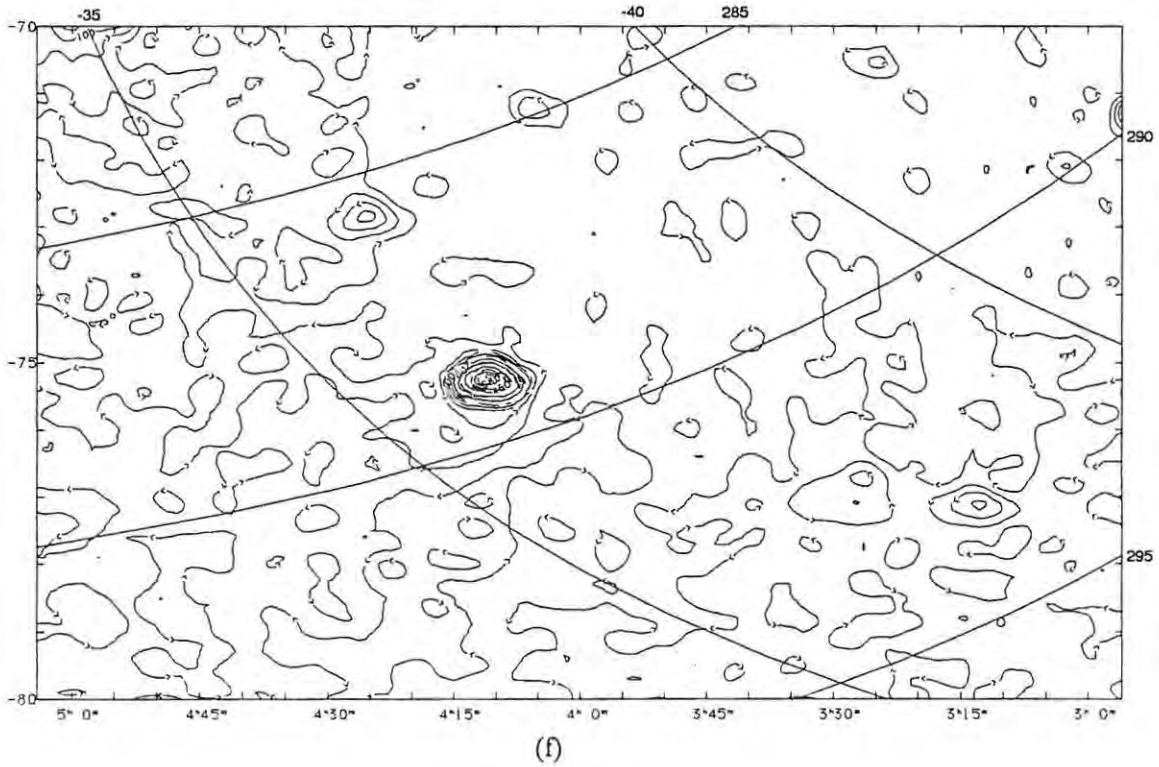
-35
-40
285
-70
290
-75
295
-80
5h 0m
4h45m
4h30m
4h15m
4h 0m
3h45m
3h30m
3h15m
3h 0m

(f)

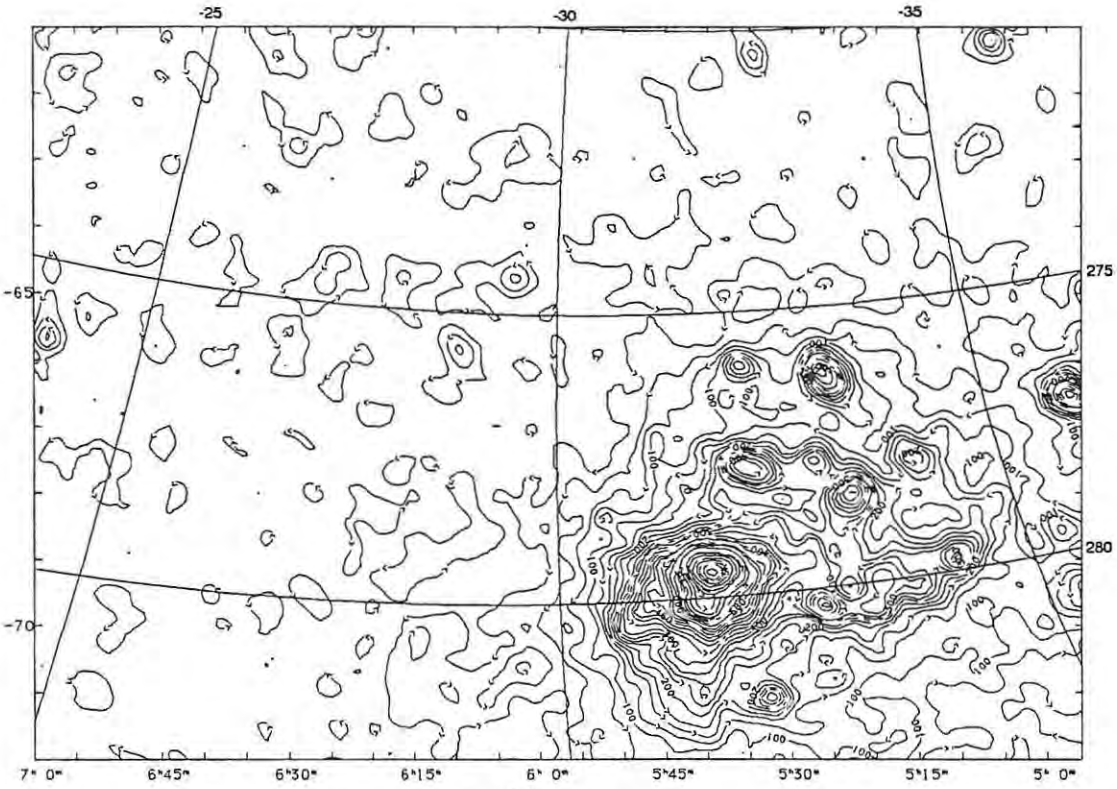
-25
-30
-35
-65
-70
275
280
7h 0m
6h45m
6h30m
6h15m
6h 0m
5h45m
5h30m
5h15m
5h 0m

(g)

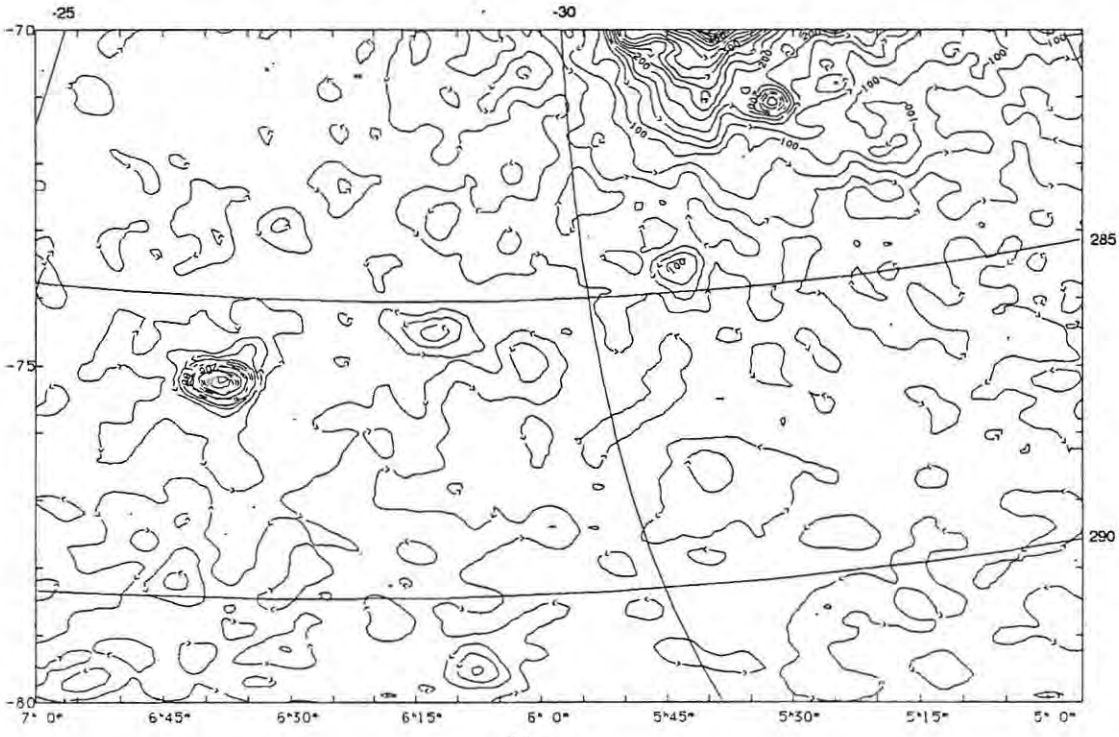
-25
-30
-70
-75
-80
285
290
7h 0m
6h45m
6h30m
6h15m
6h 0m
5h45m
5h30m
5h15m
5h 0m

(h)

Table 7.1. Contour levels for Figures 7.1 to7.3.

From [mK]	In steps of [mK]	To [mK]	With labels at
25	25	300	100, 200, 300 mK
340	40	500	460 mK
550	50	600	
680	80	1000	680 mK, 1 K
1150	150	1600	1.6 K
1800	200	2000	
2500	500	4500	3 K

distribution of negative temperatures at the lowest parts of the map is consistent with the expected r.m.s. noise deviations.

The contour levels used in Figures 7.1 through 7.3 are detailed in Table 7.1. Contour labels and unlabelled contours are not drawn where the temperature gradient is too steep, but labelled contours are always drawn. The arrows on unlabelled contours show anti-clockwise around an increase in temperature.

Figures 7.2 and 7.3 are contour maps of the Large and Small Clouds respectively, transformed onto individual field-centred projections. The integrated 2.3 GHz flux densities were measured to be 412 ± 50 Jy and 37 ± 6 Jy respectively. This measurement was performed by integrating the flux over expanding concentric circles on the sky until a base level was reached. The base level was determined by the constraint that the integrated flux should not increase or decrease monotonically once the circles had expanded beyond the boundaries of the object being measured.

It must be noted that the observations were made with a linearly polarised feed with the E-vector aligned East-West, so there may be some systematic error in these fluxes. For this reason an accurate spectral index cannot be calculated, but comparison with the 408 MHz flux densities of Haslam *et al.* (1981) indicates that the SMC has a strong non-thermal character. The spectral index of the integrated LMC flux appears somewhat flatter, which is to be expected as the thermal emission from 30 Doradus and numerous other H II regions forms a large component of the total.

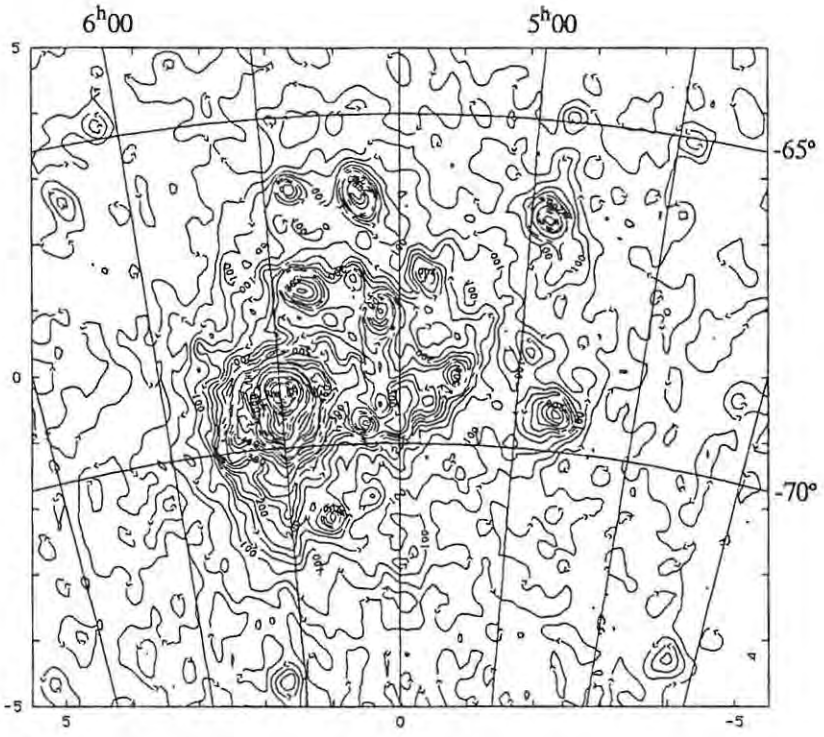

Figure 7.2. The Large Magellanic Cloud. Contours of antenna temperature rotated onto field centred coordinates. The contour levels are detailed in Table 7.1. The superimposed grid lines represent 1950.0 Equatorial coordinates.

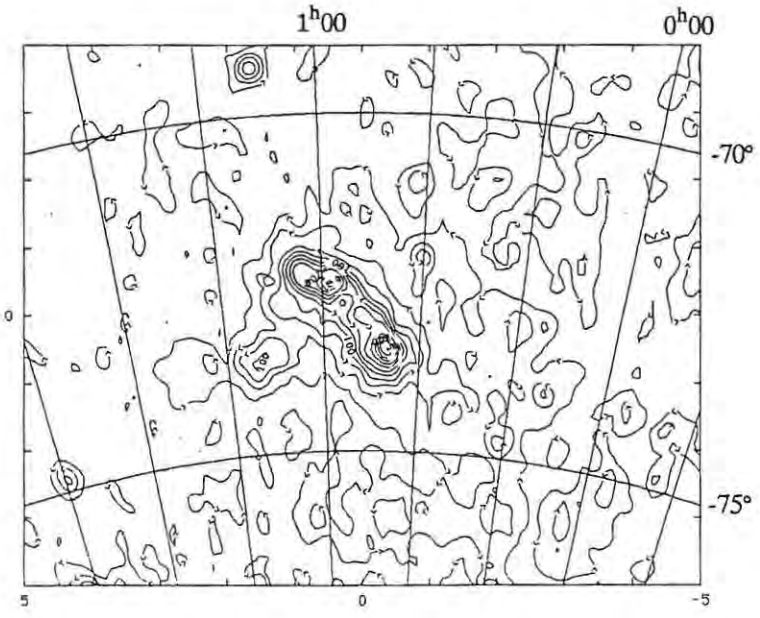

Figure 7.3. The Small Magellanic Cloud. Contours of antenna temperature rotated onto field centred coordinates. The contour levels are detailed in Table 7.1. The superimposed grid lines represent 1950.0 Equatorial coordinates.

The flux density of the emission from one square degree around the 30 Doradus region is estimated to be 100 ± 20 Jy. This value agrees with those at other frequencies quoted by Mills, Turtle and Watkinson (1978). This emission has a spectrum which is very flat over a wide range of frequencies, implying that it is thermal.

Figure 7.4 is a contour map of brightness temperature for the whole region with the data smoothed to the 0°.85 beamwidth of the 408 MHz survey (Haslam *et al.*, 1982), and overlaid with a map from Haslam *et al.* (1981). The contour intervals are 100 times smaller than those of the 408 MHz map, which compensates closely for a non-thermal spectrum of index –0.7. This is shown in the similarities e.g. in the outer regions of the LMC, and by the way the 2.3 GHz data is much steeper near 30 Doradus, a thermal source. Figure 7.5 is a portion of the same heavily smoothed data plotted in Equatorial co-ordinates, with contours plotted at 6 mK intervals from 0 to 60 mK. This is overlaid with a contour map of H I column densities from Mathewson *et al.* (1979).

The map parameters of pointing, flux calibration, base levels, residual noise, final resolution and side effects of the reduction process are discussed below.

7.3.1. Noise Measurement

The r.m.s. noise was measured on 24 square degrees of the map which appeared to be free of sources, and a value of 34 mK was obtained. The expected noise may be deduced from the DVM integration time of 0.1 s and the fact that each bin usually contains three samples on each observation. As each raster is observed three times, the total integration time on each sample of the final map is 0.9 s. In section 2.1. the r.m.s. noise was calculated from the receiver noise temperature to be 15 mK for 1 s integration time. Adding the 10 mK r.m.s. for confused sources brings the expected noise up to 18 mK. The extra noise must be attributed to residual scanning effects and the fact that the median rather than the mean is taken when combining observations of a raster.

After filtering to remove all spatial frequencies higher than those present in the telescope beam the noise was reduced to 21 mK. A 3×3 median filter on the same data reduced the r.m.s. noise to 18 mK and following this with the above low pass filter yielded 17 mK.

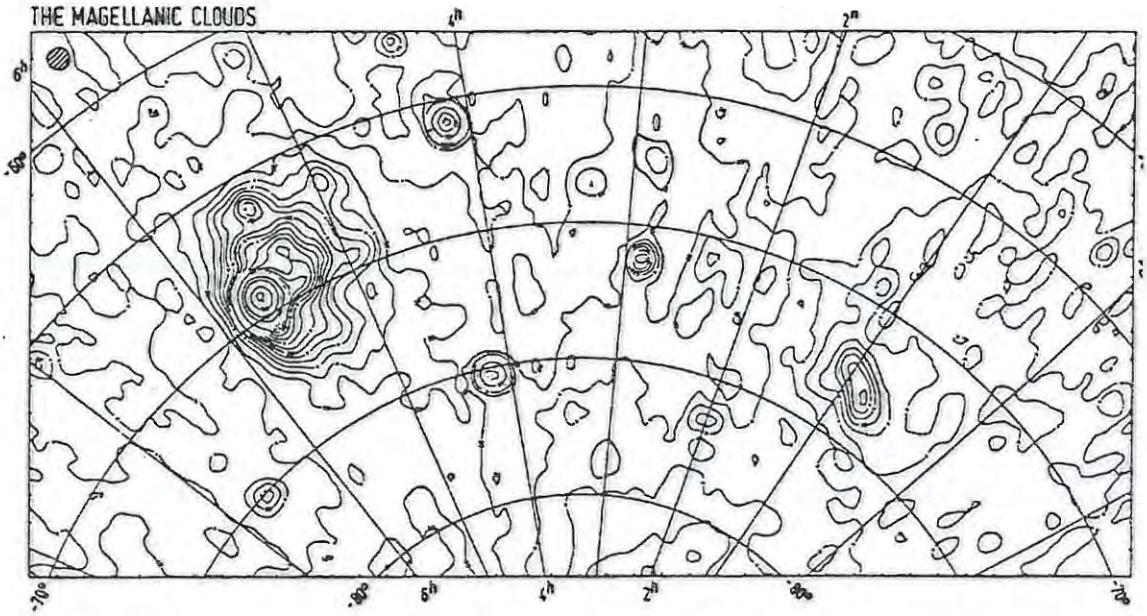
THE MAGELLANIC CLOUDS

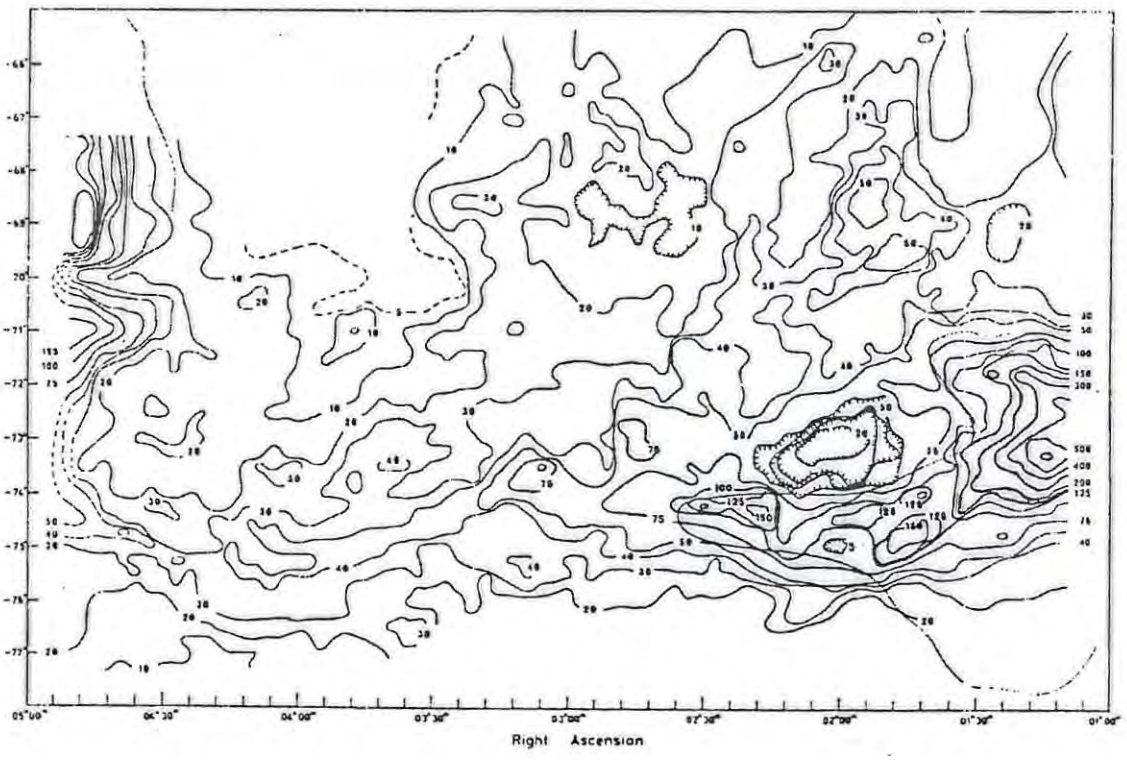
Right Ascension

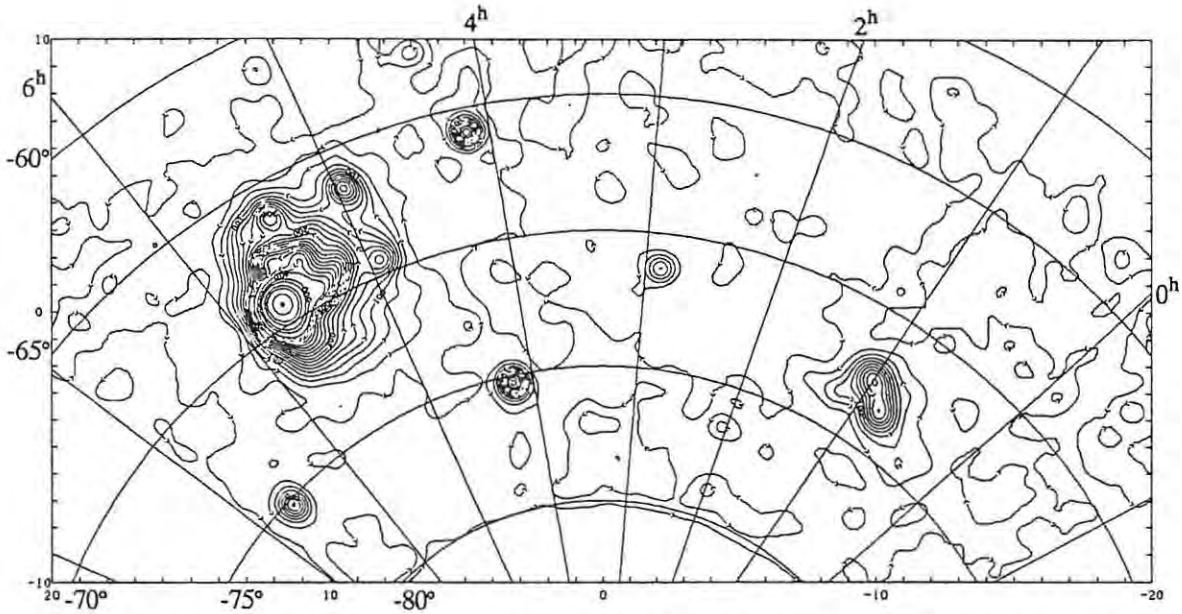

Figure 7.4. 408 MHz comparison map. Contours of beam brightness temperature for the entire region rotated onto field centred coordinates and smoothed to the 0?85 beamwidth of the 408 MHz survey. The overlay is from Haslam *et al.*,1981. The contour intervals for the 2.3 GHz map are 100 times smaller than those of the 408 MHz map, a factor which closely compensates for the difference in frequency, assuming a non-thermal spectral index of –0.7. Contours are shown at 20 mK intervals from 20 to 400 mK, and then at 500, 600 and 800 mK and at 1.0, 1.5 and 2.0 K.

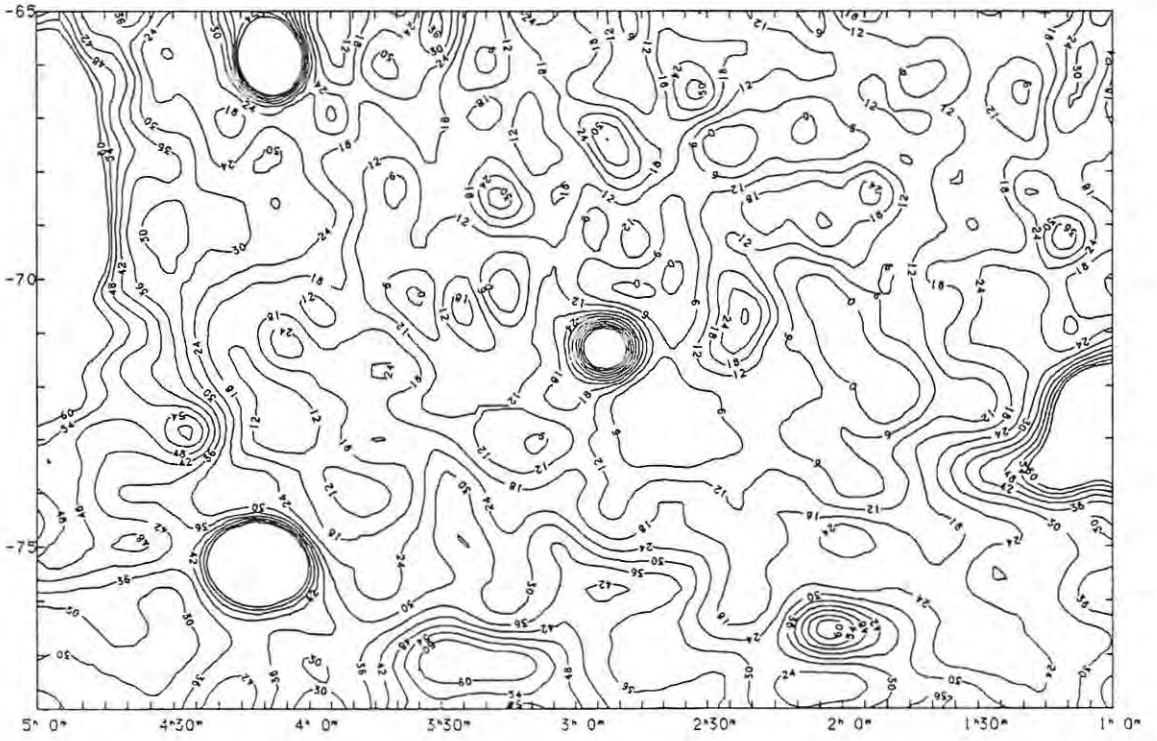

Figure 7.5. H I comparison map. A portion of the same heavily smoothed data as Figure 7.4, on Equatorial coordinates with contours spaced at 6 mK intervals from 0 to 60 mK. The overlay is from Mathewson *et al.*, 1979 and shows column densities of H I in units of 10^{19} atoms cm^{-2}.

7.3.2. Unresolved Source Comparison

Sources for which the Parkes catalogue predicts a 2300 MHz flux $S_{2300} > 0.6$ Jy are listed in Table 7.2 together with the flux actually measured and the pointing errors. The numbers were obtained by fitting (to the unfiltered data) a Gaussian beam of 20′ HPBW superimposed on a base surface to the local maximum nearest the position indicated in the catalogue. The co-ordinate residuals have a standard deviation of 2′ in both Right Ascension and Declination, and a systematic error of 4′ in Right Ascension. This is probably due to the fact that the pointing errors of the telescope were not well calibrated for this Declination range at the time of the observations.

The goodness of fit of the Gaussian beam is shown by σ, which is the r.m.s. deviation of the data from the fitted beam. This generally compares favourably with the noise level of the data, and implies an uncertainty < 0.1Jy for the majority of sources. PKS 0539–691 is 30 Doradus, which is obviously not a point source, and is included only for completeness. The larger disagreements may be due to strong polarization or intrinsic variability of the sources.

7.3.3. Establishing Base Levels

The base levels obtained with the Skymap technique are not, of course, absolute, but referred to the lowest temperature encountered within a particular source area. For this to be successful, several drift-free observations must be obtained. As this was rarely the case, the Hartebeesthoek antenna structure was modified in 1983 to permit direct observation of the South Celestial Pole (SCP). This permitted a Skymap observation of the polar cap to be made (by Jonas) from which all receiver drift was removed by using the SCP as a constant temperature reference. Drift due to the cooling of the telescope surroundings which make a contribution to the system temperature when the antenna is pointing at the SCP must be eliminated by making several observations at different local times. Drift scans were synthesised both from these observations and from the maps presented here for –80° Declination. A comparison indicates that the residual variations are less than 25 mK.

7.3.4. Final Resolution

The data were rotated onto field centred co-ordinates and all spatial frequencies above 3.5 degree^{-1} removed with a Fourier filter. This does not broaden the telescope's 20′ beam.

Table 7.2. Parkes catalogue source comparison. Sources from the Parkes catalogue with an estimated $S_{2300} > 0.6$ Jy. Fluxes and deviations from the catalogue position were measured from the maps for each source. σ is the rms deviation from a 20′ Gaussian beam.

PKS Number	$\alpha_{1950.0}$ h m s	$\delta_{1950.0}$ ° ′ ″	Optical Identity	S_{Parkes} Jy	S_{Rhodes} Jy	$\Delta\alpha$ ′	$\Delta\alpha\cos\delta$ ′	$\Delta\delta$ ′	σ mK
2332-66	23 32 20.6	-66 54 04	G	1.45	1.50	9.52	3.76	-1.83	14.0
2353-68	23 53 24.6	-68 37 42	III	0.96	0.99	15.50	5.69	2.41	14.9
0013-63	00 13 37.2	-63 26 50	III	0.97	0.98	2.58	1.16	-0.12	14.2
0036-62	00 36 32.7	-62 47 42	E	0.91	0.91	12.62	5.80	-0.85	17.6
0043-63	00 43 54.0	-63 50 33	E	0.73	0.66	1.57	0.70	-6.04	14.8
0110-69	01 10 02.3	-69 15 47		1.13	1.16	10.91	3.89	-0.59	15.9
0118-68	01 18 05.5	-68 25 14	III	0.75	0.76	6.01	2.23	1.82	16.7
0119-63	01 19 52.4	-63 24 43	Q	0.86	0.88	18.31	8.25	-1.17	14.7
0202-76	02 02 00.2	-76 34 29	Q	1.55	1.61	20.84	4.89	-0.28	21.8
0230-66	02 30 50.2	-66 39 27	III	0.76	0.77	6.58	2.62	4.50	14.0
0252-71	02 52 27.2	-71 16 49	G	3.60	4.01	11.00	3.55	-0.58	29.8
0302-623	03 02 48.4	-62 23 06	Q	1.07	1.72	7.56	3.52	-1.04	13.6
0308-611	03 08 51.3	-61 09 59	Q?	0.82	1.54	11.14	5.39	0.10	15.4
0315-68	03 15 44.3	-68 32 29	G	0.83	0.88	5.71	2.10	-0.17	12.9
0331-654	03 31 08.5	-65 28 06	IIIB	0.79	0.85	6.07	2.53	0.66	14.6
0355-66	03 55 25.8	-66 54 13	III	0.79	0.80	-2.05	-0.81	0.19	11.9
0408-65	04 07 57.8	-65 52 46	III	7.69	8.89	7.07	2.90	-2.23	39.8
0410-75	04 09 58.9	-75 14 57	III	9.18	9.45	14.32	3.67	-0.36	85.9
0420-62	04 20 19.0	-62 30 40	G	1.93	2.02	7.64	3.53	-3.57	14.7
0429-61	04 29 36.9	-61 38 55	II	1.21	1.20	13.96	6.64	0.99	16.7
0437-65	04 36 50.7	-65 04 57	Q?	0.83	0.84	17.57	7.42	0.98	13.7
0506-61	05 06 08.6	-61 13 33	Q	1.95	1.42	8.43	4.06	1.24	13.3
0507-62	05 07 23.3	-62 46 17	III	0.78	0.80	10.65	4.88	-0.20	12.3
0534-61	05 34 16.3	-61 23 46	III	0.81	0.83	7.42	3.55	-1.40	17.4
0539-691	05 39 04.0	-69 06 30	HII	30.80	44.49	6.24	2.23	-5.65	374.1
0602-64	06 02 24.8	-64 43 18	DB	0.83	0.85	8.83	3.77	-3.65	11.1
0606-79	06 06 33.5	-79 34 22		0.90	0.92	19.43	3.52	3.09	19.3
0608-65	06 08 42.8	-65 51 14	III	0.84	0.87	11.47	4.69	-2.07	12.3
0611-74	06 11 33.7	-74 31 12	III	0.83	0.85	13.63	3.63	-0.12	18.5
0637-75	06 37 23.2	-75 13 34	Q	5.79	5.85	11.52	2.93	-1.57	52.6
0658-65	06 58 04.2	-65 40 42	IIIS	1.24	1.11	8.84	3.63	2.54	17.1

Optical identification codes from the Parkes catalogue (a ? indicates a suggested identification):

D,DB,E	– galaxies of the corresponding type
G	– galaxy too faint to classify
Q	– confirmed quasi-stellar object
II	– one or more galaxies within the error box
III	– one or more stars of normal colour within the error box
IIIB	– blank
IIIS	– a star of normal colour
HII	– H II region

Plate 1 *(overleaf)*. **Radiograph of the Cloud region.** A high contrast false colour radiograph of the region on field-centred co-ordinates. The colour scale is represented by the horizontal bar above the map data, antenna temperature increasing from left to right. Full scale is 500 mK.

7.3.5. Reduction Side Effects

The chief uncertainty introduced into this particular set of data by the reduction process is due to the lack of drift free observations and the measures which had to be adopted to remove the drift. The result is that any source which extends the full length of a Declination scan or synthesised Drift scan will have been subtracted out by the reduction process.

7.4. Discussion

Plate 1 is a high contrast false colour radiograph of the entire data set projected onto a field centred co-ordinate system. The most prominent emission features are all extragalactic – the LMC on the left, the SMC on the right and numerous point sources spread across the field. The very extended feature to the South of the area between the Clouds is part of a radio spur projecting from the galactic plane. This feature is visible on the 408 MHz data (Haslam *et al.*, 1982) and coincides with nebulosity on the SRC survey Schmidt plates (King, Taylor and Tritton, 1979) and 'cirrus' on the IRAS 100 μm data.

7.4.1. The Large Magellanic Cloud

The radio emission from the LMC may be decomposed into four components:

(i) A strong extended source in the direction of the 30 Doradus complex. Ridges of emission extend from this source, some of which have an apparent spiral structure.

(ii) A broad, slightly curved ridge of emission which is coincident with the optical bar described by de Vacouleurs and Freeman (1973).

(iii) Discrete sources. Davies, Elliott and Meaburn (1976) have identified many of these sources as H II regions.

(iv) A very extended background component. This roughly elliptical disc extends from 4^h40^m to 6^h00^m in Right Ascension and from –73° to –65° in Declination. The faint optically visible outer spiral structure, dubbed regions C and D by de Vacouleurs and Freeman (1973), is not detected.

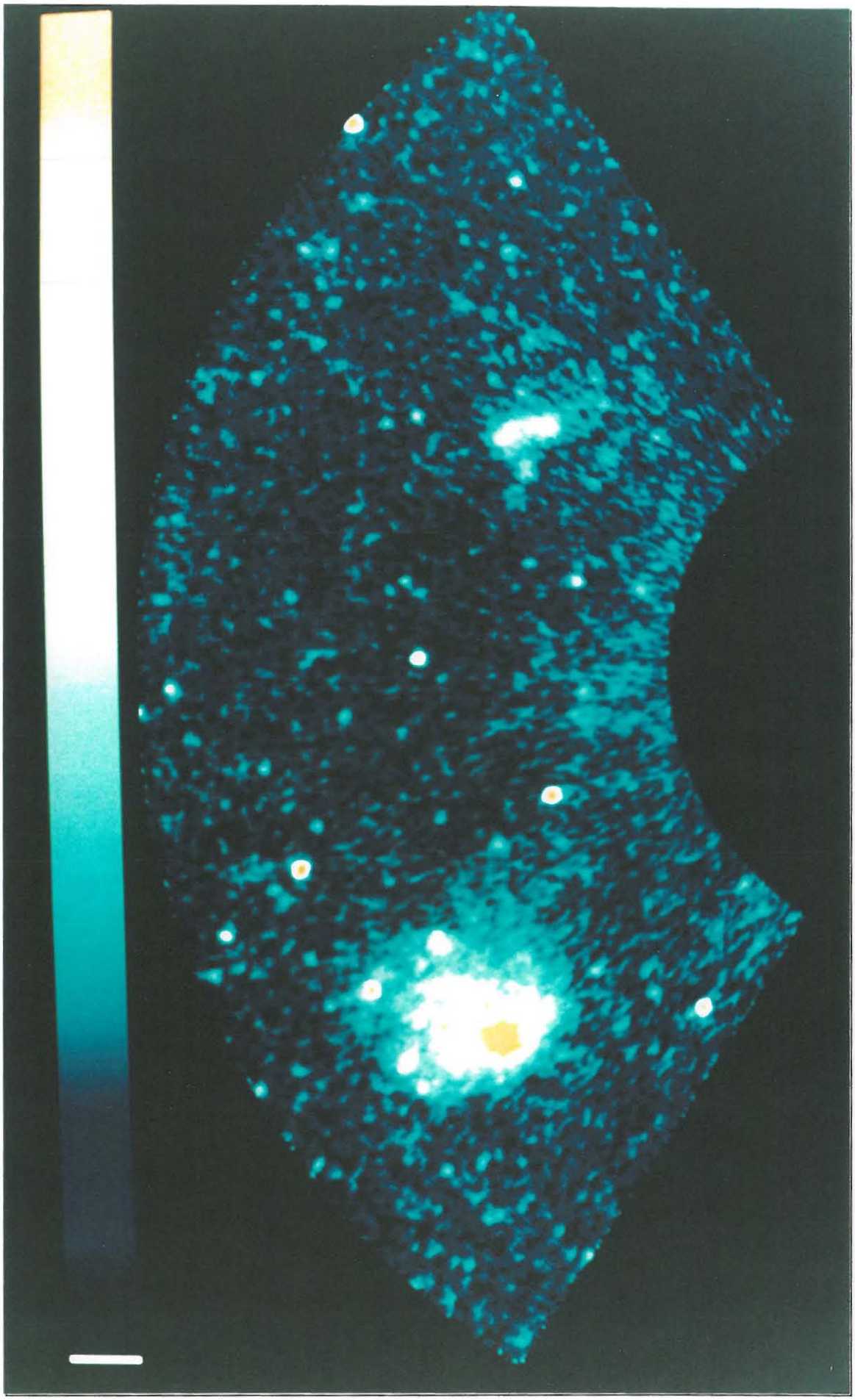

Plate 1. False colour radiograph of the Magellanic Clouds

Some evidence of spiral structure centred on 30 Doradus is visible in the radio image. This spiral structure, which is traced by ridges of emission, resembles the spiral distribution of extreme Population I objects described by Schmidt-Kaler (1977) and the hierarchical clusters of emission regions delineated by Feitzinger and Braunsfurth (1984).

7.4.2. The Small Magellanic Cloud and Intercloud Region

In the main body of the Small Cloud the contours in Figure 7.3 follow the star count isopleths down to $m_{pg} = 16$ very closely (de Vaucouleurs and Freeman, 1973), as do the H I surface density contours (Mathewson and Ford, 1984). All clearly show the 'wing' to the East of the main body around RA 1^h10 and Dec –74° (dubbed K1 by de Vaucouleurs and Freeman).

Westerlund and Glaspey (1971) extended the star counts up to RA 2^h15 and to below –75° Dec. This area is also covered by Figure 7.5, and it is interesting to note that while there is no obvious correspondence of extended sources, an unresolved 0.5 Jy continuum source corresponding to PKS 0159–747 coincides with a 'hole' in the H I and lies very near to possible clusters of blue stars identified by Westerlund and Glaspey. The optical identity offered by the Parkes catalogue is "one or more stars of normal colour within the error box". Loiseau *et al.* (1987), who have performed detailed spectral index measurements of the SMC using, amongst others, the computer readable forms of this 2.3 GHz data and the 408 MHz data of Haslam *et al.*, show a very non-thermal index (approaching –1.0) for this area. However, this may arise from the foreground spur from the Galaxy which covers this region.

Mathewson *et al.* (1979) characterise the large scale structure of their inter-Cloud H I map (Figure 7.5) as a sharp cutoff to the South and streamers pointing North toward the Magellanic Stream, with concentrations at approximately –68° Dec and RA's of 1^h50 and 3^h15. The comparison continuum map is complicated by the presence of foreground and background sources. The 0.9 Jy source PKS 0315–68 appears to coincide with one of the concentrations, but has been identified as a faint galaxy. The source PKS 0153–68, which coincides with the other peak H I concentration, only offers identification with "several stars of normal colour" which presumably rules out any optically detectable emission nebulae. On the current data, an extended source is visible on both the contour

maps (Figure 7.1(c)) and in the radiograph (Plate 1). The concentration at 01^h50 and $-69°$ and the 'hole' at 02^h00 and $-73°$ do not correspond to any noticeable features on the continuum map.

The Hα radiation detected by Johnson, Meaburn and Osman (1982) is too diffuse to attempt identification with any feature on the radio map.

Chapter Eight: Evolution and Evaluation of Skymap

The changes which have been brought about during the last seven years use of Skymap are detailed, then a critical evaluation is attempted.

8.1. Evolution

Changes have been made to Skymap to take advantage of new hardware which has become available, and to streamline the observing procedure. In the absence of the author, all revisions of the Skymap procedures have been made by J.L. Jonas of Rhodes, and modifications to the telescope control programs by M. Gaylard of the RAO staff.

8.1.1. The Observing System

Changes have been made in response to new hardware and changing priorities at the observatory.

8.1.1.1. The Radiometer

A potentially fatal blow was dealt to the project by the demise of the MASER amplifier in 1983, the stability of which had made the whole principle of night-long raster-scanned observations attractive. However, the cryogenically cooled GaAsFET amplifier obtained as a replacement compensates for its higher noise temperature by having a wider bandwidth (45 K and 40 MHz useable), and is more stable in terms both of gain and noise temperature as long as the refrigerator temperature remains below 18 K.

8.1.1.2. The Telescope Control System

The upgrade of the on-line computers to E-series machines with 512 Kword memory and the RTE-6 operating system has meant that STEER no longer has to be made memory resident at system generation time, but is simply allocated is own partition.

The modification to the telescope to enable it to point at the South Celestial Pole, as mentioned in section 7.3.3, and the extension of observing frequencies to 12.2 GHz, has stretched COMND's method of calculating pointing corrections from polynomials to its limit, and this has been replaced by a set of lookup tables, once more taking advantage of the increased memory available. In fact, with the increased computing power available, the pointing correction function has been moved into STEER

where it is performed on each interpolated co-ordinate. Error checking has also been improved, and the utility programs have been enhanced and made more user-friendly.

Replacement of the electromechanical synchros by optical encoders and the valve amplifiers in the servo system by semiconductor parts has improved reliability and tracking accuracy.

8.1.1.3. Observing Procedure and program SKYMP

To facilitate observations in the absence of any Rhodes staff member at the observatory, the startup routine of the observing program (SKYMP) was modified to read the source parameters from a file, upon entry of an observation number from the keyboard.

Further reduction in operator interaction was achieved by including an automatic temperature scale calibration at the start and end of each observation by recording output from the noise tube. A calibration factor is printed so that the correct operation of the radiometer may immediately be assessed. As telescope time became an increasingly sought after commodity, arrangements were made to abandon an observation at the first sign of improper operation or unfavourable conditions, so that another type of program might be substituted.

The larger computer memory mentioned above has also meant that program SKYMP could be assigned its own memory partition. With this assurance that it need not be swapped out, SKYMP now controls the DVMs directly (program LOGER falls away) and writes to magnetic tape via buffered Class I/O. Two new Fluke DVMs are used, interfaced via HP-IB and sampling at 20 Hz. The second DVM allows for simultaneous observations from a second radiometer operating at a frequency of 5 GHz. The output magnetic tape format has been altered to allow for this.

8.1.2. The Reduction System

In 1982, soon after the initial Skymap system had been completed, the University replaced the ICL 1900 computer to which it had been so carefully tailored with a Control Data Cyber 170/825 machine, much more powerful and with a great deal more storage. In 1984, the Physics Department acquired a VAX 11/730, which has virtual memory capability and hosts the STARLINK astronomical software package. Attached to the VAX via a parallel interface is a Tektronix 4115B high resolution colour terminal. On each occasion the Skymap software was rewritten for the new machine. A version of the

software has also been ported to the HP 1000 E-series computers at the RAO. Thus while the principles of background removal, drift removal and combining rasters have been retained, the implementation details differ considerably from those detailed in Chapter Five, and from system to system.

The most radical changes have come about through the high speed display: because bad observations can be seen and edited out interactively, the processing programs no longer need to be so defensive, and the operations of taking medians and binning which were the corner stone of the original system have been replaced by proper interpolation, resulting in better noise reduction and more accurate data. The least mean square polynomial fits have been replaced by spline fits. The drift estimation has also become a more interactive process.

The practically unlimited memory has removed the need for all the different types of data produced by program TABN in the original system, and all the sorting and selection of these data for input to subsequent processing stages. The one remaining median operation is the computation of the median sky, but input to this process is now in the form of fully sampled runs from which an estimated background has already been subtracted.

The STARLINK package provided many useful routines for operating on the complete maps and a consistent framework within which local routines could be written.

8.2. Evaluation

The Skymap project has been successful from the purely technical aspect of providing an automated continuum mapping system optimised for the Hartebeesthoek Radio Telescope, although the finishing touches were supplied after the author's departure (see section 8.1.1.3 above). A promising indication of its worth is the fact that it has been used to observe roughly one quarter of the Southern

Plate 2 *(overleaf)*. **The area surveyed with Skymap.** A false colour radiograph, displaying in Galactic co-ordinates all the data (except the Magellanic Cloud Region) so far gathered with Skymap, is dominated by the Galactic Plane. The maximum extent of the data is $65° \geq l \geq 240°$ and $-30° \leq b \leq 60°$. Sag A is identifiable as the brightest source in the centre of symmetry of the dark contour. Cen A is the bright double source opposite the South Celestial Pole. The bright striations at top centre are due to an unintentional observation of the Moon. Several well-known extended features appear outlined by the outer green contour on the Northern edge of the Plane: The North Polar Spur, the circle of Sharpless 27 surrounding ζ Oph and nearby at lower Latitude the brighter Gum 65 and RCW 129 around σ and τ Sco respectively, also covered in Chapter 6. At far right is the large ring of the Gum Nebula.

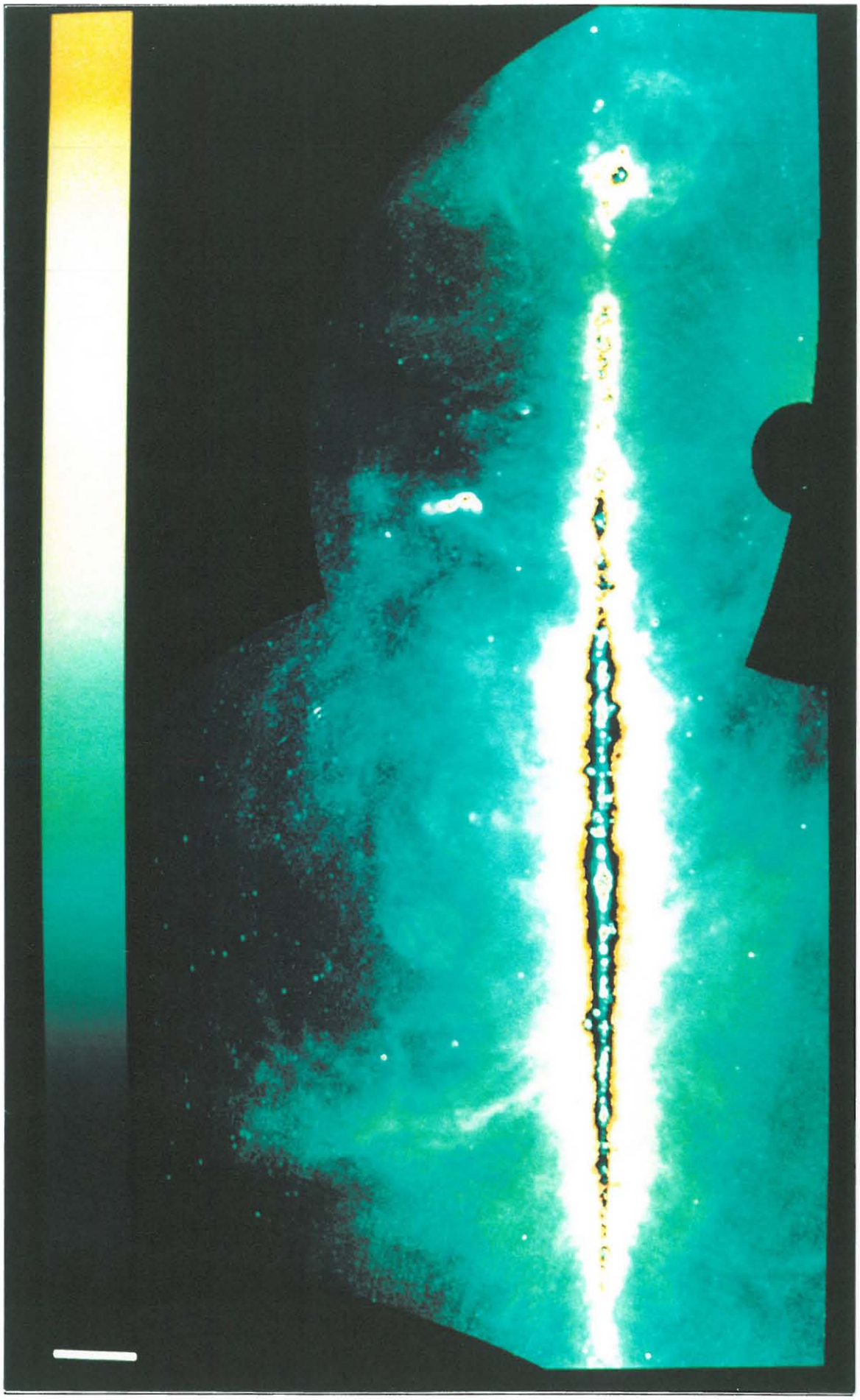

Plate 2. Area surveyed so far with Skymap (1987).

sky (see Plate 2) over a period of five years. The repeatability of the data obtained where separately mapped areas overlap (Jonas, private communication and see e.g. section 7.3.3) and the reasonable agreement between noise levels expected from consideration of the system parameters and that measured on the final map (section 7.3.1) show that the system is at least self-consistent.

It has also kept several researchers occupied, providing a basis for two M. Sc. theses, one devoted to aspects of data processing (Jonas, 1982) and the other to problems of interpreting the data (Greybe, 1984), and several publications: Jonas, de Jager and Baart (1985), Jonas (1986), Mounfort *et al.* (1987) and Woermann and Jonas (1988). Loiseau *et al.* (1987) compared the Magellanic Cloud data described in Chapter Seven with the 1.4 GHz data of Haynes *et al.* (1986) and the 408 MHz data of Haslam *et al.* (1981) to perform spectral index estimations. They rescaled the data to a standard flux density scale and smoothed it to an effective 24′ beamwidth before use. Much of the data has thus passed a rather stringent process of peer scrutiny.

8.2.1. Comparison with other mapping methods

The simplest practical method for mapping with a telescope with a steerable dish antenna is to scan across the source and subtract a linear baseline passing through the endpoints of each scan. The assumptions here are that each scan reaches 'cold sky' at its endpoints, and that the background of ground and atmospheric radiation plus any receiver drift may be approximated by a straight line. This works well even at relatively high frequencies for Galactic Plane surveys, where the source is narrow when scanning in Galactic Latitude and the source temperatures are high compared with the surroundings and the background. The limits of this technique were probably reached by the 2.7 GHz survey of Reich *et al.* (1984), where the source temperatures at the scan ends could not always be assumed to be zero and had to be measured separately.

8.2.1.1. Basket Weaving

An extension of the simple method described above is to scan in two orthogonal directions, producing much more reliable and accurate data as the two sets of scans may now be compared with one another to evaluate the baselines. This technique was used by Haynes *et al.* (1986) for the 1.4 GHz Magellanic Cloud survey, and is described by Sieber, Haslam and Salter (1979). It works very well where the background may be assumed to be linear and the source temperatures at the boundaries of

the map, zero. Loiseau *et al.* (1987) note that this introduces some uncertainty into the 1.4 GHz flux obtained for the Small Magellanic Cloud.

When larger areas are mapped, background radiation becomes more important, and the stability not only of the receiver during observations, but of the whole observing environment over the months or years spanning a set of observations, must be taken into account.

8.2.1.2. The 408 MHz All-sky Survey

This survey and the reduction technique are descibed by Haslam *et al.* (1981). Receiver stability was monitored by continuous calibration against a noise diode. Where sets of scans were made with the 'nodding' technique (see section 4.2.2), all observations from a set covering a particular range of Declination and made with the same telescope have the same background as all are made on the meridian. The scans, including any background radiation, are made consistent by subtracting a straight line from each scan and comparing the values measured at intersections of up and down scans. Any scan which cannot be made to agree with its intersecting scans by altering the parameters of its baseline is rejected. These consistent scans are then assembled into a map. The background and any other errors in baselevel and scaling are corrected by bringing these maps into agreement with older, absolutely calibrated, lower resolution surveys at each common Declination. The method of interpolating in Declination was not specified.

It was reported that for the sets of observations made at Parkes, no systematic baselevel adjustment with elevation (i.e. background correction) was necessary. At the other extreme, some observations of the North polar cap made from Jodrell Bank had to be made from the pole down to elevation 8° rather than in the preferred position from the pole through the zenith. A background for the low elevation observations was measured by observing some scans at both positions and comparing these matched pairs. This background was used to correct all low elevation observations before comparing intersections.

8.2.1.3. 1420 MHz Stockert Surveys

Reich (1978 and 1982) has observed the Northern sky down to Declination –19° using the 25 m Stockert telescope at 1420 MHz. The observations were performed as Azimuth scans at 50.571° (through the North Pole) and 40° and 20° Elevation.

The lower Elevation scans were corrected for a non-linear backgound by the subtraction of a lower envelope fitted to a set of scans taken at high Galactic Latitude, after which the procedure followed was essentially the same as for the 408 MHz survey above. Separate maps were compiled from observations taken at each Elevation. The final maps were given an absolute baselevel by comparison with absolutely calibrated sky-horn measurements, and scaled from observations of standard sources.

A technique called 'unsharp masking' was used to correct for local non-linear scanning effects. This is reminiscent of Skymap's median sky comparison, involving fitting a second order curve to the difference between individual scans and a map heavily smoothed orthogonal to the scan direction.

Reich and Steffen (1981) mapped the Southern part of Loop IV with nodding scans down to Elevation 8°. The background was constructed by taking medians across the scans at each Elevation to remove strong sources. A system temperature offset was subtracted from each scan, removing any gradient in RA.

8.2.1.4. Skymap comparison

From the above it is seen that when backgound radiation becomes a problem, similar techniques of restricting the scanning pattern in local co-ordinates, measuring backgrounds in areas thought to be free of extended sources, and removing point sources from the background measurements by taking medians, have been followed.

The Skymap system of Dec scans is basically simpler than those involving intersecting scans: by repeating observations exactly to detect interference or drift, and by relying on the noise-adding radiometer and cryogenic amplifier to maintain accurate levels and consistent gains over the whole map, there is no opportunity for the interpolation, iterative intersection comparison and baseline adjustment, and offline calibration possible with the nodding or Azimuth scans and the correlation radiometers used in their observation.

Removing a separate background from each observation relieves the observer from the constraint of making each observation in a set at exactly the same local co-ordinate, allowing e.g. multiple observations of a source of small extent to be completed in one night.

Conversely, when drift or interference is present on too many of the observations for them to be simply re-observed, the process of drift removal for Skymap via the median sky approach makes the operation much more complex and error prone.

The recently acquired capability to scan to the South Celestial Pole will improve this situation. Since scanning to the pole regularly during an observation upsets the observing pattern, particularly if the source area lies at low or Northern Latitudes, the policy adopted by the Rhodes group is to make a greatly undersampled survey of the whole sky which, by including the South Pole, may be corrected for drift, and then used to provide base levels for other maps much in the same way that Skymap uses the median sky. This will also allow for the correction of drift caused by the cooling of the telescope surroundings. Simply scanning to the pole during an observation does not help, as this changes the ground radiation contribution to the system temperature. Great care will have to be taken with the observation of this reference survey to eliminate contamination by such effects, as the Pole is at an Elevation of only 25.89°.

References

Alvarez, H., Aparici, J., May, J.: 1987, *Astron. Astrophys.* **176**, 25–33.

Baart, E.E., de Jager, G., Mountfort, P.I.: 1980, *Astron. Astrophys.* **92**, 156.

Berkhuijzen, E.M.: 1971, *Astron. Astrophys.* **14**, 359.

Blaauw, A.: 1978, Internal Motions and Age of the Sub-association Upper Scorpio in *Problems of Physics and Evolution of the Universe*, p. 101, ed. V.L. Mirzoyan, American Academy of Sciences, Yerevah.

Bracewell, R.N.: 1965, *The Fourier Transform and its Applications*, p. 77, McGraw-Hill, New York.

Brenner, N.: 1976, The Fast Fourier Transform and Appendices A–H in *Methods of Experimental Physics* **12C**, p. 284, eds. L. Marton and M.L. Meeks, Academic Press, New York.

Broten, N.W.: 1972, *Australian J. Phys.* **25**, 599–612.

Cappa de Nicolau, C.E., Pöppel, W.G.L.: 1986, *Astron. Astrophys.* **164**, 274–299.

Churchwell, E., Walmsley, C.M.: 1973, *Astron. Astrophys.* **23**, 117.

Davies, R.D., Elliott, K.H., Meaburn, J.: 1976, *Mem. R. Astron. Soc.* **81**, 89.

Day, G.A., Caswell, J.L., Cooke, D.J.: 1972, *Australian J. Phys. Astrophys. Suppl.* **25**, 1.

de Vaucouleurs, G., Freeman, K.C.: 1973, Structure and Dynamics of Barred Spiral Galaxies, in particular of the Magellanic Type, in *Vistas in Astronomy Volume 14*, ed. A. Beer, Pergamon Press, Oxford.

Ekers, J.A. (Ed.): 1969, *Australian J. Phys. Astrophys. Suppl.* **7**, 1.

Emerson, D.T., Klein, U.: 1979, Observations of Extended Radio Sources Using a Multiple Beam Technique in *Image Formation from Coherence Functions in Astronomy*, p. 293, Ed. C. van Schooneveld, D. Reidel, Dordrecht, Holland.

Feitzinger, J.V., Braunsfurth, E.: 1984, The Spatial Distribution of Young objects in the Large Magellanic Cloud – A Problem of Pattern Recognition in *IAU Symposium No. 108 Structure and Evolution of the Magellanic Clouds*, p. 93, eds. S. van den Bergh and K.S. de Boer, D. Reidel, Dordrecht, Holland.

Garrison, R.F.: 1967, *Astrophys. J.* 147, 1003.

Greybe, A.: 1984, M.Sc. Thesis, Rhodes University.

Gutierrez-Moreno, A., Moreno, H.: 1968, *Astrophys. J. Suppl.* **15**, 459.

Gum, C.S.: 1955, *Mem. R. Astron. Soc.* **67**, 155.

Hardie, R.H., Crawford, D.L.: 1961, *Astrophys. J.* **133**, 843.

Haslam, C.G.T., Quigley, M.J.S., Salter, C.J.: 1970, *Mon. Not. R. Astron. Soc.* **147**, 405.

Haslam, C.G.T., Wilson, W.E., Cooke, D.J., Cleary, M.N., Graham, D.A., Wielebinski, K., Day, G.A.: 1975, *Proc. Astron. Soc. Australia* **2**, 331.

Haslam, C.G.T., Klein, U., Salter, C.J., Stoffel, H., Wilson, W.E., Cleary, M.N., Cooke, D.J., Thomasson, P.: 1981, *Astron. Astrophys.* **100**, 209.

Haslam, C.G.T., Salter, C.J., Stoffel, H., Wilson, W.E.: 1982, *Astron. Astrophys. Suppl. Ser.* **47**, 1.

Haynes, R.F., Caswell, J.L., Simons, L.W.J.: 1978, *Australian J. Phys. Astrophys. Suppl.* **45**, 1.

Haynes, R.F., Klein, U., Wielebinski, R., Murray, J.D.: 1986, *Astron. Astrophys.* **159**, 22.

Higgs, L.A., Ramana, K.V.V.: 1968a, *J. R. Astron. Soc. Canada* **62**, 5.

Higgs, L.A., Ramana, K.V.V.: 1968b, *Astrophys. J.* **160**, 193.

Hill, E.R.: 1968, *Australian J. Phys.* **21**, 735.

Hindman, J.V.: 1967, *Australian J. Phys.* **20**, 147.

Jackson, F.: 1976, Honours Project, Rhodes University.

Jenkins, C.R.: 1976, Radio Astronomy Observatory, Hartebeesthoek, Internal Report 14, NITR, CSIR.

Johnson, P.G., Meaburn, J., Osman, A.M.I.: 1982, *Mon. Not. R. Astron. Soc.* **198**, 985.

Jonas, J.L.: 1982, *Observation and Processing of 2.3 GHz Radio Astronomy Survey Data*, M.Sc. Thesis, Rhodes University.

Jonas, J.L.: 1986, *Mon. Not. R. Astron. Soc.* **219**, 1–12.

Jonas, J.L., de Jager, G., Baart, E.E.: 1985, *Astron. Astrophys. Suppl. Ser.* **62**, 105–128.

Kazès, I., Le Squeren, A.M., Gadea, F.: 1975, *Astron. Astrophys.* **42**, 9.

Kellerman, K.I.: 1972, *Astron. J.* **77**, 531.

King, D.J., Taylor, K.N.R., Tritton, K.P.: 1979, *Mon. Not. R. Astron. Soc.* **188**, 719.

Kraus, J.D.: 1966, *Radio Astronomy*, McGraw-Hill, New York.

Landecker, T.L., Wielebinski, R.: 1970, *Australian J. Phys. Astrophys. Suppl.* **16**, 1.

Loiseau, N., Klein, U., Greybe, A., Wielebinski, R., Haynes, R.F.: 1987, *Astron. Astrophys.* **178**, 62–76.

Marcelin, M., Boulesteix, J., Georgelin, Y.P.: 1985, *Nature* **316**, 705.

Mathewson, D.S., Ford, V.L., Schwarz, M.P., Murray, J.D.: 1979, The Magellanic Stream: Observational Considerations in *IAU Symposium No. 84, The Large Scale Characteristics of the Galaxy*, p. 547, ed. W.B. Burton, D. Reidel, Dordrecht, Holland.

Mathewson, D.S., Ford, V.L.: 1984, H I Surveys of the Magellanic Stream in *IAU Symposium No. 108 Structure and Evolution of the Magellanic Clouds*, p. 125, eds. S. van den Bergh and K.S. de Boer, D. Reidel, Dordrecht, Holland.

Mathewson, D.S., Healey, J.R.: 1964, Continuum Radio Emission from the Magellanic Clouds in *IAU Symposium No. 20 The Galaxy and the Magellanic Clouds*, p. 245, eds. F.J. Kerr and A.W. Rodgers, Australian Academy of Science, Canberra.

McGee, R.X., Brooks, J.W., Batchelor, R.A.: 1972, *Australian J. Phys.* **25**, 581–597.

McGee, R.X., Milton, J.A.: 1966, *Australian J. Phys.* **19**, 343.

McGee, R.X., Newton, L.M.: 1981, *Proc. Astron. Soc. Australia* **4**, 189.

McGee, R.X., Newton, L.M., Butler, P.W.: 1978, *Mon. Not. R. Astron. Soc.* **183**, 799.

Mezger, P.G., Henderson, A.P.: 1967, *Astrophys. J.* **147**, 471.

Mills, B.Y.: 1955, *Australian J. Phys.* **8**,368–389.

Mills, B.Y., Turtle, A.J., Watkinson, A.: 1978, *Mon. Not. R. Astron. Soc.* **185**, 263–276.

Mills, B.Y., Turtle, A.J., Little, A.G., Durdin, J.M.: 1984, *Australian J. Phys.* **37**, 321–357.

Mountfort, P.I., Jonas, J.L., de Jager, G., Baart, E.E.: 1987, *Mon. Not. R. Astron. Soc.* **226**, 917–926.

Neugebauer, G., Beichman, C.A.: 1985, in *Infrared Astronomical Satellite (IRAS) Catalogs and Atlases Explanatory Supplement*, p. I-1, eds. C.A. Beichman, G. Neugebauer, H.J. Habing, P.E. Clegg and T.J. Chester, Jet Propulsion Laboratory, Pasadena, California.

Nicolson, G.D.: 1970, *IEEE Trans. Microwave Theory and Tech.* **MTT-18**, 169.

Panagia, N.: 1973, *Astron. J.* **78**, 929.

Price, R.M.: 1974, Continuum Radio Emission and Galactic Structure in *IAU Symposium No. 60 Galactic Radio Astronomy*, p. 637, Eds. F.J. Kerr and S.C. Simonson III, D. Reidel, Dordrecht, Holland.

Reich, W.: 1978, *Astron. Astrophys.* **64**, 407–421.

Reich, W.: 1982, *Astron. Astrophys. Suppl. Ser.* **48**, 219–217.

Reich, W., Fürst, E., Steffen, P., Reif, K., Haslam, C.G.T.: 1984, *Astron. Astrophys. Suppl. Ser.* **58**, 197–248.

Reich, W., Steffen, P.: 1981, *Astron. Astrophys.* **93**, 27–34.

Rodgers, A.W., Campbell, C.T., Whiteoak, J.B., Bailey, H.H., Hunt, V.O.: 1960, *An Atlas of H-Alpha Emission in the Southern Milky Way*, Mt Stromlo Observatory, Canberra.

Rossano, G.S.: 1978, *Astron. J.* **83**, 3.

Rubin, R.H.: 1968, *Astrophys. J.* **154**, 391.

Sancisi, R.: 1974, Expanding Shells of Neutral Hydrogen as Birthplaces of Stellar Associations in *IAU Symposium No. 60 Galactic Radio Astronomy*, p. 637, Eds. F.J. Kerr and S.C. Simonson III, D. Reidel, Dordrecht, Holland.

Schmidt-Kaler, Th.: 1977, *Astron. Astrophys.* **54**, 771.

Shain, C.A.: 1959, Observations of Extragalactic Radio Emission in *IAU Symposium No. 9/URSI Symposium No. 1, Paris Symposium on Radio Astronomy*, p. 328, ed. R.N. Bracewell, Stanford University Press, Stanford, California.

Sieber, W., Haslam, C.G.T., Salter, C.J.: 1979, *Astron. Astrophys.* **74**, 361–368.

Sivan, J.P.: 1974, *Astron. Astrophys. Suppl. Ser.* **16**, 163.

Stumpf, P., Schraml, J.: 1974, *Astron. Astrophys. Suppl.* **15**, 517.

Tiuri, M.E.: 1966, Radio Telescope Receivers in *Radio Astronomy*, p. 293, J.D. Kraus, McGraw-Hill, New York.

Tukey, J.W.: 1977, *Exploratory Data Analysis*, Addison-Wesley, Reading, Massachusetts.

Wall, J.V.: 1979, *Q. J. R. Astron. Soc.* **20**, 138.

Woermann, B., Jonas, J.L.: 1988, *Mon. Not. R. Astron. Soc.* **234**, 971–974.

Wright, A.E., Bolton, J.G.: 1976, *Australian J. Phys. Astrophys. Suppl.* **39**, 1.